PONTIFICIA
UNIVERSIDAD
CATÓLICA
DEL PERÚ

TECHNISCHE UNIVERSITÄT
ILMENAU

Pontificia Universidad Católica del Perú

Escuela de Posgrado

Tesis de Maestría

Energy-Based Control for the Cart-Pole System in Implicit Port-Hamiltonian Representation

Para optar el grado académico de
Magíster en Ingeniería de Control y Automatización

Presentado por:
Ing. Alex Smith Huaman Loayza

Profesor Responsable (TU Ilmenau):	Univ.-Prof. Dr.-Ing. Johann Reger
Supervisor (TU Ilmenau):	M. Sc. Oscar B. Cieza Aguirre
Profesor Responsable (PUCP):	Dr. Ing. Carlos Gustavo Pérez Zuñiga

Noviembre, 2019

Abstract

This master thesis is devoted to the design, analysis, and experimental validation of an energy-based control strategy for the well-known benchmark cart-pole system in implicit Port-Hamiltonian (PH) representation. The control scheme performs two tasks: swing-up and (local) stabilization. The swing-up controller is carried out on the basis of a generalized energy function and consists of bringing the pendulum trajectories from the lower (stable) position to a limit cycle (homoclinic orbit), which passes by the upright (unstable) position, as well as the cart trajectories to the desired point. The (local) stabilizing controller is designed under a novel algebraic Interconnection and Damping Assignment Passivity-Based Control (IDA-PBC) technique and ensures the upright (asymptotic) stabilization of the pendulum as well as the cart at a desired position. To illustrate the effectiveness of the proposed control scheme, this work presents simulations and real-time experiments considering physical damping, i.e., viscous friction. The results are additionally contrasted with another energy-based control strategy for the cart-pole system in explicit Euler-Lagrange (EL) representation.

TECHNISCHE UNIVERSITÄT
ILMENAU

Control Engineering Group

Alex Huaman

Energy-Based Control for the Cart-Pole System in Implicit Port-Hamiltonian Representation

Master Thesis in Engineering Cybernetics and Systems Theory

15 November 2019

Please cite as:
Alex Huaman, "Energy-Based Control for the Cart-Pole System in Implicit Port-Hamiltonian Representation," Master Thesis (Masterarbeit), Technische Universität Ilmenau, Department of Computer Science and Automation, November 2019.

Technische Universität Ilmenau
Department of Computer Science and Automation
Control Engineering Group

Helmholtzplatz 5 (Zusebau) · 98693 Ilmenau · Germany
http://www.tu-ilmenau.de/en/control-engineering-group

ET LUX IN TENEBRIS LUCET
MCMXVII

PONTIFICIA
UNIVERSIDAD
CATÓLICA
DEL PERÚ

TECHNISCHE UNIVERSITÄT
ILMENAU

Energy-Based Control for the Cart-Pole System in Implicit Port-Hamiltonian Representation

Master Thesis in Engineering Cybernetics and Systems Theory

submitted by

Alex Smith Huaman Loayza

born in Lima, Perú

in the

Control Engineering Group

Department of Computer Science and Automation
Technische Universität Ilmenau

Responsible Professor (TU Ilmenau):	**Univ.-Prof. Dr.-Ing. Johann Reger**
Supervisor (TU Ilmenau):	**M. Sc. Oscar B. Cieza Aguirre**
Responsible Professor (PUCP):	**Dr. Ing. Carlos G. Pérez Zuñiga**
Submission Date:	**15 November 2019**

ET LUX IN TENEBRIS LUCET
MCMXVII

Declaration

I declare that the work is entirely my own and was produced with no assistance from third parties.
I certify that the work has not been submitted in the same or any similar form for assessment to any other examining body and all references, direct and indirect, are indicated as such and have been cited accordingly.

(Alex Huaman)
Ilmenau, 15 November 2019

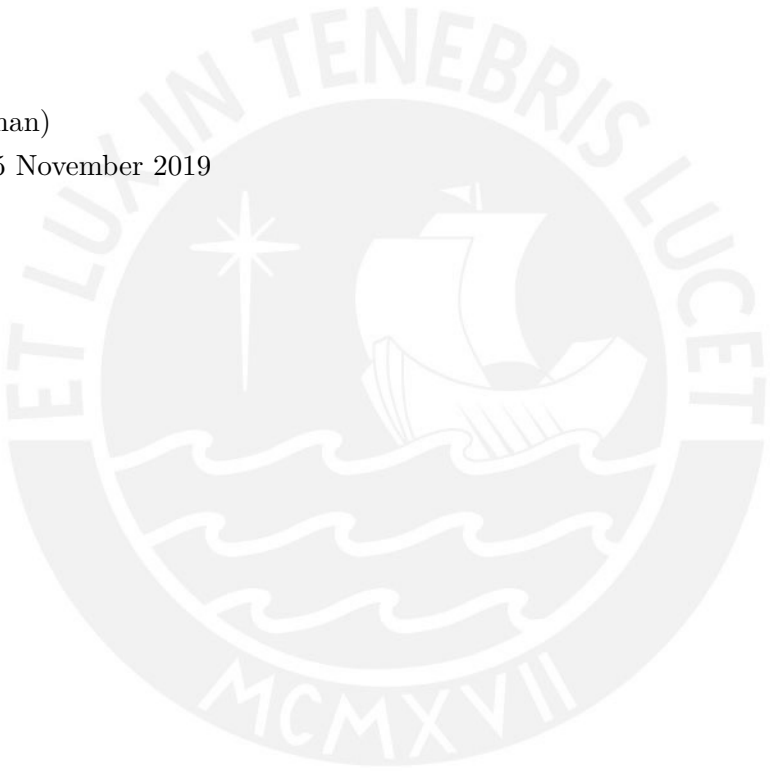

ET LUX IN TENEBRIS LUCET
MCMXVII

Acknowledgment

The author gratefully acknowledge the financial support from Deutscher Akademischer Austauschdienst (DAAD), Germany.
Foremost, I would like to express my deepest gratitude to Prof. Johann Reger and M.Sc. Oscar Cieza for their valuable and constructive suggestions during the planning and development of this research work. I would also like to thank Dr. Gustavo Pérez for his advice and assistance in keeping the progress of this work on schedule.
Last but not least, I wish to thank my mother for her support and encouragement throughout my life.

Before I forget! Thank you, dear reader, for reading the first page. I wish you a great journey through this manuscript.

ET LUX IN TENEBRIS LUCET
MCMXVII

Abstract

This master thesis is devoted to the design, analysis and experimental validation of an energy-based control strategy for the well-known benchmark cart-pole system in implicit Port-Hamiltonian (PH) representation. The control scheme performs two tasks: swing-up and (local) stabilization. The swing-up controller is carried out on the basis of a generalized energy function and consists of bringing the pendulum trajectories from the lower (stable) position to a limit cycle (homoclinic orbit), which passes by the upright (unstable) position, as well as the cart trajectories to the desired point. The (local) stabilizing controller is designed under a novel algebraic Interconnection and Damping Assignment Passivity-Based Control (IDA-PBC) technique and ensures the upright (asymptotic) stabilization of the pendulum as well as the cart at a desired position. To illustrate the effectiveness of the proposed control scheme, this work presents simulations and real-time experiments considering physical damping, i.e., viscous friction. The results are additionally contrasted with another energy-based control strategy for the cart-pole system in explicit Euler-Lagrange (EL) representation.

ET LUX IN TENEBRIS LUCET
MCMXVII

Kurzfassung

Diese Masterarbeit widmet sich dem Entwurf, der Analyse und der experimentellen Validierung einer energiebasierten Regelstrategie für das bekannte Benchmarksystem des inversen Pendels auf einem Wagen in impliziter Port-Hamiltonscher (PH) Darstellung. Das Regelungssystem erfüllt zwei Aufgaben: das Aufschwingen und (lokale) Stabilisierung. Das Aufschwingen erfolgt auf Grundlage der generalisierten Energiefunktion und besteht darin, sowohl die Trajektorien des Pendels von der unteren (stabilen) Position in einen Grenzzyklus (homokliner Orbit) zu bringen, wobei die (instabile) aufrechte Lage passiert wird, als auch den Wagen in einer gewünschten Position einzustellen. Die (lokale) Regelung zur Stabilisierung ist nach einer neuartigen algebraischen *Interconnection and Damping Assignment Passivity-Based Control* (IDA-PBC) Methode konzipiert und gewährleistet die aufrechte (asymptotische) Stabilisierung des Pendels sowie die Positionierung des Wagens an einem gewünschten Referenzpunkt. Um die Funktionalität des entworfenen Regelungssystems zu veranschaulichen, werden in dieser Masterarbeit Simulationen und Echtzeit-Experimente unter Berücksichtigung der physikalischen Dämpfung, d.h. der viskosen Reibung, vorgestellt. Die Ergebnisse werden zusätzlich mit einem weiteren energiebasierten Regelungsansatz für das System des inversen Pendels auf einem Wagen in expliziter Euler-Lagrange (EL) Darstellung verglichen.

ET LUX IN TENEBRIS LUCET
MCMXVII

Contents

ET LUX IN TENEBRIS LUCET
MCMXVII

Chapter 1

Introduction

1.1 Motivation

The last decades have revealed an increasing interest in the control of a class of mechanical systems, namely, Underactuated Mechanical Systems (UMSs). These systems are characterized by the fact that they have fewer actuators than Degrees of Freedom (DOF). UMSs are widely used in real-life scenarios, examples of such applications include manufacturing, transportation, aerospace industry, military purposes, robotics, among others, see e.g. [1, 2]. The typical and widely extended control approaches developed for fully-actuated mechanical systems, e.g. [3, 4], cannot be applied directly to UMSs. Therefore, much research focuses on the development of new control techniques and the feasibility of their real-time implementation.

Energy-based control methodology plays a central role in the development of algorithms that exploit the passivity and energy properties of mechanical systems. Those (passivity and energy) refer to the properties of dynamical systems that result useful for their stability and robustness analysis. Here, two essential types of controllers have been developed. The first is an approach similar to the classical Lyapunov-based design method which defines a more general class of energy storage functions, see e.g. [5, 6]. The second is the so-called energy-shaping control approach, first introduced in [7], which *shapes* the system's energy (kinetic plus potential) through feedback providing a closed-loop system that preserves the mechanical structure. Whereas shaping the potential energy (plus damping injection) is enough to stabilize fully-actuated mechanical systems; shaping the kinetic energy is (in most cases) absolutely necessary for the stabilization of UMSs, as

well as to improve their transient response. When dealing with UMSs, the applicability of total energy-shaping is restricted by the so-called matching conditions, i.e., solution of Partial Differential Equations (PDEs). This approach leads to the development of the Interconnection and Damping Assignment Passivity-Based Control (IDA-PBC) method.

In general, there are at least two different representations for Port-Hamiltonian (PH) systems: (i) the explicit representation, where systems are described by Ordinary Differential Equations (ODEs), and (ii) the implicit representation, where systems are described by Differential Algebraic Equations (DAEs). The difference between those representations relies on the consideration of (physical) constraints [8]. So far, there exist many results on the control of UMSs in the explicit formulation and only a few in the implicit representation, see e.g. [9, 10], with only one reported physical implementation, see [11]. Since there are some aspects not yet implemented, the aim of this thesis is the experimental validation of these algorithms in the cart-pole test-bench located at the Control Engineering Group, TU-Ilmenau.

1.2 Literature Review

In order to place this thesis in the appropriate context, we present below a brief overview of the cart-pole system and the control algorithms developed over the last few years.

The cart-pole, or inverted pendulum on a cart, is one of the most common and popular problems in nonlinear control. It is widely used as a benchmark example for nonlinear control, owing to its nonlinear, underactuated and non-minimum phase properties. The motivation for controlling the cart-pole system is vast due to its wide range of applications in balance problems, such as, the control of rockets and the anti-seismic control of buildings [5]. The cart-pole system, as shown in Figure 1.1, consists of a free pendulum (underactuated variable) mounted on a cart (actuated variable) that can be moved linearly along the horizontal axis. In spite of its simple structure, this system is considered, among others, one of the most fundamental benchmarks. The inverted pendulum on a cart posses a stable equilibrium point when the pendulum is at the downward position and an unstable equilibrium point when the pendulum is at the upright vertical position. The main control task considered for the cart-pole system is to swing-up the pendulum from the stable equilibrium to the unstable equilibrium point and then to stabilize the pendulum at the upright vertical position with the cart at some desired (or target) position.

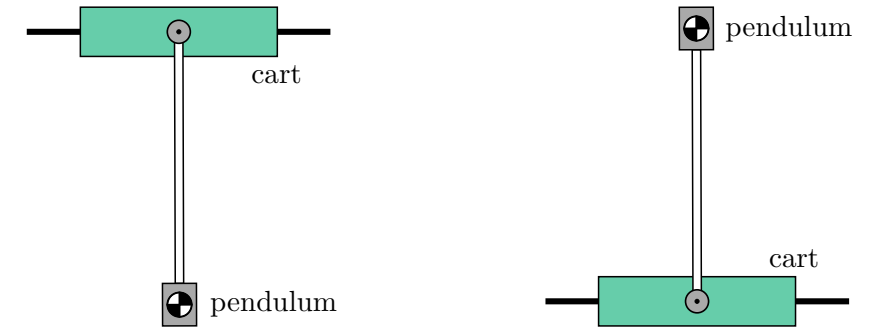

Figure 1.1 – Equilibria of the cart-pole system

Although the cart-pole benchmark is a well-studied control problem; a lot of effort is still put in the design of nonlinear controllers for the swing-up (trajectory tracking) and the (local) stabilization. The solution to this control problem was first reported in [12] and few years later in [13]. The cart-pole system has been taken as a case study in many books to solve the linear optimal control problem, e.g. in [14], and the nonlinear control problem, e.g. in [15]. In the literature, there are many control approaches and those range from the classical linear state feedback [16, 17] to robust control [18], hybrid control [19–21], Sliding Mode Control (SMC) [22–24], backstepping [25], model predictive control [26–28], PID adaptive control [29], feedforward control [30], singular perturbation method [31], energy-shaping [32], immersion and invariance [33], fuzzy logic [34, 35], neural networks [36], among others.

One can address the tracking control problem of a given reference trajectory for the actuated variable(s) of UMSs via the so-called Partial Feedback Linearization (PFL) approach, see [37]. On that basis, a fundamental question arises: Can be further achieved by controlling other variable(s) besides to the actuated variable? This question has been answered by several authors using many different approaches, e.g. in [38–40], where the total mechanical energy stands out as an important variable related to the motion of UMSs, see [41, 42]. The typical energy-based control approach provided by [42, 43] exploits the passivity properties of the system and has been widely applied to some mechanical systems (in explicit representation) with underactuation degree one, among them, the cart-pole benchmark. This approach consists in defining a generalized energy function to stabilize a homoclinic orbit that contains the desired equilibrium, but the equilibrium itself is not stabilized. That is to say, two essential tasks are solved: (i) trajectory planning, i.e., finding a feasible trajectory which connects initial and final states in a given finite time and (ii) trajectory tracking, i.e., finding a feedback control law that drives the tracking error to zero. As far as the cart-pole system is concerned,

several research works have been developed on the basis of this swing-up strategy, see e.g. [44–47].

In the literature, there exist a large number of research papers related to the (local) stabilization control problem using Passivity-Based Control (PBC). We focus on the so-called IDA-PBC technique for (explicit) UMSs, first introduced in [48]. IDA-PBC performs a total energy-shaping assigning a desired (or target) PH structure to the closed-loop in order to regulate the dynamics of a given nonlinear system, e.g. the cart-pole. However, there exists one fundamental limitation. The synthesis of the control law (as well as the equivalent Controlled Lagrangian [49, 50]) requires solving the matching conditions as a result of the energy-shaping process. These matching conditions yield a linear PDE with state-dependent coefficients for the potential energy and a quasi-linear PDE for the kinetic energy. In the last few years, great effort has been devoted to simplify or completely avoid the computation of these PDEs, whose solution is a nontrivial task. Concerning total energy-shaping, several research works with illustration for the cart-pole system have been reported. In [51], it has been proved that the PDEs can be *explicitly solved* with the parameterization of the target dynamics. In [52], the PDE associated with the kinetic energy can be reduced or eliminated under a change of coordinates in the original system with modified target dynamics. In [53, 54], the computation of PDEs are completely avoided through a constructive procedure using new passive outputs; however, it tends to lose the PH structure of the closed-loop.

Recently, the typical energy-based and PBC methodology have been extended to UMSs in implicit PH representation allowing to perform two tasks for the cart-pole system under the implicit framework. (i) *Swing-Up*: Castaños and Gromov in [9] reports an alternative approach for UMSs in implicit PH representation and consists in defining a generalized energy function to address the tracking control problem of homoclinic orbits (limit cycles) thus leading to the formulation of swing-up strategies. Their results are tested on the simple pendulum and the cart-pole system. (ii) *(Local) Stabilization*: Cieza and Reger in [10] introduces a generalization of the IDA-PBC method for UMSs in implicit PH representation and provides an algebraic solution to the IDA-PBC problem (avoiding PDEs). Under this novel approach, they perform the total energy-shaping for the (local) stabilization of the cart-pole system on a inclined plane avoiding the computation of PDEs.

The control techniques mentioned throughout this section are summarized in Table 1.1. It can be observed that there exist numerous control strategies for systems in explicit

Representation	Control strategy	Research paper
Explicit	Bang-bang control	[16, 17]
	Robust control	[18]
	Hybrid control	[19–21]
	Sliding mode control	[22–24]
	Backstepping	[25]
	Model predictive control	[26–28]
	PID adaptive control	[29]
	Feedforward control	[30]
	Singular perturbation	[31]
	Energy-shaping	[32]
	Immersion and invariance	[33]
	Fuzzy logic	[34, 35]
	Neural networks	[36]
	Energy-based control	[41–47]
	Passivity-based control	[51–54]
Implicit	**Energy-based control**	[9]
	Passivity-based control	[10]

Table 1.1 – List of some control strategies applied to the cart-pole

representation. However, the formulation of control techniques for systems in implicit representation is, nowadays, an emerging field.

1.3 Objectives

Design an energy-based control scheme to swing-up and (local) stabilize the cart-pole system modeled in implicit PH representation and perform analytical and experimental validation.

The specific objectives of this work are:

- Design a swing-up controller on the basis of a generalized energy function for the cart-pole system in implicit PH representation and perform the stability analysis.
- Design a (locally) asymptotically stabilizing IDA-PBC for the cart-pole system in implicit PH representation that guarantees optimal (local) transient response.
- Perform simulations and real-time experiments in order to verify the closed-loop performance.

- Compare the results with another control scheme for the cart-pole system in explicit Euler-Lagrange (EL) representation.

1.4 Outline

The content presented in this thesis is organized as follows.

Chapter 2 provides an overview of the theoretical background required for all upcoming chapters. It includes the fundamentals of PBC and briefly recalls the typical IDA-PBC methodology for UMSs in explicit PH representation.

Chapter 3 presents the so-called PID Passivity-Based Control (PID-PBC) technique with total energy-shaping and the typical energy-based control approach using a generalized energy function for UMSs in explicit EL representation.

Chapter 4 deals with the cart-pole system in explicit EL representation and performs the design, analysis and experimental validation of the control algorithms discussed in Chapter 3 with mild modifications to accomplish the tracking of a homoclinic orbit.

Chapter 5 provides a novel IDA-PBC method with total energy-shaping and an alternative approach to the typical energy-based control using a (generalized) admissible energy function for UMSs in implicit PH representation.

Chapter 6 addresses the cart-pole system in implicit PH representation and performs the design, analysis and experimental validation of the control algorithms introduced in Chapter 5 with slight modifications to accomplish the tracking of a homoclinic orbit.

Chapter 7 closes this manuscript with conclusions and future work.

Chapter 2

Theoretical Fundamentals

This chapter is devoted to recall some essential concepts and statements used throughout this thesis. For a general introduction to nonlinear dynamical systems, the reader is referred to the excellent books [15, 55–57]. The chapter is structured as follows. Section 2.1 presents statements about the stability analysis of nonlinear systems, most of the content of this section relies on [5, 6, 15]. Section 2.2 provides definitions about dissipativity and passivity as well as some related statements that are relevant to the remaining sections, most of the content of this section is taken from [58–60]. Section 2.3 presents the theoretical background about PBC with emphasis on the fundamentals of Interconnection and Damping Assignment (IDA), most of the content of this section is based on [57, 61–64]. Section 2.4 briefly discusses the stabilization control problem for UMSs under the typical IDA-PBC approach, for a complete overview over the field the reader is referred to [10, 48, 51, 54], the survey paper [64] and the references within.

2.1 Stability of Nonlinear Systems

This section explores the stability analysis of equilibrium points in the sense of Lyapunov. Lyapunov stability theory plays an important role in systems theory since it provides sufficient conditions for stability and asymptotic stability. Furthermore, an extension of the underlying theory is stated in order to analyze the stability of invariant sets based on the well-known LaSalle's invariance principle.

2.1.1 Preliminaries

Consider the autonomous system

$$\dot{x} = f(x), \qquad x_0 = x(0), \tag{2.1}$$

where $x \in \mathcal{D}$ and $f : \mathcal{D} \to \mathbb{R}^n$ is a locally Lipschitz[1] map from a domain $\mathcal{D} \subset \mathbb{R}^n$ into $\mathbb{R}^n$. The solution of (2.1) starting from $x_0 = x(0) \in \mathcal{D}$ is denoted by $x(t)$, $\forall\, t \geq 0$. Let $x^\star \in \mathcal{D}$ be an equilibrium point of (2.1), which satisfies

$$f(x^\star) = 0.$$

Unless otherwise stated, it is assumed without loss of generality that the equilibrium point is at the origin of $\mathbb{R}^n$, i.e., $x^\star = 0$. For the nonzero case, the equilibrium point can be shifted to the origin via a change of variables, e.g. $\tilde{x} = x - x^\star$.

Definition 2.1 (Lyapunov stability [5])**:** *The equilibrium point $x^\star = 0$ of (2.1) is*

(1) stable if, for each $\varepsilon > 0$, there exists a $\delta = \delta(\varepsilon) > 0$ such that

$$\|x(0)\| < \delta \quad \Rightarrow \quad \|x(t)\| < \varepsilon, \quad \forall\, t \geq 0;$$

(2) unstable if it is not stable;

(3) asymptotically stable if it is stable and δ can be chosen such that

$$\|x(0)\| < \delta \quad \Rightarrow \quad \lim_{t \to \infty} x(t) = 0;$$

(4) exponentially stable if there exist two strictly positive numbers α and λ independent of time and initial conditions such that

$$\|x(0)\| < \delta \quad \Rightarrow \quad \|x(t)\| \leq \alpha \|x(0)\| \exp(-\lambda t), \quad \forall\, t \geq 0;$$

where $\|\cdot\|$ is the Euclidean norm. ■

Under some abuse of notation, it can be said that the system (2.1) is stable (unstable) if $x^\star$ is a stable (unstable) equilibrium point of (2.1). It should be underscored that

[1] Locally Lipschitz means that $\exists\, L > 0$ such that $\|f(x) - f(y)\| \leq L \|x - y\|$, $\forall\, x, y \in \mathcal{D}$.

Definition 2.1 is a local statement since it describes the behavior of a system near an equilibrium point.

2.1.2 Direct Method of Lyapunov

The direct method of Lyapunov, also called the second method of Lyapunov, allows determining the stability of a system without knowing its analytical solution.

Definition 2.2 ((Semi-)Definiteness [5])**:** *Let $\mathcal{D} \subset \mathbb{R}^n$ be a domain containing $x = 0$. A function $V = V(x)$ with $V : \mathcal{D} \to \mathbb{R}$ is called positive (negative) definite, if*

(1) $V(0) = 0$ *and*

(2) $V(x) > 0 \quad (V(x) < 0) \quad \forall\, x \in \mathcal{D} \setminus \{0\}$.

Moreover, if instead of (2)

(3) $V(x) \geq 0 \quad (V(x) \leq 0) \quad \forall\, x \in \mathcal{D} \setminus \{0\}$,

then V is called positive (negative) semi-definite. If neither of the above cases applies to V, then it is said to be indefinite. ■

Definition 2.3 (Lyapunov function [6])**:** *Let $\mathcal{D} \subset \mathbb{R}^n$ be a domain containing $x = 0$. Let $V : \mathcal{D} \to \mathbb{R}$ be a continuously differentiable function. $V(x)$ is called a Lyapunov function if it is positive definite and $\dot{V}(x)$ is negative semi-definite in $\mathcal{D}$.* ■

Theorem 2.1 (Lyapunov's direct method [15])**:** *Let $x^\star = 0$ be an equilibrium point for* (2.1) *and $\mathcal{D} \subset \mathbb{R}^n$ be a domain containing $x^\star = 0$. Let $V : \mathcal{D} \to \mathbb{R}$ be a continuously differentiable function (w.r.t. x), such that, if*

(1) $V(x)$ *is positive definite in $\mathcal{D}$ and*

(2) $\dot{V}(x)$ *is negative semi-definite in $\mathcal{D}$,*

then $x^\star = 0$ is stable. Moreover, if instead of (2)

(3) $\dot{V}(x)$ *is negative definite in $\mathcal{D}$,*

then $x^\star = 0$ is asymptotically stable. ■

Regarding the case that $V(x)$ is positive definite and $\dot{V}(x)$ is negative semi-definite, the following corollary is recalled.

Corollary 2.1 (Barbashin-LaSalle [15])**:** *Let $x^\star = 0$ be an equilibrium point for* (2.1)*. Let $V : \mathcal{D} \to \mathbb{R}$ be a continuously differentiable positive definite function on a domain $\mathcal{D}$ containing the origin $x^\star = 0$, such that $\dot{V}(x) \leq 0$ in $\mathcal{D}$. Let $\mathcal{S} = \{x \in \mathcal{D} \mid \dot{V}(x) = 0\}$ and suppose that no solution can stay identically in $\mathcal{S}$, other than the trivial solution $x(t) \equiv 0$. Then, the origin is asymptotically stable.* ■

Corollary 2.1 is equivalent to Theorem 2.1 when $\dot{V}(x)$ is negative definite, i.e., $\mathcal{S} = \{0\}$. Similar to Definition 2.1, Theorem 2.1 and Corollary 2.1 deal with local stability. Within the scope of this work, global stability is not addressed.

2.1.3 LaSalle's Invariance Principle

LaSalle's theorem can also be used in cases where the system has an equilibrium set, instead of an isolated equilibrium point [15]. Recall the following definitions.

Definition 2.4 (Invariant set [6])**:** *A set $\mathbb{M}$ is said to be invariant set with respect to* (2.1) *if*

$$x(0) \in \mathbb{M} \quad \Rightarrow \quad x(t) \in \mathbb{M}, \tag{2.2}$$

$\forall\, t \in \mathbb{R}$. That is, if a solution $x(t)$ belongs to $\mathbb{M}$ at some time instant, then it belongs to $\mathbb{M}$ for all future and past time. A set $\mathbb{M}$ is said to be a positively invariant set with respect to (2.1) *if* (2.2) *holds $\forall\, t > 0$.* ■

Theorem 2.2 (LaSalle's invariance principle[2] [15])**:** *Let $\Omega \subset \mathcal{D}$ be a compact set that is positively invariant with respect to* (2.1)*. Let $V : \mathcal{D} \to \mathbb{R}$ be a continuously differentiable function such that $\dot{V}(x) \leq 0$ in Ω. Let Γ be the set of all points in Ω where $\dot{V}(x) = 0$. Let $\mathbb{M}$ be the largest invariant set in Γ. Then every solution $x(t)$ starting in Ω approaches $\mathbb{M}$ as $t \to \infty$.* ■

It is noteworthy here that Theorem 2.2 does not require $V(x)$ to be positive definite. For asymptotic stability analysis of an equilibrium point, one can utilize the invariance principle by establishing that the largest invariant set $\mathbb{M}$ is the origin and suppose that no solution can stay identically in $\mathbb{M}$, other than the trivial solution $x \equiv 0$. For stability

[2] Also known as Barbashin-Krasovskii-LaSalle invariance principle.

at an invariant set, define an ε-neighborhood of $\mathbb{M}$ by

$$\mathcal{B}_\varepsilon = \{x \in \mathbb{R}^n \mid \text{dist}(x, \mathbb{M}) < \varepsilon\}, \tag{2.3}$$

where $\text{dist}(x, \mathbb{M})$ is the minimum distance from x to a point p in $\mathbb{M}$, that is,

$$\text{dist}(x, \mathbb{M}) = \inf_{p \in \mathbb{M}} \|x - p\|.$$

It is said that $x(t)$ approaches a set $\mathbb{M}$ as t approaches infinity, if for each $\varepsilon > 0$ there exists $T > 0$, such that

$$\text{dist}(x, \mathbb{M}) < \varepsilon, \quad \forall\, t > T.$$

Definition 2.5 (Stability of an invariant set [6])**:** *Let $\mathbb{M}$ be an invariant set of* (2.1)*. The invariant set $\mathbb{M}$ is*

(1) stable if for each $\varepsilon > 0$ there exists a $\delta > 0$ such that

$$x(0) \in \mathcal{B}_\delta \quad \Rightarrow \quad x(t) \in \mathcal{B}_\varepsilon, \quad \forall\, t \geq 0;$$

(2) unstable if it is not stable;

(3) asymptotically stable if it is stable and $\delta > 0$ can be chosen such that

$$x(0) \in \mathcal{B}_\delta \quad \Rightarrow \quad \lim_{t \to \infty} \text{dist}\big(x(t), \mathbb{M}\big) = 0;$$

where $\mathcal{B}_\varepsilon$ and $\mathcal{B}_\delta$ are given by (2.3)*.* ■

2.1.4 Indirect Method of Lyapunov

The indirect method of Lyapunov, also called the first method of Lyapunov, uses the linearization of a system to determine the local stability of the original system.

Theorem 2.3 (Lyapunov's indirect method [15])**:** *Let $x^\star = 0$ be an equilibrium point of* (2.1)*, where $f : \mathcal{D} \to \mathbb{R}^n$ is continuously differentiable and $\mathcal{D}$ is a neighborhood of the origin. Let*

$$\mathbf{A} = \left.\frac{\partial f(x)}{\partial x}\right|_{x = x^\star},$$

then the equilibrium point is

(1) asymptotically stable if all eigenvalues of $\mathbf{A}$ *are in the open left-half plane or*

(2) unstable if there exists at least one eigenvalue in the open right-half plane. ■

2.2 Dissipativity and Passivity

Dissipativity is a fundamental property of physical systems closely related to the phenomena of loss or dissipation of energy [58]. Dealing with the notion of dissipativity requires the definition of the following functions.

- *Supply rate*, is the rate at which energy flows into the system.
- *Storage function*, is a function that measures the amount of energy that is stored inside the system.

Consider the nonlinear system

$$\begin{aligned} \dot{x} &= f(x,u), \quad x \in \mathcal{X} \subseteq \mathbb{R}^n, \quad u \in \mathcal{U} \subseteq \mathbb{R}^m, \\ y &= h(x,u), \quad y \in \mathcal{Y} \subseteq \mathbb{R}^p, \end{aligned} \tag{2.4}$$

that under $u = 0$ has an equilibrium at $x^\star = 0$, that is, $f(0,0) = 0$. For all initial conditions $x(0) = x_0$ and input functions $u = u(t)$, the solution $x(t) = \varphi(x_0, u(t), t)$, $\forall\, t \geq 0$ is unique. Let $s : \mathcal{U} \times \mathcal{Y} \to \mathbb{R}$ be the supply rate of (2.4), which satisfies $\forall\, x_0 \in \mathcal{X}$ and $\forall\, u(t) \in \mathcal{U}$ the following relationship

$$\int_0^t \left| s(u(\tau), y(\tau)) \right| \mathrm{d}\tau < \infty, \quad \forall\, t \geq 0.$$

Definition 2.6 (Dissipativity [59])**:** *System* (2.4) *is said to be dissipative with respect to the supply rate* s*, if there exists a non-negative storage function* $V(x) \geq 0$*,* $V : \mathcal{X} \to \mathbb{R}^+$*, such that* $\forall\, x_0 \in \mathcal{X}$ *and* $\forall\, u(t) \in \mathcal{U}$ *the integral dissipation inequality*

$$V(x(t)) - V(x_0) \leq \int_0^t s(u(\tau), y(\tau))\, \mathrm{d}\tau \tag{2.5}$$

holds. If the equality remains in (2.5)*, then* (2.4) *is called conservative or lossless.* ■

Remark: If V is continuously differentiable, then (2.5) can be rewritten as the differential dissipation inequality

$$\frac{\partial V(x)}{\partial x} f(x,u) \leq s(u(t), y(t)), \quad \forall\, t \geq 0.$$

Definition 2.7 (Passivity [59])**:** *System* (2.4) *with* $\mathcal{U} = \mathcal{Y} = \mathbb{R}^m$ *is said to be passive if it is dissipative with respect to the supply rate* $s(u, y) = u^\top y$*, and the storage function* $V(x)$ *satisfies* $V(0) = 0$*.* ■

Definition 2.8 (Zero-state observability [60])**:** *System* (2.4) *is said to be Zero-State Observable (ZSO) if no solution of* $\dot{x} = f(x, 0)$ *can stay identically in* $\mathbb{S} = \{x \in \mathbb{R}^n \mid h(x, 0) = 0\}$*, other than the trivial solution* $x(t) \equiv 0$*.* ■

Definition 2.9 (Zero-state detectability [60])**:** *System* (2.4) *is said to be Zero-State Detectable (ZSD) if no solution of* $\dot{x} = f(x, 0)$ *can stay identically in* $\mathbb{S} = \{x \in \mathbb{R}^n \mid h(x, 0) = 0\}$*, other than* $x(t) = 0$ *when* $t \to \infty$*.* ■

Passivity is a structural property derived from the fact that energy is dissipated in physical systems. In essence, a passive system cannot store more energy than is supplied by the environment, i.e., there can be no internal creation of energy. In the context of PBC, Definitions 2.8-2.9 are widely used to prove asymptotic stability.[3]

2.3 Passivity-Based Control

The basis of Passivity-Based Control (PBC) is motivated by recalling the following theorem.

Theorem 2.4 (Passivity and stability [57])**:** *Let the system* (2.4) *be passive with a storage function* $V \in \mathcal{C}^1$ *and* $h(x, u)$ *be* $\mathcal{C}^1$ *in* u *for all* x*. Then the following properties hold:*

(i) If V *is positive definite, then the equilibrium* $x^\star = 0$ *of* (2.4) *with* $u = 0$ *is stable.*

(ii) If (2.4) *is ZSD, then the equilibrium* $x^\star = 0$ *of* (2.4) *with* $u = 0$ *is stable.*

(iii) When there is no throughput, $y = h(x)$*, then the feedback* $u = -y$ *achieves asymptotic stability of* $x^\star = 0$ *if and only if* (2.4) *is ZSD.*

When the storage function V *is radially unbounded, these properties are global.* ■

[3] Clearly, for systems of the form (2.4), the ZSO property implies ZSD, i.e., ZSD is weaker than ZSO.

2.3.1 Port-Hamiltonian Systems

In the literature, Port-Hamiltonian (PH) systems are also referred to as Port-Controlled Hamiltonian with Dissipation (PCHD) systems, e.g. in [59], or Port-Controlled Hamiltonian (PCH) systems, e.g. in [65]. This section focuses on PH systems whose dynamics is described by the standard input-state-output representation.

Consider the PH system of the form[4]

$$\dot{x} = \big[J(x) - R(x)\big]\partial_x^\top H + g(x)u, \tag{2.6a}$$

$$y = g^\top(x)\partial_x^\top H, \tag{2.6b}$$

where $x \in \mathbb{R}^n$ are the states variables. The input $u \in \mathbb{R}^m$ and the output $y \in \mathbb{R}^m$ are conjugated variables, i.e., their product gives a power quantity. The interconnection matrix $J : \mathbb{R}^n \to \mathbb{R}^{n\times n}$ is skew-symmetric $J(x) = -J^\top(x)$, $\forall\, x \in \mathbb{R}^n$, and captures the internal interconnection structure of the system; while the full rank input matrix $g : \mathbb{R}^n \to \mathbb{R}^{n\times m}$ represents the interconnection of the system with its environment. The damping matrix $R : \mathbb{R}^n \to \mathbb{R}^{n\times n}$ is symmetric positive semi-definite $R(x) = R^\top(x) \succeq 0$, $\forall\, x \in \mathbb{R}^n$ and characterizes the energy dissipation. The continuously differentiable Hamiltonian function $H : \mathbb{R}^n \to \mathbb{R}$ represents the total energy stored in the system.

Definition 2.10 (Underactuated system [58])**:** *System* (2.6) *is said to be underactuated if* $\operatorname{rank}(g) < \dim(x)$. ■

Via the skew-symmetry of $J(x)$, we obtain[5]

$$\begin{aligned}\dot{H}(x) &= \frac{\partial H}{\partial x}\Big(\big[J(x) - R(x)\big]\partial_x^\top H + g(x)u\Big)\\ &= -\left(\frac{\partial H}{\partial x}\right) R \left(\frac{\partial H}{\partial x}\right)^\top + y^\top u \quad \leq \quad y^\top u\end{aligned} \tag{2.7}$$

for the rate of change of the system's energy, where (2.7) is non-positive due to $R(x) \succeq 0$. As a consequence, if $H(x)$ is bounded from below,[6] then system (2.6) is passive with non-negative storage function $H(x)$ and the stability of the equilibrium point $x^\star$ follows from Theorem 2.1.

[4] We define the differential operator $\partial_x h = \frac{\partial h}{\partial x}$ and $\partial_x^\top h = \left(\frac{\partial h}{\partial x}\right)^\top$ for any vector or scalar function $h(x)$.

[5] Here, and throughout the rest of the document, the arguments of some functions that have been previously defined will be omitted.

[6] Suppose $H(x)$ is bounded from below, i.e., there exists a constant $c > -\infty$ such that $H(x) \geq c$ or $H(x) - c \geq 0$. Hence, the storage function $H(x)$ is non-negative by adding a constant.

2.3.2 Interconnection and Damping Assignment

The control objective of IDA-PBC is to transform the nominal system (2.6) by means of some state-feedback control law into a target (or desired) PH system[7] with a stable equilibrium point at $x^\star \in \mathbb{R}^n$.

Consider the target PH system

$$\dot{x} = \big[J_d(x) - R_d(x)\big]\partial_x^\top H_d, \tag{2.8}$$

where $J_d(x) = -J_d^\top(x)$ and $R_d(x) = R_d^\top(x) \succeq 0$, $\forall\, x \in \mathbb{R}^n$.

The nominal system (2.6a), with g assumed to be full rank, can be transformed into (2.8) whenever the following matching

$$g(x)u = \big[J_d(x) - R_d(x)\big]\partial_x^\top H_d - \big[J(x) - R(x)\big]\partial_x^\top H$$

is satisfied. The equilibrium point $x^\star$ of the closed-loop system (2.8) is (asymptotically) stable if

(i) the target damping matrix satisfies ($R_d = R_d^\top \succ 0$) $R_d = R_d^\top \succeq 0$ and

(ii) the desired Hamiltonian H_d has an isolated minimum at $x^\star$.

For PH systems of the form (2.6), verifying Definition 2.10, the existence of the left-inverse of g leads to one fundamental limitation, that is, the projected matching equation must be satisfied. Recall the following lemma.

Lemma 2.1 (Existence of the pseudo-inverse [63])**:** *Let $g : \mathbb{R}^n \to \mathbb{R}^{n\times m}$ such that* $\operatorname{rank}(g) = m < n$. *Define $g_\perp \in \mathbb{R}^{(n-m)\times n}$ as the full rank left annihilator of g, i.e., $g_\perp g = 0$. For any $f \in \mathbb{R}^n$ and $u \in \mathbb{R}^m$, then*

$$f + g(x)u = 0 \quad \Leftrightarrow \quad \begin{cases} 0 = g_\perp f \\ u = -(g^\top g)^{-1} g^\top f \end{cases}$$

where $\begin{bmatrix} g_\perp & g^\top \end{bmatrix}^\top$ is full rank. ■

[7] In other words, the PH structure of the closed-loop is preserved.

Proposition 2.1 (Standard IDA-PBC [64])**:** *System* (2.6a)*, with* g *assumed to be full rank and* $\operatorname{rank}(g) < \dim(x)$*, can be transformed into* (2.8) *whenever the following matching condition*

$$0 = g_\perp \left([J_d - R_d] \partial_x^\top H_d - [J - R] \partial_x^\top H \right) \tag{2.9}$$

is satisfied. As a consequence, the uniquely defined control law is given by

$$u = (g^\top g)^{-1} g^\top \left([J_d - R_d] \partial_x^\top H_d - [J - R] \partial_x^\top H \right), \tag{2.10}$$

where $g_\perp(x)$ *is the full rank left-annihilator of* $g(x)$*.* ■

From Proposition 2.1 it follows that in the IDA-PBC design procedure the key step is the solution of (2.9). Hence, to solve the matching condition there are, roughly speaking, three ways to proceed.

(i) *Non-Parameterized IDA-PBC:* Consider $R_d = R_d^\top \succ 0$ and $J_d = -J_d^\top$ both fixed and solve the matching condition (2.9) as a PDE, whose solution defines the admissible storage function H_d.

(ii) *Algebraic IDA-PBC:* Consider H_d fixed, with $x^\star = \arg\min H_d$ an isolated minimum, and solve the algebraic equation (2.9) with respect to R_d, J_d and $g_\perp$.

(iii) *Parameterized IDA-PBC:* The desired storage function H_d is restricted to a certain class, e.g. in mechanical systems H_d equals the sum of kinetic and potential energy. Fixing the structure of H_d yields a new matching condition, which is solved as a PDE.

2.4 IDA-PBC for Explicit UMS

To make this thesis self–contained we briefly recall the typical IDA-PBC [48] for UMSs with no natural damping described in explicit[8] PH representation of the form[9]

$$\begin{bmatrix} \dot{q} \\ \dot{p} \end{bmatrix} = \begin{bmatrix} 0 & I_n \\ -I_n & 0 \end{bmatrix} \begin{bmatrix} \partial_q^\top H \\ \partial_p^\top H \end{bmatrix} + \begin{bmatrix} 0 \\ G(q) \end{bmatrix} u \tag{2.11}$$

[8] Explicit systems are those modeled as ODEs. In the literature the term *explicit* is usually avoided.
[9] Let I_n be the $n \times n$ identity matrix and 0 be a matrix of zeros with appropriate dimension.

with total stored energy[10]

$$H(q,p) = \frac{1}{2}p^\top M^{-1}(q)p + V(q),$$

where $q \in \mathbb{R}^n$ are the explicit generalized coordinates, $p \in \mathbb{R}^n$ are its associated momenta, $u \in \mathbb{R}^m$, with $m \leq n$, are the inputs, $G : \mathbb{R}^n \to \mathbb{R}^{n\times m}$ is the full rank input matrix, $M : \mathbb{R}^n \to \mathbb{R}^{n\times n}$ is the inertia matrix that satisfies $M(q) = M^\top(q) \succ 0$ and $V : \mathbb{R}^n \to \mathbb{R}$ is the potential energy assumed to be bounded from below. The Hamiltonian $H : \mathbb{R}^n \times \mathbb{R}^n \to \mathbb{R}$ equals the energy of the systems, namely, kinetic plus potential.

Definition 2.11 (Explicit UMS [58])**:** *The (explicit) mechanical system* (2.11) *is said to be underactuated if* $\text{rank}(G) < \dim(q)$. ■

The control objective is to transform the nominal system (2.11) by means of some state-feedback control law into a target PH system with a stable equilibrium at the desired point $(q, \dot{q}) = (q^\star, 0)$. Consider the target (or desired) PH system

$$\begin{bmatrix}\dot{q}\\ \dot{p}\end{bmatrix} = \begin{bmatrix}0 & J(q)\\ -J^\top(q) & -W(q,p)\end{bmatrix}\begin{bmatrix}\partial_q^\top H_d\\ \partial_p^\top H_d\end{bmatrix} \tag{2.12}$$

with target energy function

$$H_d(q,p) = \frac{1}{2}p^\top M_d^{-1}(q)p + V_d(q),$$

where $M_d : \mathbb{R}^n \to \mathbb{R}^{n\times n}$ is the target inertia matrix that satisfies $M_d(q) = M_d^\top(q) \succ 0$, $J = M^{-1}(q)M_d(q)$, $V_d : \mathbb{R}^n \to \mathbb{R}$ is the target potential energy, $W : \mathbb{R}^n \times \mathbb{R}^n \to \mathbb{R}^{n\times n}$ is a matrix that extends the scope of the typical IDA-PBC and $H_d : \mathbb{R}^n \times \mathbb{R}^n \to \mathbb{R}$ is the new shaped Hamiltonian.

Proposition 2.2 (Explicit IDA-PBC [10])**:** *System* (2.11) *can be transformed into* (2.12) *whenever the following kinetic and potential matching conditions*

$$G_\perp\Big(\partial_q^\top(M^{-1}p) - J^\top\partial_q^\top(M_d^{-1}p) - 2WM_d^{-1}\Big) = 0, \tag{2.13a}$$

$$G_\perp\Big(\partial_q^\top V - J^\top\partial_q^\top V_d\Big) = 0, \tag{2.13b}$$

[10]From now on, $V(q)$ represents the system's potential energy.

are satisfied. As a consequence, the uniquely defined control law is given by

$$u_{E} = \left(G^{\top}G\right)^{-1}G^{\top}\left(\partial_{q}^{\top}H - J^{\top}\partial_{q}^{\top}H_{d} - W\partial_{p}^{\top}H_{d}\right),$$

where $G_{\perp}$ is the full rank left-annihilator of G and $W(q,p) \coloneqq \frac{1}{2}W_{1}(q,p) + W_{2}(q)$ for W_{1} affine in p. ■

Proposition 2.3 (Explicit stability [10])**:** *Assume that the conditions of* Proposition 2.2 *are satisfied. Then $(q^{\star},0) \in \{(q,\dot{q}) \in \mathbb{R}^{n}\times\mathbb{R}^{n} \mid G_{\perp}\partial_{q}^{\top}H = 0\}$ is a stable equilibrium of the closed-loop system* (2.12) *for any $W_{2} + W_{2}^{\top} \succeq 0$ if $q^{\star} = \arg\min V_{d}$ is an isolated minimum and*

$$p^{\top}M_{d}^{-1}W_{1}M_{d}^{-1}p = 0.$$

Furthermore, if $y_{E} \coloneqq (W_{2} + W_{2}^{\top})^{\frac{1}{2}}M_{d}^{-1}p$ is a detectable output of (2.12)*, then the equilibrium point $(q^{\star},0)$ is asymptotically stable.*[11] ■

Propositions 2.2-2.3 summarize the explicit IDA-PBC methodology for UMSs. The success of IDA-PBC relies on the possibility of solving the matching conditions, where the kinetic matching condition (2.13a) is a non-homogeneous, first order, quasi-linear PDE and the potential matching condition (2.13b) is a linear PDE.

[11] Skew-symmetry of W_{1} is a sufficient, but not necessary, condition for $p^{\top}M_{d}^{-1}W_{1}M_{d}^{-1}p = 0$. We write ${A^{\frac{1}{2}}}^{\top}A^{\frac{1}{2}} = A$ for any square positive definite matrix A.

Chapter 3

Energy-Based Control for Explicit UMS

Energy-shaping for UMSs is a well-established robust design technique [53]. In the typical IDA-PBC approach the feedback control law exists under certain requirements called matching conditions, where the main drawback is to solve the set of nonlinear PDEs. Recent research work has shown that for a class of UMSs the total energy-shaping can be performed without solving PDEs, that is the case of the so-called PID-PBC introduced in [53] and widely extended in [54, 66, 67]. Conversely, an energy-based controller is derived using a generalized energy function and taking advantage of the passivity properties of UMSs. The latter approach is often used for two specific tasks: (i) the stabilization at an isolated equilibrium point and, more recently, (ii) the tracking of homoclinic orbits (limit cycles). This chapter is organized as follows. Section 3.1 presents a truly constructive procedure for the total energy-shaping of a class of UMSs, that does not require the solution of PDEs. The design in [53] proceeds in two steps. First, we perform Partial Feedback Linearization (PFL) and if the Lagrangian structure is preserved then two new passive outputs are immediately identified. Second, the application of a Proportional–Integral–Derivative (PID) controller under a suitable combination of these passive outputs completes the design procedure. Section 3.2 provides the typical energy-based control approach using a more general energy function for UMSs with no class restriction. The latter approach is performed in two stages. First, we analyze the passivity properties of the system and identify its passive output. Second, we define a (generalized) admissible storage function for the stabilization at an energy level-set.

3.1 PID Passivity-Based Control

Consider the UMS whose dynamics is described by the Euler-Lagrange (EL) equations of motion in matrix form

$$M(q)\ddot{q} + C(q,\dot{q})\dot{q} + \partial_q^\top V(q) = G(q)u, \tag{3.1}$$

where $q \in \mathbb{R}^n$ are the (explicit) generalized coordinates, $u \in \mathbb{R}^m$, with $m \leq n$, are the inputs, $M : \mathbb{R}^n \to \mathbb{R}^{n\times n}$ is the inertia matrix that satisfies $M(q) = M^\top(q) \succ 0$, $C(q,\dot{q})\dot{q}$ are the Coriolis and centrifugal forces, with $C : \mathbb{R}^n \times \mathbb{R}^n \to \mathbb{R}^{n\times n}$ built via the Christoffel symbols,[12] $V : \mathbb{R}^n \to \mathbb{R}$ is the potential energy assumed to be bounded from below and $G : \mathbb{R}^n \to \mathbb{R}^{n\times m}$ is the full rank input matrix which verifies the following assumption.

Assumption 3.1: *The input matrix is constant and of the form*

$$G = \begin{bmatrix} 0_{s\times m} \\ I_m \end{bmatrix},$$

where $s \coloneqq n - m$.

To delimit the class of UMSs supported in this approach, and in agreement with Assumption 3.1, the generalized coordinates are partitioned into its underactuated and actuated components as[13] $q = \mathrm{col}(q_u, q_a)$, with $q_u \in \mathbb{R}^s$ and $q_a \in \mathbb{R}^m$. Likewise, the inertia matrix is partitioned as

$$M(q) = \begin{bmatrix} m_{uu}(q) & m_{au}^\top(q) \\ m_{au}(q) & m_{aa}(q) \end{bmatrix},$$

where $m_{uu} : \mathbb{R}^n \to \mathbb{R}^{s\times s}$, $m_{au} : \mathbb{R}^n \to \mathbb{R}^{m\times s}$ and $m_{aa} : \mathbb{R}^n \to \mathbb{R}^{m\times m}$. As done in [53], the class of UMSs is identified imposing the following assumption.

Assumption 3.2:

(a) *The inertia matrix depends only on the underactuated variables* q_u*, i.e.,* $M(q) = M(q_u)$.

(b) *The sub-block matrix* m_{aa} *of the inertia matrix is constant.*

[12] Also known as Christoffel symbols of the First Kind, see [68, p. 201]

[13] Given any scalars or column vectors $a_1, \ldots, a_n$, we write $\mathrm{col}(a_1, \ldots, a_n) = \begin{bmatrix} a_1^\top & \ldots & a_n^\top \end{bmatrix}^\top$.

(c) *There exist functions* $V_a : \mathbb{R}^m \to \mathbb{R}$ *and* $V_u : \mathbb{R}^s \to \mathbb{R}$ *such that the potential energy can be written as*

$$V(q) = V_a(q_a) + V_u(q_u),$$

where $V_u(q_u)$ *is assumed to be bounded from below.*[14]

Problem Formulation: *Find a mapping* $u : \mathbb{R}^n \times \mathbb{R}^n \to \mathbb{R}^m$ *such that the system* (3.1) *in closed-loop with the state-feedback control law* u *has a stable equilibrium at the desired point* $(q, \dot{q}) = (q^\star, 0)$ *with target (or desired) Lyapunov function*

$$H_d(q, \dot{q}) = \frac{1}{2}\dot{q}^\top M_d(q)\dot{q} + V_d(q), \tag{3.2}$$

where $M_d(q) = M_d^\top(q) \succ 0$ *and* $q^\star = \arg\min V_d(q)$ *is an isolated minimum.*

3.1.1 Partial Feedback Linearization

The first stage is the application of a collocated PFL that transforms the system (3.1) into the so-called Spong's Normal Form (SNF).[15]

Proposition 3.1 (Spong's normal form [37])**:** *System* (3.1) *under* Assumption 3.1 *is feedback equivalent to*

$$\begin{aligned} m_{uu}(q)\ddot{q}_u + \begin{bmatrix} I_s & 0_{s\times m} \end{bmatrix} C(q, \dot{q})\dot{q} + \partial_{q_u}^\top V &= -m_{au}^\top(q)\, \upsilon, \\ \ddot{q}_a &= \upsilon. \end{aligned} \tag{3.3}$$

That is, there exist two mappings $\hat{u}_1, \hat{u}_2 : \mathbb{R}^n \times \mathbb{R}^n \to \mathbb{R}^m$ *such that the system* (3.1) *in closed-loop with the state-feedback control law* $u = \hat{u}_1(q, \dot{q})\upsilon + \hat{u}_2(q, \dot{q})$ *takes the form* (3.3).[16] ■

The second stage is to verify if the Lagrangian structure is preserved even for UMSs in SNF representation.

[14] The lower boundedness on $V_u(q_u)$ is introduced in order to deal only with passive outputs (instead of cyclo-passive outputs), see Definition 3.1.

[15] Collocated PFL refers to the global linearization of the active (actuated) variables via an invertible change of control inputs [37].

[16] See [37] for the explicit expression of $\hat{u}_1$ and $\hat{u}_2$.

Proposition 3.2 (Preservation of the Lagrangian structure [53])**:** *Consider the system* (3.3) *fulfilling* Assumption 3.2.

(i) *The system satisfies the EL equations with Lagrangian function*

$$\tilde{L}(q,\dot{q}) = \frac{1}{2}\begin{bmatrix}\dot{q}_u^\top & \dot{q}_a^\top\end{bmatrix}\begin{bmatrix}m_{uu}(q_u) & 0_{s\times m}\\ 0_{m\times s} & I_m\end{bmatrix}\begin{bmatrix}\dot{q}_u\\ \dot{q}_a\end{bmatrix} - V_u(q_u)$$

and input matrix $\tilde{G}(q_u) = \begin{bmatrix}-m_{au}^\top(q_u)\\ I_m\end{bmatrix}$.

(ii) *The system may be rewritten as*

$$\begin{aligned} m_{uu}(q_u)\ddot{q}_u + c_u(q_u,\dot{q}_u)\dot{q}_u + \partial_{q_u}^\top V(q_u) &= -m_{au}^\top(q_u)\,\upsilon \\ \ddot{q}_a &= \upsilon, \end{aligned} \tag{3.4}$$

where the skew-symmetry property $\dot{m}_{uu}(q_u) = c_u(q_u,\dot{q}_u) + c_u^\top(q_u,\dot{q}_u)$ *is satisfied.*

(iii) *The operator* $\upsilon \mapsto \dot{q}_a - m_{au}^\top(q_u)\dot{q}_u$ *is cyclo-passive with storage function*

$$\tilde{H}(q,\dot{q}) = \frac{1}{2}\begin{bmatrix}\dot{q}_u^\top & \dot{q}_a^\top\end{bmatrix}\begin{bmatrix}m_{uu}(q_u) & 0_{s\times m}\\ 0_{m\times s} & I_m\end{bmatrix}\begin{bmatrix}\dot{q}_u\\ \dot{q}_a\end{bmatrix} + V_u(q_u).$$

However, the operator is passive if $V_u(q_u)$ *is bounded from below.* ■

3.1.2 New (Cyclo) Passive Outputs

Definition 3.1 (Cyclo-passivity [59])**:** *System* (2.4) *is said to be cyclo-passive if there exists a differentiable function* $H : \mathcal{X} \to \mathbb{R}^+$ *(called storage function) that satisfies the power balance inequality*

$$\dot{H} \leq y^\top u,$$

when evaluated along the trajectories of (2.4)*. Moreover, if* $H(x)$ *is bounded from below, then* (2.4) *is said to be passive.* ■

The corollary below identifies two new (cyclo) passive outputs for the system (3.4).[17]

[17] From now on, we will consider passive outputs (instead of cyclo-passive) since we assume $V_u(q_u)$ is bounded from below.

Corollary 3.1 (New (cyclo) passive outputs [53])**:** *Consider the UMS* (3.4) *verifying* Assumption 3.2. *Define the (new) input* υ *and the (new) outputs*

$$\begin{aligned} y_u &\coloneqq -m_{au}(q_u)\dot{q}_u, \\ y_a &\coloneqq \dot{q}_a. \end{aligned} \tag{3.5}$$

The operators $\upsilon \mapsto y_u$ *and* $\upsilon \mapsto y_a$ *are (cyclo) passive with storage functions*

$$\begin{aligned} H_u(q_u, \dot{q}_u) &= \frac{1}{2}\dot{q}_u^\top m_{uu}(q_u)\dot{q}_u + V_u(q_u), \\ H_a(\dot{q}_a) &= \frac{1}{2}\dot{q}_a^\top \dot{q}_a, \end{aligned}$$

respectively. The time-derivatives of these functions along the trajectories of (3.4) *verifies* $\dot{H}_u = \upsilon^\top y_u$ *and* $\dot{H}_a = \upsilon^\top y_a$. ■

3.1.3 PID Controller

The controller design is completed adding a PID structure with a suitable weighted sum of the two passive outputs identified in Corollary 3.1. The PID-PBC state-feedback law has the following well-known form

$$k_e\, \upsilon = -\left(K_P\, y_d + K_I \int_0^t y_d(\tau)\, \mathrm{d}\tau + K_D\, \dot{y}_d \right), \tag{3.6}$$

with

$$y_d \coloneqq k_a y_a + k_u y_u, \tag{3.7}$$

where k_e, k_a, $k_u \in \mathbb{R}$ are nonzero constants with $k_a \neq k_u$ and K_P, K_I, $K_D \in \mathbb{R}^{m\times m}$ verifying $K_P \succ 0$ and K_I, $K_D \succeq 0$.

For practical implementation, and to avoid the computation of the integral and derivative term, some lengthy but straightforward calculations shows that (3.6) is equivalent to

$$K(q_u)\, \upsilon = -K_P\, y_d - K_I \int_0^t y_d(\tau)\, \mathrm{d}\tau - S(q, \dot{q}), \tag{3.8}$$

where the mapping $K : \mathbb{R}^s \to \mathbb{R}^{m\times m}$ is given by

$$K(q_u) \coloneqq k_e I_m + k_a K_D + k_u K_D m_{au}(q_u) m_{uu}^{-1}(q_u) m_{au}^\top(q_u), \tag{3.9}$$

and $S : \mathbb{R}^n \times \mathbb{R}^n \to \mathbb{R}^m$ is the globally defined mapping

$$S(q, \dot{q}) \coloneqq k_u K_D \left[-\dot{m}_{au}\dot{q}_u + m_{au} m_{uu}^{-1} (c_u \dot{q}_u + \partial_{q_u} V_u) \right]. \tag{3.10}$$

To compute the integral term, we assume the following integrability assumption.

Assumption 3.3: *There exists a mapping $V_N : \mathbb{R}^s \to \mathbb{R}^m$ such that*

$$\dot{V}_N \coloneqq -m_{au}(q_u)\dot{q}_u. \tag{3.11}$$

That is, $V_N(q_u) = \int_1^0 m_{au}(sq_u)q_u \, \mathrm{d}s + V_N(0)$.

Replacing (3.11) in (3.7) yields $y_d = k_a\dot{q}_a + k_u\dot{V}_N(q_u, \dot{q}_u)$. Clearly, the integral term can be expressed as

$$\int_0^t y_d(\tau) \, \mathrm{d}\tau \coloneqq k_a q_a + k_u V_N(q_u) + \kappa, \tag{3.12}$$

where κ is a constant defined as $\kappa \coloneqq -k_a q_a^\star - k_u V_N(q_u^\star)$ with target values given by $q_u^\star \in \mathbb{R}^s$ and $q_a^\star \in \mathbb{R}^m$.

To ensure that the control law (3.8) is well-defined, the following assumption is imposed.

Assumption 3.4: *Consider the controller tuning gains k_e, k_a, $k_u \in \mathbb{R} \setminus \{0\}$ and K_I, $K_D \in \mathbb{R}^{m\times m}$ verifying K_I, $K_D \succeq 0$ such that the following hold.*

(a) $\det\left[K(q_u)\right] \neq 0, \quad \forall\, q_u \in \mathbb{R}^s$.

(b) *The target inertia matrix*

$$M_d(q_u) \coloneqq \begin{bmatrix} k_e k_u m_{uu}(q_u) + k_u^2 m_{au}^\top(q_u) K_D m_{au}(q_u) & -k_a k_u K_D m_{au}(q_u) \\ -k_a k_u m_{au}^\top(q_u) K_D^\top & k_e k_a I_m + k_a^2 K_D \end{bmatrix} \tag{3.13}$$

is symmetric positive definite; and the target potential energy

$$V_d(q) \coloneqq k_e k_u V_u(q_u) + \frac{1}{2}\left\| k_a q_a + k_u V_N(q_u) + \kappa \right\|_{K_I}^2 \tag{3.14}$$

is proper and verifies $q^\star = \arg\min V_d(q)$ is an isolated minimum.

To analyze the stability of the system (3.4) in closed–loop with the PID-PBC state-feedback law (3.8), and after some calculations, the target (closed-loop) Lyapunov

function (3.2) with (3.13) and (3.14) can be rewritten as follows

$$\begin{aligned} H_d(q,\dot{q}) = k_e\big[k_a H_a(\dot{q}_a) + k_u H_u(q_u,\dot{q}_u)\big] &+ \frac{1}{2}\|k_a y_a + k_u y_u\|^2_{K_D} \\ &+ \frac{1}{2}\|k_a q_a + k_u V_N(q_u) + \kappa\|^2_{K_I}. \end{aligned} \tag{3.15}$$

The time-derivative of (3.15) along the trajectories of (3.4) yields

$$\dot{H}_d = (k_a y_a + k_u y_u)^\top \Big[K(q_u)\upsilon + K_I(k_a q_a + k_u V_N(q_u) + \kappa) + S(q,\dot{q})\Big].$$

Replacing (3.8), with (3.7) and (3.12), in the latter gives

$$\dot{H}_d = -\|k_a y_a + k_u y_u\|^2_{K_P}.$$

Under the Assumption 3.4(b), the target storage function (3.2) is a proper Lyapunov function and the stability is proved invoking Theorem 2.1. Furthermore, if (3.7) is a detectable output of the closed-loop system, then the equilibrium point $(q^\star, 0)$ is asymptotically stable.

This section closes with a proposition that summarizes the development presented above and whose proof also follows from above.

Proposition 3.3 (Explicit PID-PBC)**:** *Consider the UMS* (3.1)*, satisfying* Assumptions 3.1-3.2*, in closed-loop with* $u = \hat{u}_1(q,\dot{q})\upsilon + \hat{u}_2(q,\dot{q})$*, where* υ *is given by* (3.8)*, has a stable equilibrium at the desired point* $(q,\dot{q}) = (q^\star, 0)$ *with (target) Lyapunov function* (3.2) *satisfying* Assumption 3.4*. Furthermore, if* (3.7) *is a detectable output of the closed-loop system, then the equilibrium point is asymptotically stable.* ■

3.2 Classical Energy-Based Control

This section provides the typical energy-based control approach using a more general class of energy function for the control of UMSs in explicit EL representation. This approach is performed in two steps. First, we analyze the passivity properties of the system and identify its passive output. Second, we define a (generalized) admissible storage function for the stabilization at an energy level-set.

3.2.1 Passivity

Consider the UMS (3.1) whose dynamics is described by the EL equations of motion in matrix form. The total mechanical energy of (3.1) is given by

$$E(q,\dot{q}) = \frac{1}{2}\dot{q}^\top M(q)\dot{q} + V(q). \tag{3.16}$$

Taking the time-derivative of (3.16) along the trajectories of (3.1) yields

$$\dot{E}(q,\dot{q}) = \dot{q}^\top G(q)\, u.$$

The operator $u \mapsto y \coloneqq G^\top \dot{q}$ is passive with storage function (3.16).[18]

3.2.2 Controller Design

Since the UMS (3.1) is passive, with input u and output y, then the following assumption is introduced.

Assumption 3.5: *There exists a mapping $z : \mathbb{R}^n \to \mathbb{R}^m$ such that*

$$\left(\frac{\partial\, z(q)}{\partial q}\right)^\top = G(q).$$

That is, there exists a function z such that $\dot{z} \coloneqq y$.

[18] From now on, we will consider a passive system (instead of cyclo-passive) since we assume $E(q,\dot{q})$ is bounded from below.

Problem Formulation: *Find a mapping* $u : \mathbb{R}^n \times \mathbb{R}^n \to \mathbb{R}^m$ *such that the system* (3.1) *in closed-loop with the state-feedback control law* u *achieves*

$$\lim_{t\to\infty} E = E^\star, \qquad \lim_{t\to\infty} y = 0, \qquad \lim_{t\to\infty} f(z) = 0. \tag{3.17}$$

The goal is to stabilize the passive output y *and reach the desired (or target) mechanical energy* $E^\star \in \mathbb{R}$ *which imposes a restriction on the underactuated variables.*

We now recall the standard procedure of the classical energy-based control approach [5,6] for UMSs of the form (3.1). Examine whether there exists a control law to achieve the control objectives in (3.17) via the following (generalized) function[19]

$$U(q,\dot{q}) = \frac{1}{2}k_E\big(E(q,\dot{q}) - E^\star\big)^2 + f(z) + \frac{1}{2}\| y \|^2_{K_V}, \tag{3.18}$$

where $k_E \in \mathbb{R}$ is a positive constant, $K_V \in \mathbb{R}^{m\times m}$ verifies $K_V = K_V^\top \succ 0$ and $f : \mathbb{R}^m \to \mathbb{R}$ such that $f(z) \geq 0$.

Taking the time-derivative of (3.18) along the trajectories of (3.1) yields

$$\dot{U}(q,\dot{q}) = y^\top \Big[k_E\big(E(q,\dot{q}) - E^\star\big)u + \partial_z^\top f + K_V\,\dot{y}\Big].$$

Selecting

$$k_E\big(E(q,\dot{q}) - E^\star\big)u + \partial_z^\top f + K_V\,\dot{y} = -K_\Delta\, y \tag{3.19}$$

for some $K_\Delta \in \mathbb{R}^{m\times m}$, $K_\Delta = K_\Delta^\top \succ 0$, results in

$$\dot{U} = -\| y \|^2_{K_\Delta} \leq 0.$$

Now, it is discussed under what condition the controller u can be obtained from (3.19).

Taking the time-derivative of $y = G^\top \dot{q}$ along the trajectories of (3.1) yields

$$\dot{y} = \Big[G^\top(q)M^{-1}(q)G(q)\Big]u + N_1(q,\dot{q}), \tag{3.20}$$

where $N_1(q,\dot{q}) = \dot{G}^\top\dot{q} - G^\top M^{-1}\big(C\dot{q} + \partial_q^\top V\big)$. Replacing (3.20) into (3.19) gives

$$N_2(q,\dot{q})u = -K_V N_1(q,\dot{q}) - K_\Delta\, y - \partial_z^\top f,$$

[19] According to Definition 2.3, the function U does not necessarily qualify as a Lyapunov candidate function.

such that

$$u = -N_2^{-1}(q,\dot{q})\Big[K_V N_1(q,\dot{q}) + K_\Delta\, y + \partial_z^\top f\Big] \tag{3.21}$$

is free of singularities if

$$\big|N_2(q,\dot{q})\big| \neq 0, \qquad \forall\,(q,\dot{q}), \tag{3.22}$$

where $N_2(q,\dot{q}) = k_E(E - E^\star)I_m + K_V(G^\top M^{-1} G)$.

Lemma 3.1 (Global positive definite condition [43])**:** *If the total mechanical energy E of the system* (3.1) *is bounded from below, then there exists a positive parameter K_V such that N_2 is globally positive definite.* ■

Subsequently, stability can be proved by invoking Theorem 2.2 to analyse the motion of the system (3.1) under the control law (3.21) with the aim of investigating whether the closed-loop solution satisfies the control objectives stated in the problem formulation.

Keep in mind that one application of this approach is to solve the swing-up control problem for the cart-pole system in explicit EL representation.

Chapter 4

Energy-Based Control for Explicit UMS: The Cart-Pole Analysis

This chapter provides the design, stability analysis and experimental validation of the control algorithms discussed in Chapter 3. The well-known benchmark cart-pole system is taken as a case study owing to its nonlinear, underactuated and non-minimum phase properties, which remain a topic of interest in the field of nonlinear control systems. The design of the nonlinear control scheme has been carried out on the basis of the explicit EL representation of the cart-pole system in SNF. This chapter is organized as follows. Section 4.1 describes the test-bench used in this work. Section 4.2 presents the standard EL equations of motion for the cart-pole system and its formulation in SNF. Section 4.3 performs the design of a swing-up controller based on the classical energy-based control approach with mild modifications for the cart-pole system in SNF. The effectiveness of the nonlinear controller is verified by simulations and real-time experiments. Section 4.4 performs the design of a (local) stabilizing controller under the so-called PID-PBC methodology, as well as the formulation of a novel approach to ensure an optimal (local) transient response. The effectiveness of the nonlinear controller is verified by simulations and real-time experiments. Section 4.5 describes the overall (explicit) control strategy for the cart-pole system in SNF. The chosen scheme is based on a two-stage control strategy, such that one controller will swing-up the pendulum and another will (locally) stabilize it. All numerical simulations presented in the following were performed using MATLAB®/ Simulink (R2018a) platform.

4.1 Physical Setup

The cart-pole system consist of a rotating single-arm pendulum whose pivot point is mounted on a cart, which can move linearly along the horizontal axis. The pendulum is free to swing about its pivot point and has no direct control actuation. The schematic of the test-bench used to perform real-time experiments is depicted in Figure 4.1.

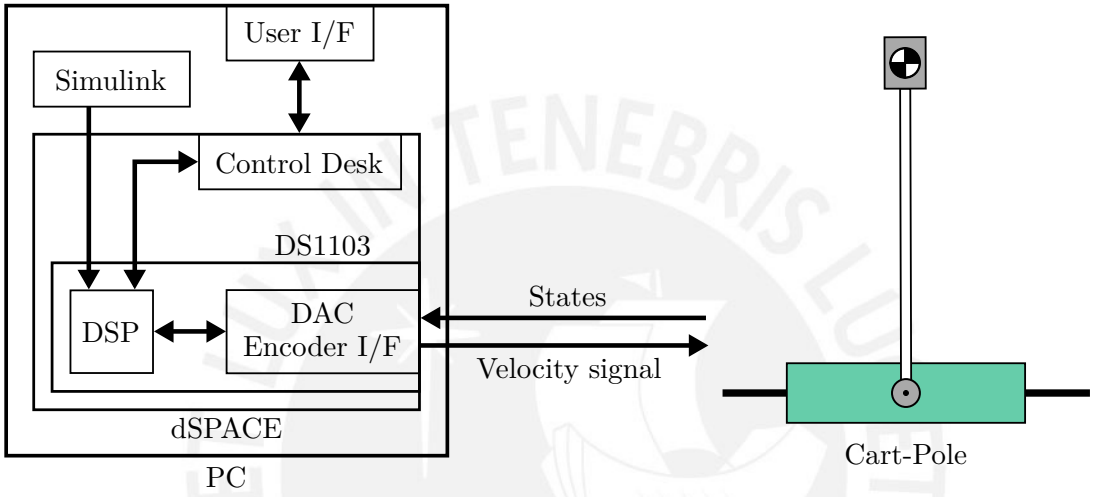

Figure 4.1 – Schematic of the experimental control system

There exist two options to control the cart-pole system: (i) via an inner velocity loop or (ii) via an inner current loop, which may be mapped to force control. Nevertheless, dealing with the inner current loop involves knowing the values of more system parameters like masses, inertias, gear features, frictions, among others. To avoid these

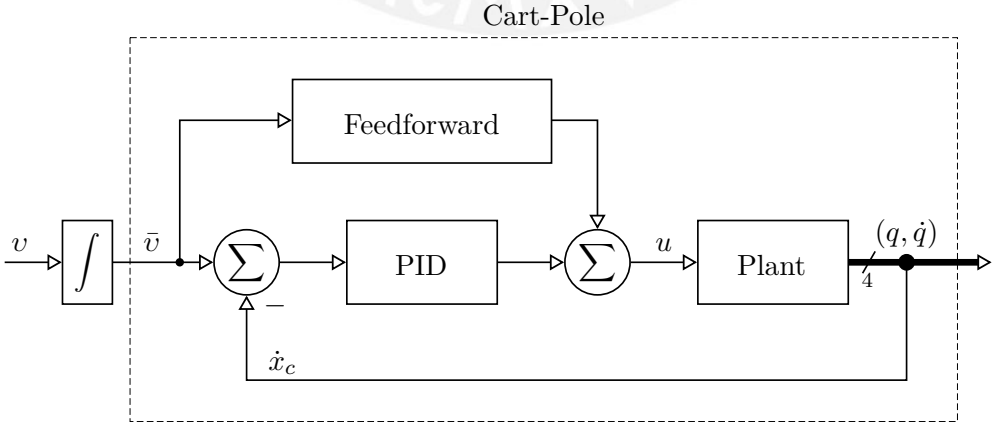

Figure 4.2 – Block diagram of the cart-pole with inner velocity loop

cumbersome parameters, which most likely involve an exhaustive (non-free of error) system identification, we decided to use the inner velocity loop. This inner loop with an integrator in the input can be approximated to the cart-pole system in SNF.

Figure 4.2 depicts the block diagram of the physical setup with the inner velocity loop. The inner loop consists of the plant with a PID + Feedforward controller, where u is the input of the plant and $(q, \dot{q})$ are the outputs (states). The (real) input $\bar{v}$ represents the desired (or target) cart velocity and the outputs are measured by encoders allowing full-state feedback. Note that the virtual input v represents the desired cart acceleration and the outputs denote the generalized coordinates in explicit representation.

Figure 4.3 displays the physical setup, located at laboratory of the Control Engineering Group (Fachgebiet Regelungstechnik), Department of Computer Science and Automation, TU Ilmenau.

Figure 4.3 – Cart-pole system at TU-Ilmenau

The parameter values of the cart-pole system are shown in Table 4.1.

Parameter	Description	Value
l	Length of the pendulum	$0.484\,\mathrm{m}$
g_r	Gravitational acceleration	$9.81\,\mathrm{m/s^2}$
r_1	Viscous friction in the joint	$0.0276\,\mathrm{N\,m\,s/rad}$

Table 4.1 – Cart-pole system parameter values

4.2 Model Derivation

The mathematical (explicit) model of the cart-pole system as shown in Figure 4.4 is derived via the Euler-Lagrange formulation. Consider the cart-pole system satisfying the following ideal assumptions.

- The pendulum is a point mass located at the top of the pole.
- There exists no Coulomb friction.

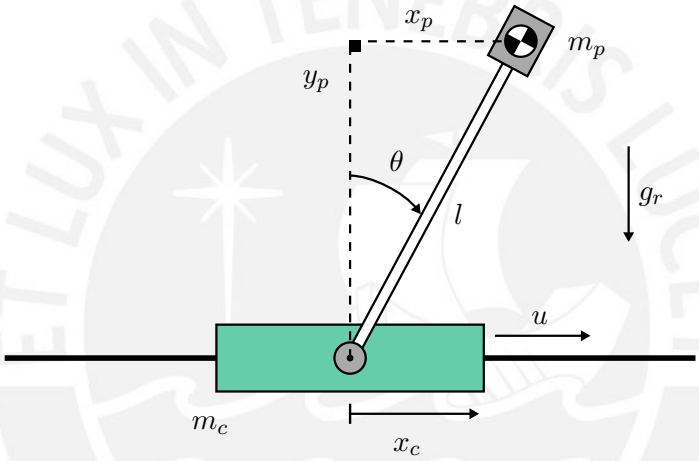

Figure 4.4 – Cart-pole system diagram

The parameters of the cart-pole system are shown in Table 4.2.

Parameter	Description	Units
θ	Angle with respect to the vertical axis	rad
x_c	Cart position	m
u	Force applied on the cart	N
m_p	Mass of the pendulum	kg
m_c	Mass of the cart	kg
l	Length of the pendulum	m
g_r	Gravitational acceleration	$\mathrm{m/s^2}$
r_1	Viscous friction in the joint	N m s/rad
r_2	Viscous friction in the rail	N s/m

Table 4.2 – Cart-pole system parameters

For a complete overview of the model derivation, the reader is referred to [5, p. 25]. The EL equations of motion for the cart-pole system can be written in the standard form as

$$m_p l^2 \ddot{\theta} + m_p l \cos\theta \ddot{x}_c - m_p g_r l \sin\theta = -r_1 \dot{\theta}, \tag{4.1a}$$

$$(m_c + m_p)\, \ddot{x}_c + m_p l \cos\theta \ddot{\theta} - m_p l \sin\theta \dot{\theta}^2 = u - r_2 \dot{x}_c. \tag{4.1b}$$

It is clear that the system (4.1) verifies Assumption 3.1 with input matrix $G_u = \mathrm{col}(0, 1)$. Notice that equations (4.1a) and (4.1b) represent the standard dynamics of the cart-pole system and require exact knowledge of the system parameters.

According to Section 4.1, it is required that the standard system takes the so-called SNF. As stated in Proposition 3.1, we can transform (4.1) into

$$l^2 \ddot{\theta} - g_r l \sin\theta = -l \cos\theta \upsilon - r_1 \dot{\theta}, \tag{4.2a}$$

$$\ddot{x}_c = \upsilon, \tag{4.2b}$$

where $q = \mathrm{col}(\theta, x_c) \in \mathbb{R}^2$, $n = 2$, are the generalized coordinates and $\upsilon \in \mathbb{R}$, $m = 1$, is the new input which directly commands the cart acceleration. The inertia matrix, potential energy and input vector are now given by

$$M(q) = \begin{bmatrix} l^2 & 0 \\ 0 & 1 \end{bmatrix}, \qquad V(q) = g_r l(\cos\theta - 1) \quad \text{and} \quad G(q) = \begin{bmatrix} -l\cos\theta \\ 1 \end{bmatrix}, \tag{4.3}$$

respectively. The potential energy has been initially chosen to be zero at the origin, i.e. $V(0) = 0$, and is clearly bounded from below. Due to PFL, the mass of the cart, the mass of the pendulum and the viscous friction between the cart and the rail have no effect on the new dynamics (4.2).

For unforced mechanical systems, that is $\upsilon = 0$, the equilibrium points are found via

$$\frac{\partial V(q)}{\partial q} = 0 \qquad \Rightarrow \qquad -g_r l \sin\theta = 0.$$

System (4.2) has a subset of infinite equilibrium points, where

- $\theta = \pi \pmod{2\pi}$, $\dot{\theta} = 0$, $x_c = x_c^\star$ and $\dot{x}_c = 0$ are the stable equilibrium points; and
- $\theta = 0 \pmod{2\pi}$, $\dot{\theta} = 0$, $x_c = x_c^\star$ and $\dot{x}_c = 0$ are the unstable equilibrium points,

with $x_c^\star$ set as an arbitrary target value for the cart position.[20]

[20] For the problem to be well-posed, we establish later that $\theta \in [0, 2\pi[$. See Section 4.3.3.

4.3 Explicit Swing-Up Controller

This section deals with the tracking of homoclinic orbits (limit cycles) that contains the desired (unstable) equilibrium of the system. Consider an ideal cart-pole system (massless bar) in SNF given by (4.2) and assume there is no friction, i.e., $r_1 = 0$.

Problem Formulation: *Find a mapping* $\upsilon : \mathbb{R}^2 \times \mathbb{R}^2 \to \mathbb{R}$ *such that the trajectories of the pendulum can be brought into a homoclinic orbit (limit cycle) reaching the desired energy level-set* $\bar{E} \to \bar{E}^\star$ *and holding the cart stable at the target position* $x_c \to x_c^\star$ *with* $\dot{x}_c \to 0$.

Under the design procedure described in Section 3.2, we proceed to analyze the passivity properties of the system. The mechanical energy $E : \mathbb{R}^2 \times \mathbb{R}^2 \to \mathbb{R}$ is built using (4.3) and takes the form

$$E(q, \dot{q}) = \frac{1}{2}\dot{q}^\top M(q)\dot{q} + V(q). \tag{4.4}$$

Taking the time-derivative of (4.4) along the trajectories of the system (4.2) yields $\dot{E} = \dot{q}^\top G\upsilon$. The operator $\upsilon \mapsto y := G^\top \dot{q}$ is passive with storage function (4.4).

Following Section 3.2, we can synthesize a control law but the requirements of the *problem formulation* are not met because the system (4.2) is passive with a combined output of actuated and underactuated variables, i.e., $y = -l\cos\theta\dot{\theta} + \dot{x}_c$. Therefore, we introduce a mild modification in order to stabilize the cart position x_c instead of y.

4.3.1 New Energy Function

This section focuses on finding a new energy function $\bar{E} = E + E_\mu$, which allows to fulfill the requirements of the *problem formulation*.[21]

Let $\bar{E} : \mathbb{R}^2 \times \mathbb{R}^2 \to \mathbb{R}$ be the new (open-loop) energy function defined as

$$\bar{E}(q, \dot{q}) = \frac{1}{2}\dot{q}^\top \bar{M}(q)\dot{q} + V(q), \tag{4.5}$$

where

$$\bar{M}(q) = \begin{bmatrix} l^2 & l\cos\theta \\ l\cos\theta & k_c \end{bmatrix}, \qquad V(q) = g_r l\,(\cos\theta - 1)$$

[21] We define $E_\mu : \mathbb{R}^2 \times \mathbb{R}^2 \to \mathbb{R}$ as $E_\mu(q, \dot{q}) := l\cos\theta\dot{\theta}\dot{x}_c + \frac{1}{2}(k_c - 1)\dot{x}_c^2$.

and $k_c \in \mathbb{R}$ is a strictly positive constant. Clearly, $\bar{M}(q) = \bar{M}^\top(q) \succ 0$ if and only if $k_c > 1$. The new energy function $\bar{E}$, which is slightly different from the original mechanical energy E, takes similarly a constant value for each equilibrium point, i.e.,

- $\bar{E}(q, \dot{q}) = 0$ at the unstable equilibrium points and
- $\bar{E}(q, \dot{q}) = -2g_r l$ at the stable equilibrium points.

4.3.2 Stabilization around the Homoclinic Orbit

Definition 4.1 (Homoclinic Orbit [5])**:** *A homoclinic orbit is a single orbit where a stable manifold and an unstable manifold intersect. This orbit leaves the saddle point in one direction, and returns in another direction. Eventually, this orbit converges to the same saddle point.* ■

Let us verify that the new energy (4.5) is a suitable function for the controller design. In view of (4.5), if the system (4.2) reaches $\bar{E} = 0$ and $\dot{x}_c = 0$, then

$$\frac{1}{2} l^2 \dot{\theta}^2 = g_r l \, (1 - \cos\theta) \tag{4.6}$$

represents a particular trajectory that corresponds to a homoclinic orbit, where $\dot{\theta} = 0$ only when $\theta = 0$. In this particular case, the pendulum swings until it reaches its unstable equilibrium point, i.e, $(\theta, \dot{\theta}) = (0, 0)$. In general, if the system can be brought to the homoclinic orbit (4.6), then the task of swinging-up the pendulum has been solved. This means that the pendulum will eventually get close to its unstable equilibrium point if it follows the homoclinic orbit.

Remark: If $\bar{E} > 0$ and $\dot{x}_c = 0$, then $\dot{\theta}^2 > 0$ when $\theta = 0$. In other words, when the pendulum reaches $\theta = 0$, it will do so with angular velocity $\dot{\theta} \neq 0$.

Based on (4.5), a new controller is derived in order to approach the trajectories of the pendulum into the homoclinic orbit (4.6). Define the target storage function as[22]

$$U(q, \dot{q}) = \frac{1}{2} k_E (\bar{E} - \bar{E}^\star)^2 + \frac{1}{2} k_x (x_c - x_c^\star)^2 + \frac{1}{2} K_V \, \dot{x}_c^2, \tag{4.7}$$

[22] Also known as (generalized) admissible energy function or (generalized) admissible storage function.

where k_E, k_x, $K_V \in \mathbb{R}$ are strictly positive constants, $x_c^\star \in \mathbb{R}$ is the target cart position and $\bar{E}^\star \in \mathbb{R}$ is the non-negative target energy fixed as $\bar{E}^\star = 0$.

Taking the time-derivative of (4.7) along the trajectories of (4.2) yields

$$\dot{U}(q,\dot{q}) = \dot{x}_c\Big[\big[k_E(\bar{E}-\bar{E}^\star)\beta + K_V\big]\upsilon + k_E(\bar{E}-\bar{E}^\star)\alpha + k_x(x_c - x_c^\star)\Big], \tag{4.8}$$

where $\alpha(q,\dot{q}) = \sin\theta(g_r\cos\theta - l\dot{\theta}^2)$ and $\beta(q) = k_c - (\cos\theta)^2$. Clearly, $\beta(q) > 0$ if and only if $k_c > 1$.

One can choose υ such that

$$\Big[k_E(\bar{E}-\bar{E}^\star)\beta + K_V\Big]\upsilon + k_E(\bar{E}-\bar{E}^\star)\alpha + k_x(x_c - x_c^\star) = -K_\Delta\dot{x}_c \tag{4.9}$$

for some strictly positive constant $K_\Delta \in \mathbb{R}$, which leads to

$$\dot{U}(q,\dot{q}) = -K_\Delta\dot{x}_c^2. \tag{4.10}$$

Moreover, the singularities in (4.9) are avoided provided that

$$\Big|k_E(\bar{E}-\bar{E}^\star)\beta + K_V\Big| \neq 0, \qquad \forall\,(q,\dot{q}).$$

According to Lemma 3.1, the expression above holds if the following lower bound constraint for K_V is fulfilled

$$K_V > (2g_r l + \bar{E}^\star)k_E \max_\theta(\beta) \quad \Rightarrow \quad K_V > (2g_r l + \bar{E}^\star)k_E k_c. \tag{4.11}$$

Now, the control law υ can be rewritten from (4.9) as

$$\upsilon(q,\dot{q}) = -\frac{K_\Delta\dot{x}_c + k_E(\bar{E}-\bar{E}^\star)\alpha + k_x(x_c - x_c^\star)}{k_E(\bar{E}-\bar{E}^\star)\beta + K_V}. \tag{4.12}$$

4.3.3 Stability Analysis

In view of (4.10) is negative semi-definite and the homoclinic orbit is not an isolated equilibrium point, the stability analysis will be performed based on LaSalle's invariance principle, see Theorem 2.2.[23] Under some abuse of notation, we define $\theta \in \mathbb{S}$, i.e.,

[23] LaSalle's invariance principle can be used when, instead of an isolated equilibrium point, the system has an equilibrium set [15].

$\theta \in [0, 2\pi[\simeq \mathbb{S}$.[24] Since U in (4.7) is a non-increasing function, see (4.10), every solution of the system (4.2) in closed-loop with (4.12) starts in Ω and remains in Ω for all $t \geq 0$. The set Ω is defined as

$$\Omega = \Big\{(q, \dot{q}) \in \mathbb{S} \times \mathbb{R}^2 \mid U(q, \dot{q}) \leq c\Big\},$$

where c is an appropriate positive constant, such that Ω is closed and bounded. Let Γ be the set of all points in Ω such that $\dot{U} = 0$. The set Γ is defined as

$$\Gamma = \Big\{(q, \dot{q}) \in \Omega \mid \dot{U} = 0\Big\}.$$

Let $\mathbb{M}$ be the largest invariant set in Γ. Via LaSalle's theorem every solution starting in Ω approaches $\mathbb{M}$ as $t \to \infty$.

Since $\dot{U} = 0$ holds identically in Γ. From (4.10), if $\dot{U} = 0$, then $\dot{x}_c = 0$, $U = \text{const.}$, $x_c = \text{const.}$ and $\ddot{x}_c = \upsilon = 0$ in Γ. Using (4.7), it is clear that $\bar{E} = \text{const.}$ in Γ. The resulting constants can be summarized as

$$\bar{E} = \text{const.}, \qquad x_c = \text{const.}, \qquad \dot{x}_c = 0, \qquad \upsilon = 0. \tag{4.13}$$

From (4.12) and (4.13), it follows that the control law has been chosen such that

$$0 = k_E(\bar{E} - \bar{E}^\star)\alpha + k_x(x_c - x_c^\star). \tag{4.14}$$

Now, it is evident that $(\bar{E} - \bar{E}^\star)\alpha$ must be constant in Γ. Since $\bar{E}$ is also constant and $\bar{E}^\star$ is fixed to be 0, two cases are discussed below.

- $\underline{\bar{E} = 0}$: This is the simplest case. Here, $x_c = x_c^\star$. Recall that $\bar{E} = 0$ means that the trajectories of the pendulum are in the homoclinic orbit (4.6).

- $\underline{\bar{E} \neq 0}$: In this case, the only solution for α is to be a constant in Γ. Besides, using (4.5) we can rewrite α as $\alpha(\theta) = \sin\theta\left[3g_r\cos\theta - \bar{d}\right]$, where $\bar{d} = 2(E + g_r l)/l$. Analyzing (4.2), shows that if $\upsilon = 0$, then the cart-pole dynamics (4.2) is reduced to a simple pendulum. Therefore, if and only if the pendulum gets stuck at the equilibrium points, then α is constant and equal to 0. Hence, $x_c = x_c^\star$. Note that, at the unstable equilibrium point it is implied that $\bar{E} = 0$, which is a contradiction. The other equilibrium point may be avoided by including the following assumption.

[24] We assume $\theta \in \mathbb{S}$ instead of $\theta \in \mathbb{R}$, but *strictly speaking* $\theta \notin \mathbb{S}$ because $\mathbb{S} \subset \mathbb{R}^2$ denotes the unit circle. Indeed, we have $\bar{\mathbb{S}} = [0, 2\pi[$ is homeomorphic (or diffeomorphic) to $\mathbb{S}$ so that $\theta \in \bar{\mathbb{S}}$, i.e., $\theta \in [0, 2\pi[\simeq \mathbb{S}$. For further details about the discontinuity problem, see [6].

Assumption 4.1: *To avoid the pendulum get stuck at the downward (stable) position, it is imposed that the new energy* $\bar{E}(q,\dot{q}) > -2g_r l$*, for all* $(q,\dot{q})$*.*

Assumption 4.1 implies that a nonzero initial value must be assigned to the new kinetic energy in (4.5), i.e., $\theta(0) = \pi$ (downward pendulum position) is admissible if and only if $\dot{\theta}(0) \neq 0$. From the above, it is concluded that (4.14) is fulfilled only when $\bar{E} = 0$, $x_c = x_c^\star$ and $\dot{x}_c = 0$. Finally, the largest invariant set $\mathbb{M}$ in Γ is given by

$$\mathbb{M} = \Big\{(q,\dot{q}) \in \Omega \mid \dot{\theta}^2 = 2g_r(1-\cos\theta)/l,\ x_c = x_c^\star,\ \dot{x}_c = 0\Big\}.$$

From LaSalle's invariance principle, it has been proved that the control law (4.12) bring the system (4.2) for any $(q,\dot{q}) \in \Omega$ to the invariant set $\mathbb{M}$. Figure 4.5 depicts the level set of $U(\theta.\dot{\theta})$, the homoclinic reference for the set $\mathbb{M}$ is shown in red and the subset $\theta \in \mathbb{S}$ is restricted by dashed lines in black. Recall that, Theorem 2.2 refers to those sets Ω that are compact (closed and bounded), nothing can be said for those sets Ω that are not compact.

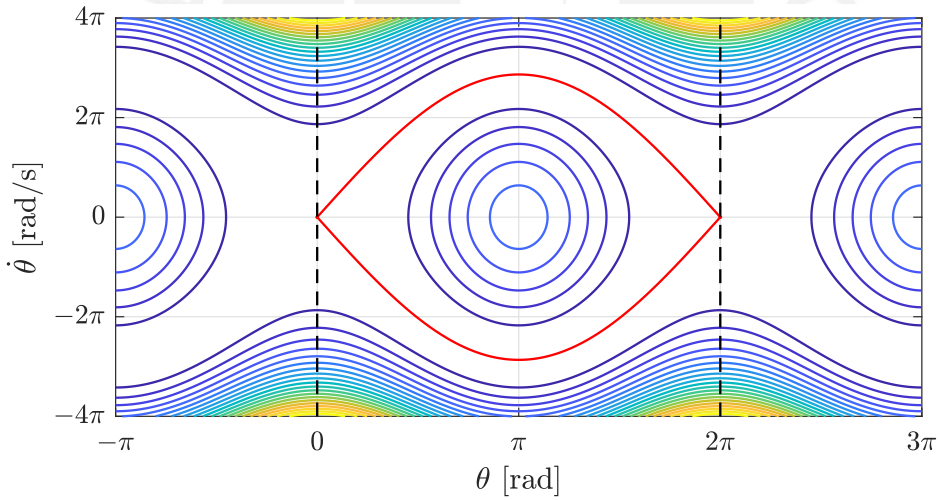

Figure 4.5 – Level set of $U(\theta,\dot{\theta})$

4.3.4 Damping Injection

In order to improve convergence (physically motivated), with no compromising stability, the well-known damping injection method can be used. The control input υ is set as

$$\upsilon \coloneqq \upsilon + \hat{\upsilon}. \tag{4.15}$$

To prove the passivity of the closed-loop it suffices to compute (4.8) with (4.15). Solving for $\hat{\upsilon}$ yields

$$\dot{U}(q,\dot{q}) = \dot{x}_c\Big[k_E(\bar{E}-\bar{E}^\star)\beta + K_V\Big]\hat{\upsilon},$$

Define the input $\hat{\upsilon}$ and the output $\hat{y} \coloneqq \dot{x}_c\Big[k_E(\bar{E}-\bar{E}^\star)\beta + K_V\Big]$. The operator $\hat{\upsilon} \mapsto \hat{y}$ is passive with storage function (4.7).

Notice that $\dot{x}_c\,\hat{y} \geq 0$, then the damping injection can be formulated as $\hat{\upsilon} = -k_y\,\dot{x}_c$, where $k_y \in \mathbb{R}$ is a strictly positive constant.

4.3.5 Simulation Results

Consider the parameters of the cart-pole system from Table 4.1, with no friction, i.e., $r_1 = 0$. The tuning gains are chosen as shown in Table 4.3. These gains satisfy the inequality in (4.11). The desired cart position is set to $x_c^\star = 0$ with target energy $\bar{E}^\star = 0$. The objective is to swing-up the pendulum from the initial states $\theta(0) = \pi$, $\dot{\theta}(0) = \pi/180$, $x_c(0) = 0$ and $\dot{x}_c(0) = 0$. These initial conditions satisfy Assumption 4.1.

k_c	k_E	k_x	K_V	K_Δ	k_y
2	1	100	20	0	4

Table 4.3 – Parameters of the explicit swing-up controller

Figure 4.6 depicts the phase portrait of $(\theta,\dot{\theta})$ and the time responses of θ, x_c, $\dot{x}_c$, U and $\bar{E}-\bar{E}^\star$ under the swing-up control problem. Simulations show that the controller (4.12) brings the trajectories of the pendulum into the homoclinic orbit (4.6) fulfilling the requirements stated in the *problem formulation*, i.e., $\bar{E} \to \bar{E}^\star$, $x_c \to x_c^\star$ and $\dot{x}_c \to 0$.

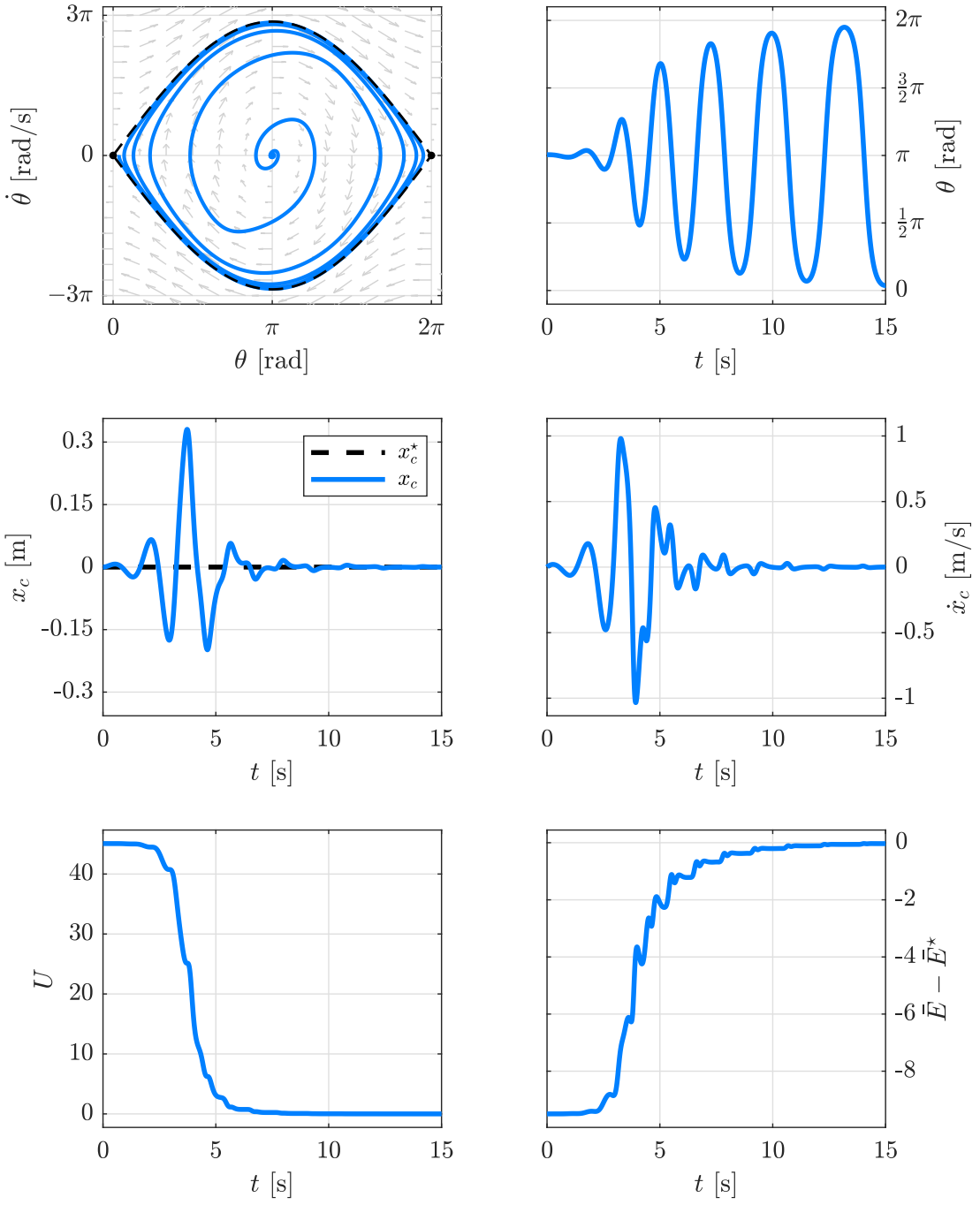

Figure 4.6 – Simulation results with no damping

4.3.6 Experimental Validation

Real-time experiments are contrasted with simulations including damping in the cart-pole dynamics. Consider the parameters of the cart-pole system from Table 4.1, including

friction, and the controller parameters from Table 4.3. The target values and initial conditions are the same as in the previous section. The first row of Figure 4.7 depicts the phase portrait of $(\theta, \dot{\theta})$ for a given $\bar{E}^\star = 0$, where unmodeled dynamics, e.g. friction, impede the increase in amplitude of θ and $\dot{\theta}$. To reduce the effect of the friction and other

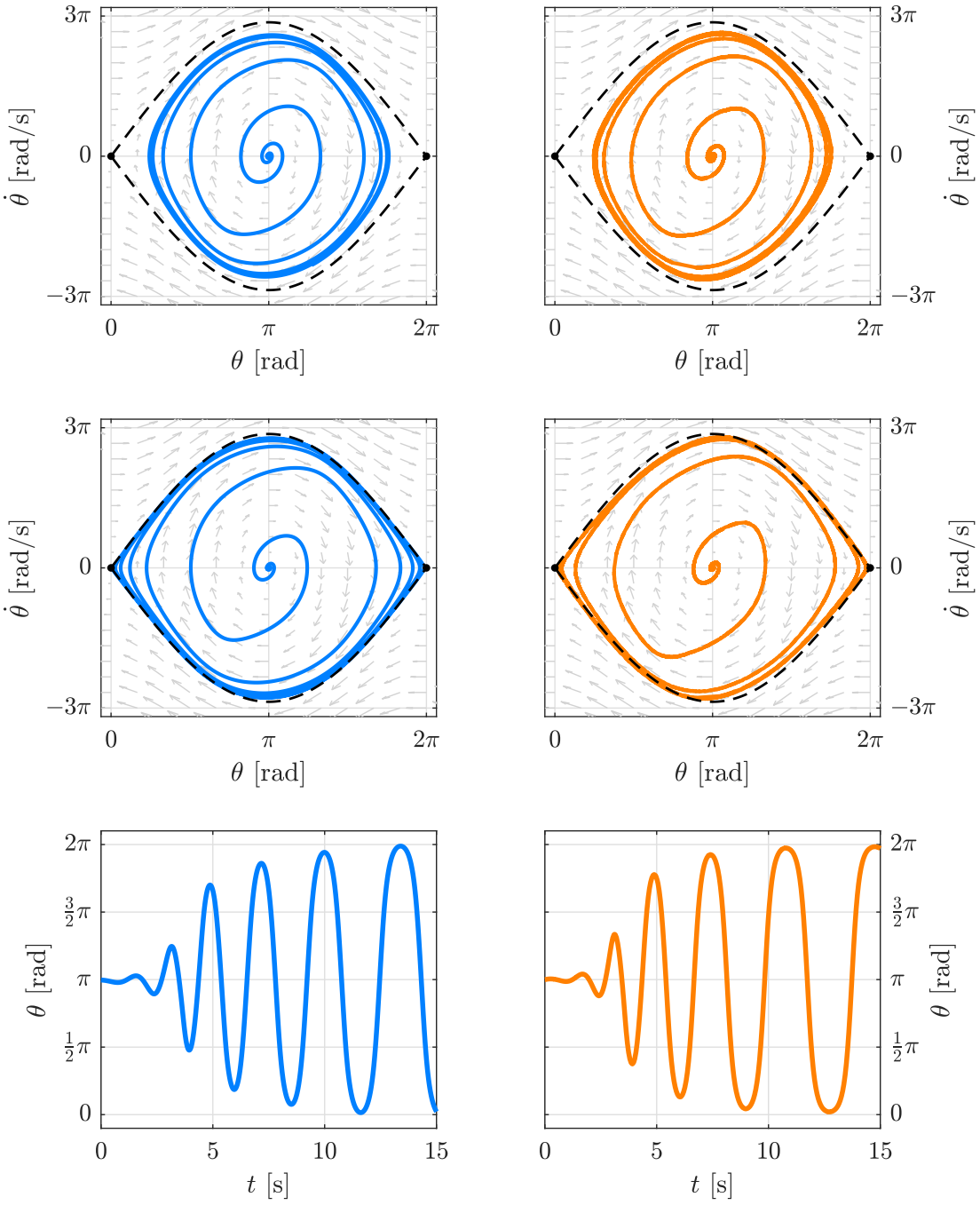

Figure 4.7 – Simulation (blue) and experimental (red) results with damping

unmodeled dynamics, we study the effectiveness of positive energy $\bar{E}(q, \dot{q})$. According to [6, 41], a good practical approach is to choose a target energy $\bar{E}^\star > 0$ such that the trajectories of the pendulum reach the homoclinic orbit (4.6).

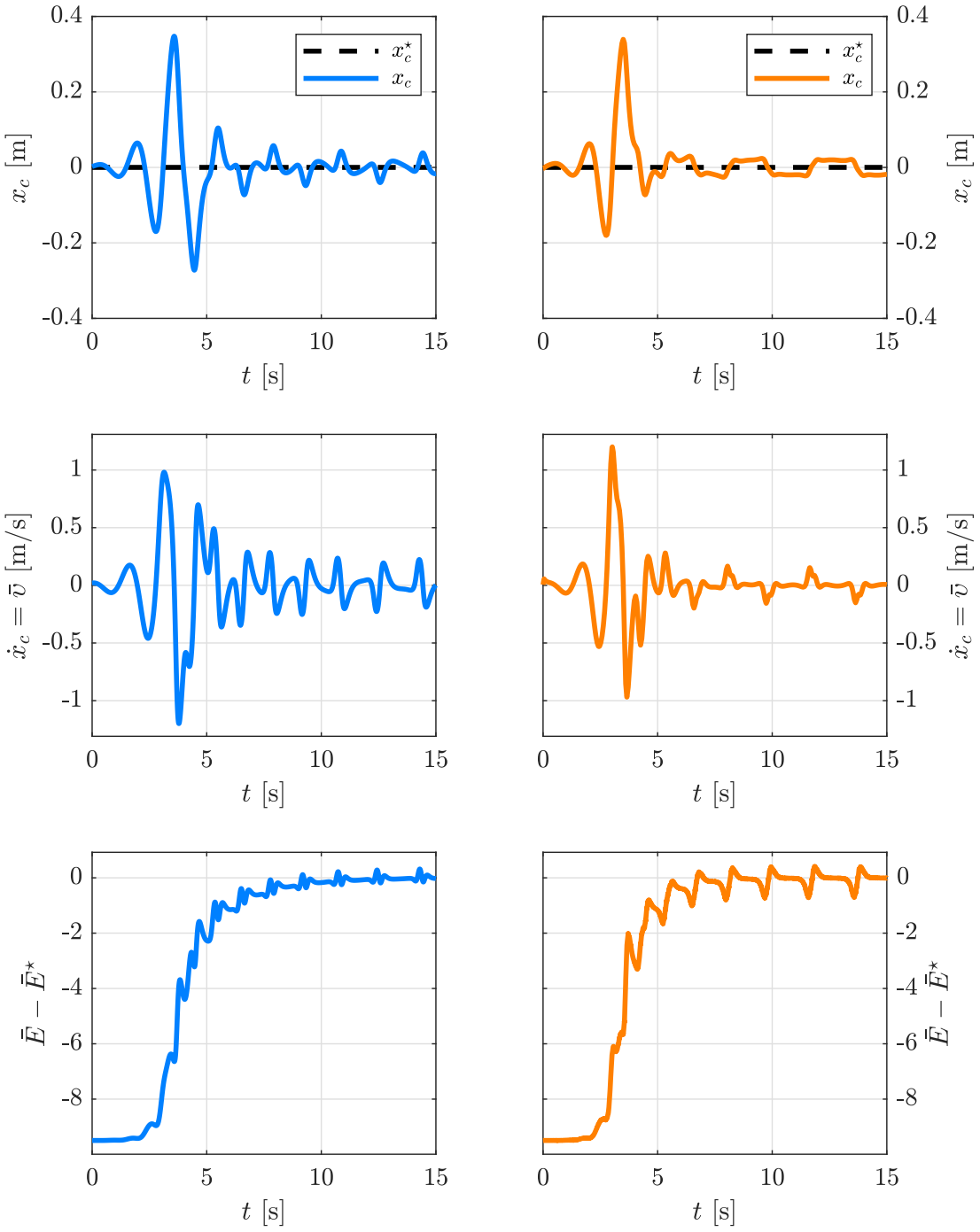

Figure 4.8 – Simulation (blue) and experimental (red) results with damping

Now, consider the same controller parameters and set the target energy as $\bar{E}^\star = 1.44$. As shown in the second row of Figure 4.7, the controller (4.12) brings the trajectories of the pendulum into the homoclinic orbit (4.6). Figure 4.8 depicts that x_c, $\dot{x}_c$ and $\bar{E}$ remain bounded near their target values.

4.4 PID-PBC

This section deals with the (local) stabilization at the unstable equilibrium point of the cart-pole system in explicit EL representation. The so-called PID-PBC approach is performed for the cart-pole system in SNF.

4.4.1 Controller Design

Consider an ideal cart-pole system (massless bar) in SNF given by (4.2) and assume there is no friction, i.e., $r_1 = 0$ with generalized coordinates $q = \text{col}(q_u, q_a) \in \mathbb{R}^2$, $n = 2$, where $q_u = \theta$ and $q_a = x_c$. From (4.1) and (4.3), the sub-blocks of the inertia matrix are given by

$$m_{uu}(\theta) = l^2, \tag{4.16a}$$

$$m_{au}(\theta) = l\cos\theta, \tag{4.16b}$$

and the sub-function of the potential energy is

$$V_u(\theta) = g_r l\left(\cos\theta - 1\right). \tag{4.17}$$

Problem Formulation: *Find a mapping $\upsilon : \mathbb{R}^2 \times \mathbb{R}^2 \to \mathbb{R}$ such that it stabilizes the upright vertical position of the pendulum and places the cart at any arbitrary position. Consider the desired equilibrium $q^\star = \text{col}(0, q_a^\star)$ with $q_a^\star = x_c^\star \in \mathbb{R}$, which is the only constant assignable equilibrium point.*

System (4.2) clearly satisfies Assumption 3.2. Applying Corollary 3.1, two new passive outputs are identified as

$$y_u = -l\cos\theta\dot{\theta},$$

$$y_a = \dot{x}_c.$$

The y_d signal defined in (3.7) takes the form

$$y_d = k_a \dot{x}_c - k_u l \cos\theta \dot{\theta}. \tag{4.18}$$

Assumption 3.3 is also satisfied with

$$V_N(\theta) = -l \sin\theta. \tag{4.19}$$

The well-defined PID-PBC state-feedback law is given by (3.8) and is rewritten as follows

$$\upsilon_{PID} = -K(\theta)^{-1} \left[K_P \, y_d + K_I \int_0^t y_d(\tau) \, \mathrm{d}\tau + S(\theta, \dot{\theta}) \right], \tag{4.20}$$

where the integral term (3.12) takes the form

$$\int_0^t y_d(\tau) \, \mathrm{d}\tau = k_a (x_c - x_c^\star) - k_u l \sin\theta, \tag{4.21}$$

and the mappings K and S result in

$$K(\theta) = k_e + k_a K_D + k_u K_D \left(\cos\theta\right)^2, \tag{4.22}$$

$$S(\theta, \dot{\theta}) = k_u K_D \left(l \sin\theta \dot{\theta}^2 - g_r \cos\theta \sin\theta \right). \tag{4.23}$$

The target (or desired) inertia matrix and potential energy function are given by

$$M_d(q) = \begin{bmatrix} k_e k_u l^2 + k_u^2 K_D \left(l \cos\theta\right)^2 & -k_a k_u K_D l \cos\theta \\ -k_a k_u K_D l \cos\theta & k_e k_a + k_a^2 K_D \end{bmatrix}, \tag{4.24}$$

$$V_d(q) = k_e k_u g_r l \left(\cos\theta - 1\right) + \frac{1}{2} K_I \left[k_a (x_c - x_c^\star) - k_u l \sin\theta \right]^2, \tag{4.25}$$

respectively. Assumption 3.4(b) is verified with

$$\left.\begin{array}{c} k_e k_a + k_a^2 K_D > 0 \\ k_e k_a k_u^2 K_D \left(\cos\theta\right)^2 > -k_e k_u \left(k_e k_a + k_a^2 K_D\right) \end{array}\right\} \quad \Rightarrow \quad M_d(q) = M_d^\top(q) \succ 0, \tag{4.26}$$

where the necessary and sufficient conditions

$$\left.\frac{\partial V_d}{\partial q}\right|_{q^\star} = 0 \qquad \text{and} \qquad \left.\frac{\partial^2 V_d}{\partial q^2}\right|_{q^\star} = \begin{bmatrix} k_u^2 K_I l^2 - k_e k_u g_r l & -k_a k_u K_I l \\ -k_a k_u K_I l & k_a^2 K_I \end{bmatrix} \succ 0 \tag{4.27}$$

are satisfied with

$$k_e k_u < 0 \qquad \Rightarrow \qquad q^\star = \arg\min V_d(q). \tag{4.28}$$

From (4.27) and (4.28), we conclude that $V_d(q)$ is proper and verifies $q^\star = \arg\min V_d(q)$ is an isolated minimum.

4.4.2 Local Optimal Controller

Solving simultaneously the set of equations (4.2a) and (4.2b) for $\ddot{\theta}$ and $\ddot{x}_c$ gives

$$\ddot{\theta} = \frac{g_r}{l}\sin(\theta) - \frac{1}{l}\cos(\theta)\upsilon - \frac{r_1}{l^2}\dot{\theta}, \tag{4.29a}$$

$$\ddot{x}_c = \upsilon. \tag{4.29b}$$

Defining the state vector $\mathbf{x} \in \mathbb{R}^4$ as $\mathbf{x} = \text{col}(q, \dot{q}) = \text{col}(\theta, x_c, \dot{\theta}, \dot{x}_c)$ and the control input $\upsilon \in \mathbb{R}$. Makes clear that (4.29) can be represented by the following affine nonlinear state-space equation $\dot{\mathbf{x}} = f(\mathbf{x}) + g(\mathbf{x})\upsilon$, for some $f : \mathbb{R}^4 \to \mathbb{R}^4$ and $g : \mathbb{R}^4 \to \mathbb{R}^4$.

Consider the linearization of the cart-pole system (4.29) in closed-loop with (4.20)

$$\begin{aligned}\dot{\tilde{\mathbf{x}}} &= \frac{\partial\left[f(\mathbf{x}) + g(\mathbf{x})\upsilon_{PID}(\mathbf{x})\right]}{\partial \mathbf{x}}\bigg|_{\mathbf{x}=\mathbf{x}^\star} \tilde{\mathbf{x}} \\ &= \frac{\partial f(\mathbf{x})}{\partial \mathbf{x}}\bigg|_{\mathbf{x}=\mathbf{x}^\star} \tilde{\mathbf{x}} + g(\mathbf{x})\big|_{\mathbf{x}=\mathbf{x}^\star} \frac{\partial \upsilon_{PID}(\mathbf{x})}{\partial \mathbf{x}}\bigg|_{\mathbf{x}=\mathbf{x}^\star} \tilde{\mathbf{x}},\end{aligned} \tag{4.30}$$

where $\tilde{\mathbf{x}} = \mathbf{x} - \mathbf{x}^\star$ and the desired equilibrium $\mathbf{x}^\star = \text{col}(q^\star, 0) = \text{col}(0, x_c^\star, 0, 0)$. Hence, the state matrix and the input-to-state matrix are provided by

$$\mathbf{A} = \frac{\partial f(\mathbf{x})}{\partial \mathbf{x}}\bigg|_{\mathbf{x}=\mathbf{x}^\star} = \begin{bmatrix} 0 & 0 & 1 & 0 \\ 0 & 0 & 0 & 1 \\ \bar{g} & 0 & -\bar{r} & 0 \\ 0 & 0 & 0 & 0 \end{bmatrix} \quad \text{and} \quad \mathbf{B} = g(\mathbf{x})\big|_{\mathbf{x}=\mathbf{x}^\star} = \begin{bmatrix} 0 \\ 0 \\ -\bar{a} \\ 1 \end{bmatrix}, \tag{4.31}$$

respectively, where $\bar{g} = g_r/l$, $\bar{r} = r_1/l^2$ and $\bar{a} = 1/l$. The (linear) feedback gain vector is computed as

$$\mathbf{K}_{LIN} = \frac{\partial \upsilon_{PID}(\mathbf{x})}{\partial \mathbf{x}}\bigg|_{\mathbf{x}=\mathbf{x}^\star} = \frac{1}{\gamma}\begin{bmatrix} k_u K_D g r + k_u K_I l & -k_a K_I & k_u K_P l & -k_a K_P \end{bmatrix}, \tag{4.32}$$

where $\gamma = k_e + k_a K_D + k_u K_D$.

The pair $(\mathbf{A}, \mathbf{B})$ is controllable and is verified computing the controllability matrix

$$\det\left(\begin{bmatrix} \mathbf{B} & \mathbf{AB} & \mathbf{A}^2\mathbf{B} & \mathbf{A}^3\mathbf{B} \end{bmatrix}\right) = -\frac{g_r^2}{l^4} \neq 0. \tag{4.33}$$

From linear systems theory, it is possible to design a state-feedback controller $\upsilon = -\mathbf{K}\tilde{\mathbf{x}}$ with $\mathbf{K} \in \mathbb{R}^{1\times 4}$ such that the closed-loop system $\dot{\tilde{\mathbf{x}}} = (\mathbf{A} - \mathbf{B}\mathbf{K})\tilde{\mathbf{x}}$ is exponentially (asymptotically) stable. For this purpose the optimal Linear Quadratic Regulator (LQR) methodology is established.

Consider the following optimization problem

$$\min_{\upsilon} \; J(\upsilon) = \int_0^\infty \tilde{\mathbf{x}}^\top \mathbf{Q}\tilde{\mathbf{x}} + \upsilon^\top \mathbf{R}\upsilon \, \mathrm{d}t, \tag{4.34a}$$

subject to

$$\dot{\tilde{\mathbf{x}}} = \mathbf{A}\tilde{\mathbf{x}} + \mathbf{B}\upsilon, \qquad \tilde{\mathbf{x}}(0) = \mathbf{x}_0, \tag{4.34b}$$

where $\mathbf{Q} = \mathbf{Q}^\top \succeq 0$ and $\mathbf{R} = \mathbf{R}^\top \succ 0$ are weighting matrices. It is well-known that the control law which minimizes the quadratic cost function (4.34a) subject to the system dynamics (4.34b) is $\upsilon = -\mathbf{K}_{LQR}\tilde{\mathbf{x}}$, where $\mathbf{K}_{LQR}$ is given by

$$\mathbf{K}_{LQR} = \mathbf{R}^{-1}\mathbf{B}^\top \mathbf{P} \tag{4.35}$$

and $\mathbf{P}$ is a solution to the Algebraic Riccati Equation (ARE)

$$\mathbf{A}^\top \mathbf{P} + \mathbf{P}\mathbf{A} - \mathbf{P}\mathbf{B}\mathbf{R}^{-1}\mathbf{B}^\top \mathbf{P} + \mathbf{Q} = 0. \tag{4.36}$$

The goal is that around the equilibrium point $\mathbf{x}^\star = \mathrm{col}(q^\star, 0)$ the behavior of the cart-pole system (4.2) in feedback with (4.20) equals the local optimal behavior of $\dot{\tilde{\mathbf{x}}} = (\mathbf{A} - \mathbf{B}\mathbf{K}_{LQR})\tilde{\mathbf{x}}$. As a consequence, the (unknown) tuning parameters of the PID-PBC state-feedback law are found by solving

$$\mathbf{K}_{LIN} = -\mathbf{K}_{LQR}. \tag{4.37}$$

4.4.3 Stability Analysis

Since, at the equilibrium point, the system (4.2) in feedback with (4.20) is (locally) equivalent to $\dot{\tilde{\mathbf{x}}} = (\mathbf{A} - \mathbf{B}\mathbf{K}_{LQR})\tilde{\mathbf{x}}$, then asymptotic stability can be verified invoking Theorem 2.3.

For the stability analysis, we considered the linearized dynamics of the cart-pole system (4.31) using the parameters from Table 4.1. The gain vector $\mathbf{K}_{LQR}$ can be found by

choosing $\mathbf{Q} = \text{diag}(1, 60, 1, 12)$, $\mathbf{R} = 1$ and solving $\mathbf{P}$ via (4.36).[25] Here, two cases are addressed.

- Negligible damping ($r_1 = 0$): The optimal LQR feedback gain is

$$\mathbf{K}_{LQR} = \begin{bmatrix} -50.2405 & -7.7460 & -11.2019 & -8.7091 \end{bmatrix} \tag{4.38}$$

  and the (closed-loop) eigenvalues are

$$\Lambda = \begin{Bmatrix} -3.2107 & -5.8772 & -2.6738 \pm 1.0821\imath \end{Bmatrix}.$$

- With damping ($r_1 = 0.0276$): The optimal LQR feedback gain is

$$\mathbf{K}_{LQR} = \begin{bmatrix} -50.7416 & -7.7460 & -11.1672 & -8.7544 \end{bmatrix} \tag{4.39}$$

  and the (closed-loop) eigenvalues are

$$\Lambda = \begin{Bmatrix} -3.2099 & -5.8788 & -2.6737 \pm 1.0821\imath \end{Bmatrix}.$$

Via Lyapunov's indirect method, (local) asymptotic stability is guaranteed because in both cases the eigenvalues of the closed-loop system are in the open left-half plane.

4.4.4 Simulation Results

Consider the parameters of the cart-pole system from Table 4.1, with no friction, i.e., $r_1 = 0$. From (4.37), using (4.32) and (4.38), one solution gives us the following tuning gains $K_P = 5.5799$, $K_I = 4.9629$, $K_D = 0.9899$, $k_e = 1$, $k_a = 1$ and $k_u = -2.6575$. These gains satisfy the inequalities in (4.26) and (4.28). The desired cart position is set to $x_c^\star = 0\,\text{m}$. The objective is to stabilize the cart-pole system from the initial states $\theta(0) = \pi/9$, $\dot{\theta}(0) = 0$, $x_c(0) = 0$ and $\dot{x}_c(0) = 0$.

Figure 4.9 depicts the time responses of the states θ, $\dot{\theta}$, x_c, $\dot{x}_c$, the control input υ and the target Hamiltonian H_d under the stabilization control problem. Simulations show that the controller (4.20) stabilizes the system (4.2) fulfilling the requirements stated in the *problem formulation*, i.e., $\theta \to 0$, $\dot{\theta} \to 0$, $x_c \to x_c^\star = 0$ and $\dot{x}_c \to 0$. It can be seen that the performance of the PID-PBC is almost the same as the LQR.

[25] We write $\text{diag}(a_1, \ldots, a_n)$ for a diagonal matrix whose diagonal entries starting in the upper left corner are $a_1, \ldots, a_n$.

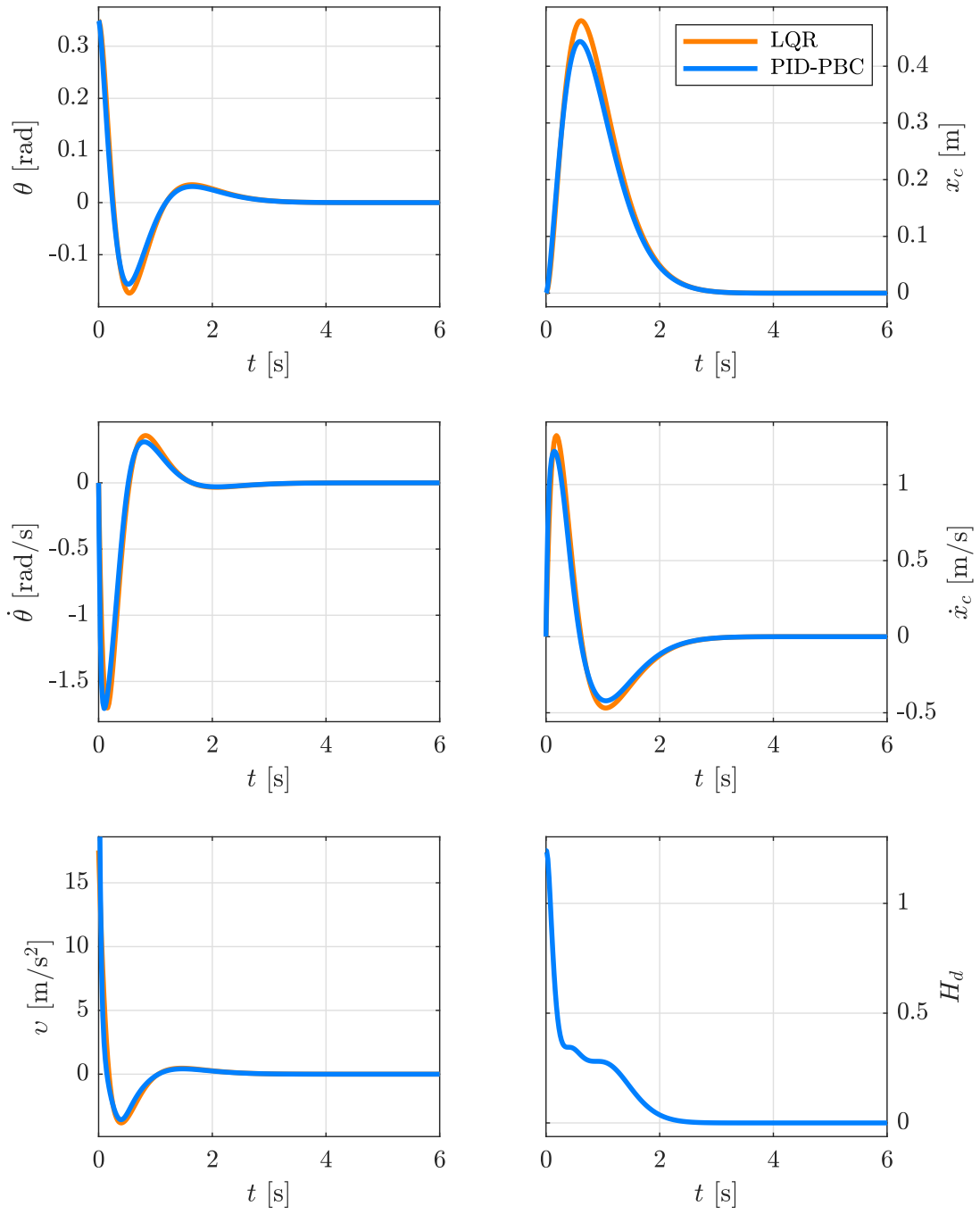

Figure 4.9 – Simulation results with no damping

4.4.5 Experimental Validation

Real-time experiments are contrasted with simulations including damping in the cart-pole dynamics. Consider the parameters of the cart-pole system from Table 4.1, including

friction. From (4.37), using (4.32) and (4.39), one solution gives us the following tuning gains as shown in Table 4.4. These gains satisfy the inequalities in (4.26) and (4.28). The desired equilibrium is set to $x_c^\star = 0.5\,\text{m}$ for $t \in [0, 5[$ s, $x_c^\star = -0.5\,\text{m}$ for $t \in [5, 10[$ s and $x_c^\star = 0\,\text{m}$ for $t \in [10, 15]$ s.

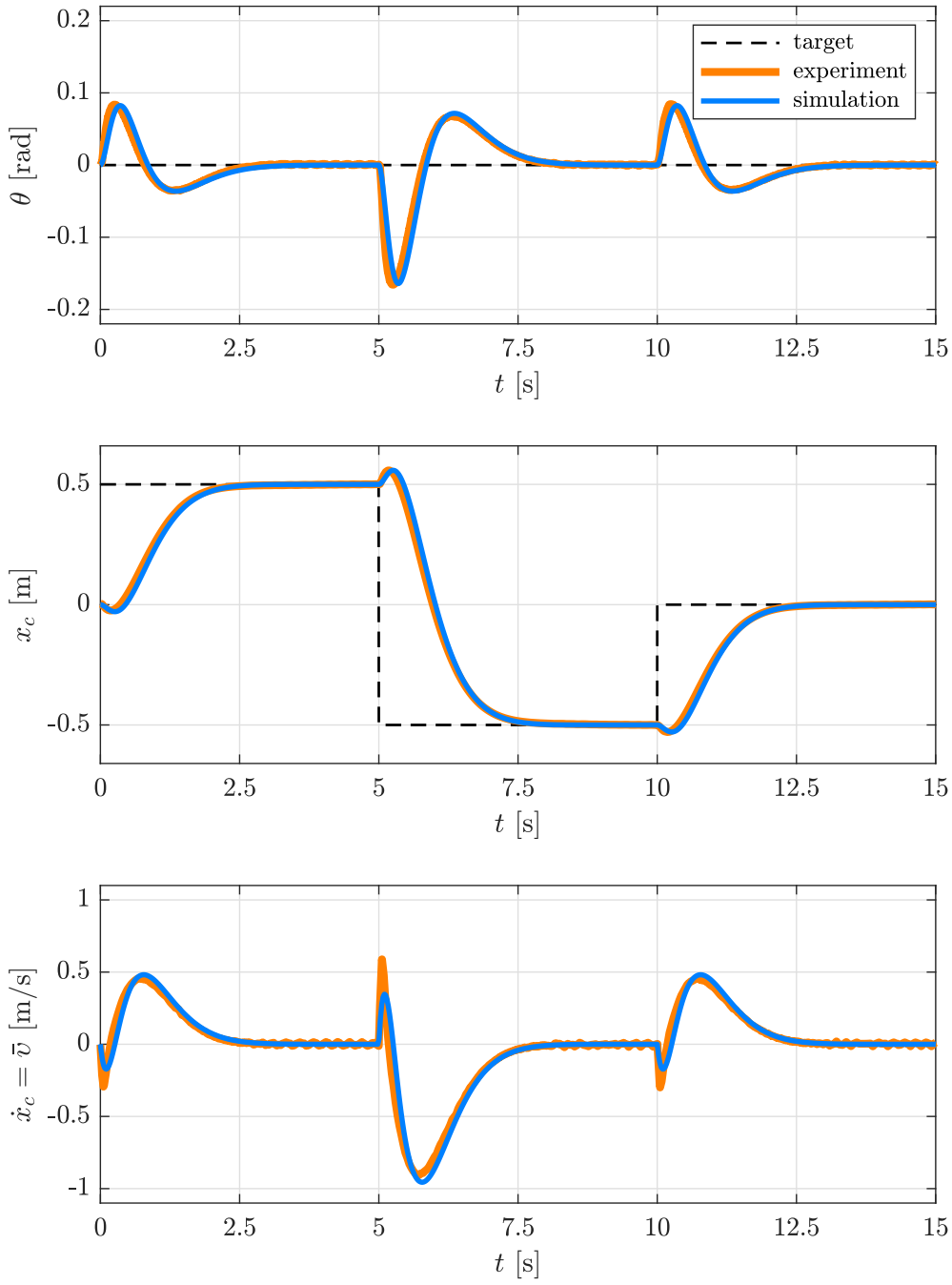

Figure 4.10 – Simulation and experimental results with damping

The objective is to stabilize the cart-pole system from the initial states $\theta(0) = 0$, $\dot{\theta}(0) = 0$, $x_c(0) = 0$ and $\dot{x}_c(0) = 0$.

K_P	K_I	K_D	k_e	k_a	k_u
5.5239	4.8876	0.9972	1	1	-2.6356

Table 4.4 – PID-PBC parameters

Figure 4.10 depicts the time responses of the states θ, x_c and the (real) control input $\bar{v}$ under the regulation control problem. Simulations and real-time experiments show that the controller (4.20) stabilizes the system (4.2) fulfilling the requirements stated in the *problem formulation*, i.e., $\theta \to 0$ and $x_c \to x_c^\star$ with continuous, smooth and bounded (real) control input $\bar{v}$. It can be seen that simulations and real-time experiments show almost the same performance.

4.5 Explicit Control Scheme

Figure 4.11 depicts an overview of the explicit control strategy which integrates both controllers: (i) swing-up and (ii) PID-PBC. The swing-up controller brings the trajectories of the pendulum into the homoclinic orbit, i.e, the pendulum will remain swinging while getting closer and closer to its upright (unstable) position. Once the system is close enough, to its unstable equilibrium point, the stabilizing controller must keep the pendulum at the upright vertical position and the cart at the target value.[26]

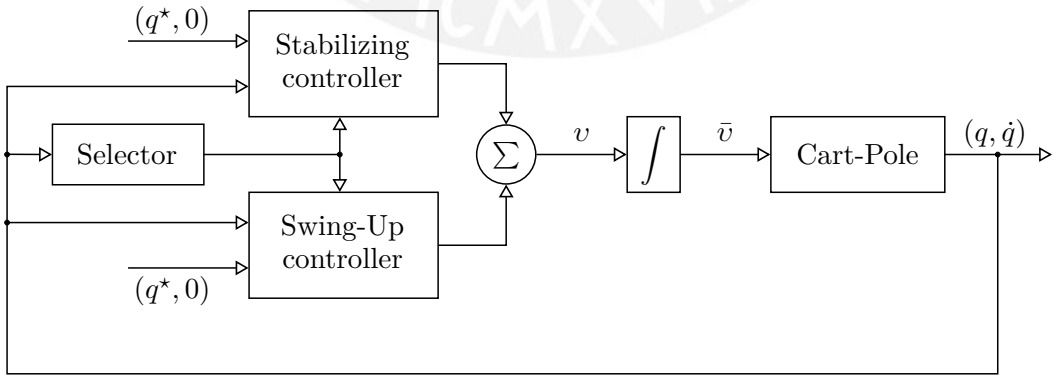

Figure 4.11 – Overview of the explicit control system

[26] In this section, *stabilizing controller* refers to PID-PBC.

Since the control scheme is initialized with the swing-up controller, then an algorithm is required to decide when to switch to the stabilizing controller. The block named *Selector* is an algorithm that decides which of the controllers must be active. To activate the stabilizing controller, we propose the following conditions $|\dot{x}| \leq 0.2\,\text{m/s}$, $|x| \leq 0.1\,\text{m}$, $|\dot{\theta}| \leq 0.4\,\text{rad/s}$ and for $|\theta|$ we develop an algorithm based on Figure 4.12.[27]

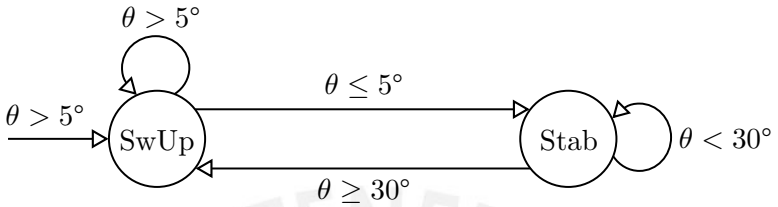

Figure 4.12 – State machine for θ

If at least one of these inequalities is not met, then the output of the swing-up controller will be applied to the system. If all of them are satisfied, then the output of the stabilizing controller will be applied to the cart-pole. Clearly, when one controller is activated the other remains deactivated. This is computationally efficient since it avoids computing both control algorithms simultaneously.

Real-time experiments are contrasted with simulations including damping in the cart-pole dynamics. (i) For the swing-up controller, consider the system parameters from Table 4.1, the controller parameters from Table 4.3, the (new) target energy set as $\bar{E}^\star = 1.44$ and the initial conditions from Section 4.3.6. (ii) For the stabilizing controller, consider the system parameters from Table 4.1 and the controller parameters from Table 4.4. For both controllers, the target cart position is set to $x_c^\star = 0\,\text{m}$.

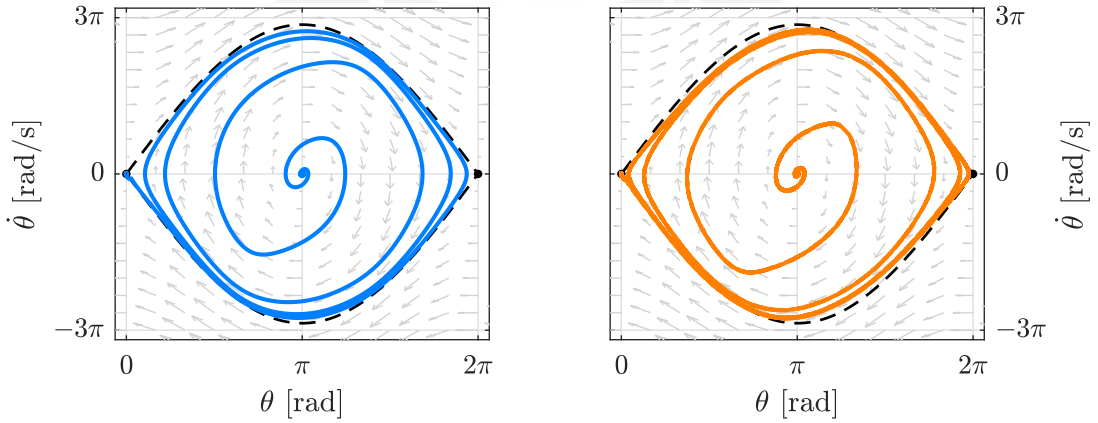

Figure 4.13 – Simulation (blue) and experimental (red) results with damping

[27] In Figure 4.12, *SwUp* refers to the swing-up controller and *Stab* refers to the stabilizing controller.

Figure 4.13 depicts the phase portrait of $(\theta, \dot{\theta})$ and Figure 4.14 depicts the time responses of the states θ, x_c and the (real) control input $\bar{v}$ under the (explicit) control scheme provided by Figure 4.11. The switch occurs at $t = 12.1\,\mathrm{s}$ in the simulations and at $t = 12.6\,\mathrm{s}$ in the real-time experiments. Note that the (real) control input $\bar{v}$ is bounded.

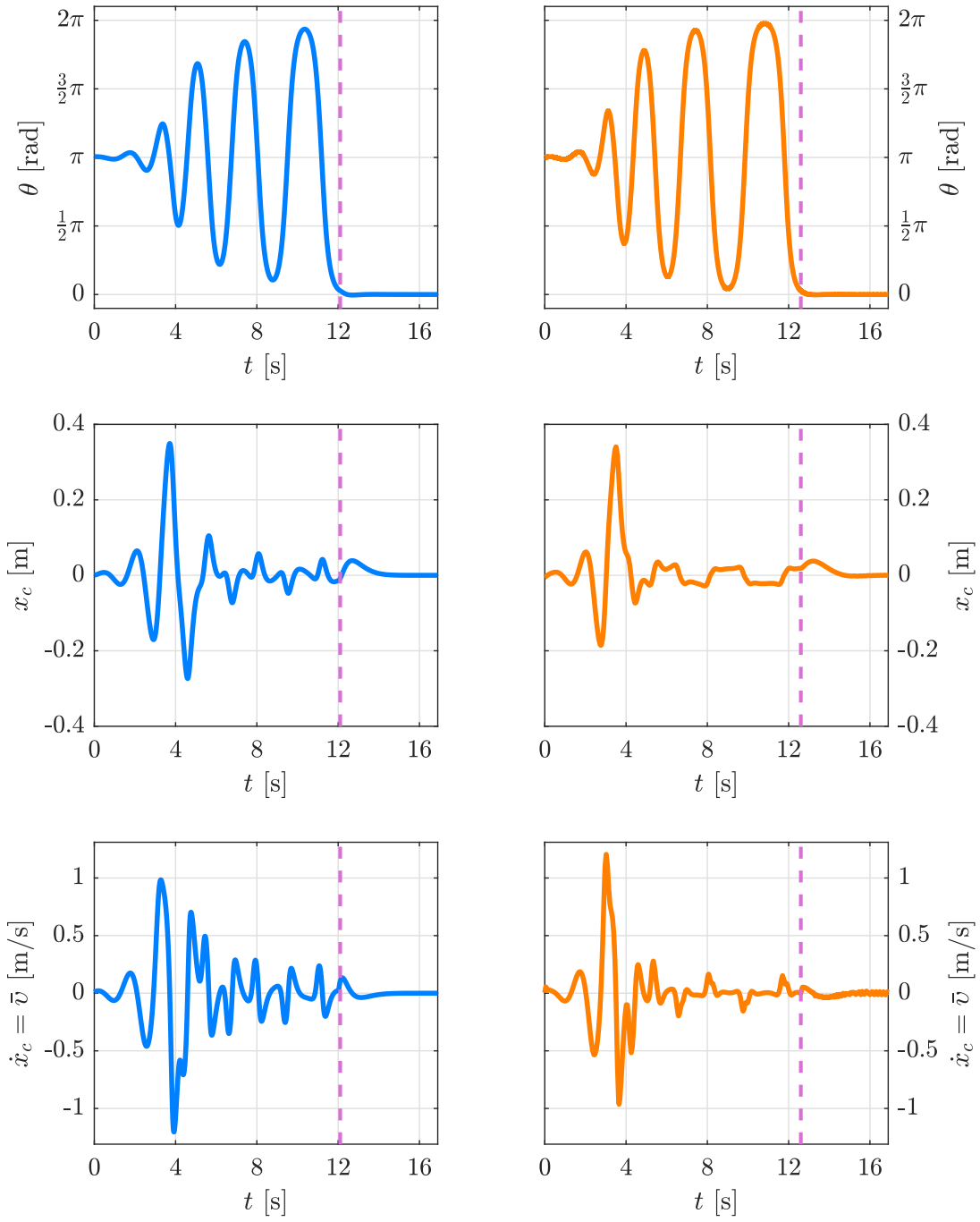

Figure 4.14 – Simulation (blue) and experimental (red) results with damping

Chapter 5

Energy-Based Control for Implicit UMS

In analytical mechanics, explicit systems are those modeled as ODEs and these representations are widely used in the design of control systems. Frequently, complex dynamical systems are modeled as simpler interconnected subsystems, where its dynamics is described by ODEs subject to a set of algebraic equations describing constraints (interconnections). The resulting implicit mechanical model becomes a system of DAEs. In the standard IDA-PBC approach, the feedback control law exists if the so-called matching conditions hold, where the main drawback is to solve a set of non-homogeneous, first order and quasi-linear PDEs, see Section 2.4. Recent research work [10] has shown that the total energy-shaping via IDA-PBC can be performed without solving PDEs for a class of UMSs in implicit PH representation and still preserving the PH structure of the closed-loop. Conversely, an energy-based controller is derived using a generalized energy function and taking advantage of the passivity properties of UMSs. The latter approach is often used for two specific tasks: (i) the stabilization at an isolated equilibrium point and, more recently, (ii) the tracking of homoclinic orbits (limit cycles). This chapter is organized as follows. Section 5.1 presents the IDA-PBC methodology for UMSs in implicit PH representation, which under some easily verifiable conditions, the computation of PDEs is avoided via algebraic equations. Section 5.2 provides the typical energy-based control approach using a more general energy function for UMSs in implicit PH representation with no class restriction. The latter approach is performed in two stages. First, we analyze the passivity properties of the system and identify its passive output. Second, we define a (generalized) admissible storage function for the stabilization at an energy level-set.

5.1 IDA-PBC for Implicit UMS

In this section it is presented the total energy-shaping via IDA-PBC for UMSs in implicit PH representation.[28] Based on [8, 59], the constrained EL equations of motion for mechanical systems with no natural damping can be rewritten as

$$\begin{bmatrix}\dot{r}\\ \dot{\rho}\end{bmatrix} = \begin{bmatrix}0 & I_{n_r}\\ -I_{n_r} & 0\end{bmatrix}\begin{bmatrix}\partial_r^\top \mathcal{H}\\ \partial_\rho^\top \mathcal{H}\end{bmatrix} + \begin{bmatrix}0\\ b(r)\end{bmatrix}\lambda + \begin{bmatrix}0\\ \mathcal{G}(r)\end{bmatrix}u, \tag{5.1a}$$

$$0 = b^\top(r)\partial_\rho^\top \mathcal{H}, \tag{5.1b}$$

with total (kinetic plus potential) stored energy

$$\mathcal{H}(r,\rho) = \frac{1}{2}\rho^\top \mathcal{M}^{-1}(r)\rho + \mathcal{V}(r), \tag{5.2}$$

where $r \in \mathbb{R}^{n_r}$ are the implicit generalized coordinates (position), $\rho \in \mathbb{R}^{n_r}$ are its associated momenta, $u \in \mathbb{R}^{n_u}$, with $n_u \leq n_r$, are the inputs, $\mathcal{G} : \mathbb{R}^{n_r} \to \mathbb{R}^{n_r \times n_u}$ is the implicit full rank input matrix, $b(r)\lambda$ represents the constraint forces with $b : \mathbb{R}^{n_r} \to \mathbb{R}^{n_r \times n_\lambda}$, and $\lambda \in \mathbb{R}^{n_\lambda}$ are the implicit variables. The implicit inertia matrix $\mathcal{M} : \mathbb{R}^{n_r} \to \mathbb{R}^{n_r \times n_r}$ satisfies $\mathcal{M}(r) = \mathcal{M}^\top(r) \succ 0$, the implicit potential energy $\mathcal{V} : \mathbb{R}^{n_r} \to \mathbb{R}$ and the implicit Hamiltonian $\mathcal{H} : \mathbb{R}^{n_r} \times \mathbb{R}^{n_r} \to \mathbb{R}$.

Definition 5.1 (Implicit UMS [9])**:** *The (implicit) mechanical system* (5.1) *is said to be underactuated if* $\operatorname{rank}(S) < \dim(r)$*, where* $S(r) \coloneqq \begin{bmatrix}\mathcal{G}(r) & b(r)\end{bmatrix}$. ■

Definition 5.2 (Holonomic system [5])**:** *Constraints* (5.1b) *are called holonomic since they can be integrated. If all constraints* (5.1b) *are integrable, then we say that the system* (5.1) *is holonomic. Otherwise,* (5.1) *is called non-holonomic.* ■

Proposition 5.1 (Well-posedness [10])**:** *Consider the implicit system* (5.1) *and define the set*

$$\mathcal{X} \coloneqq \{r \in \mathbb{R}^{n_r} \mid \operatorname{rank}(\Delta) = n_\lambda\},$$

where $\Delta(r) \coloneqq b^\top \mathcal{M}^{-1}(r)b$*. Then, for all* $r \in \mathcal{X}$*, the constrained state-space set*

$$\mathcal{X}_c = \left\{(r,\rho) \in \mathcal{X} \times \mathbb{R}^{n_r} \mid b^\top \partial_\rho^\top \mathcal{H} = 0,\ \phi_i = 0\right\}$$

[28] Implicit systems are those modeled as DAEs, where constraints are described as algebraic equations.

is a regular manifold embedded in $\mathbb{R}^{n_r \times n_r}$ *and the DAEs system* (5.1) *has differential index 1 with unique solution for* λ*. Here,*

$$\phi_i(r) \coloneqq \int_0^r b_i^\top(s)\,\mathrm{d}s + c_i$$

are the integrated (holonomic) constraints (with $\partial_r^\top \phi_i \equiv b_i$*),* c_i *is constant,* b_i *is the* i*-th column vector of* b *satisfying the integrability condition* $\partial_r b_i \equiv \partial_r^\top b_i$ *and* $b^\top \partial_\rho^\top \mathcal{H}$ *is differentiable. Otherwise, for non-integrable (non-holonomic) constraints the domain* $\mathcal{X}_c$ *reduces to*

$$\mathcal{X}_c = \left\{(r,\rho) \in \mathcal{X} \times \mathbb{R}^{n_r} \mid b^\top \partial_\rho^\top \mathcal{H} = 0\right\}. \qquad \blacksquare$$

Problem Formulation: *Find a mapping* $u : \mathcal{X} \times \mathbb{R}^{n_r} \to \mathbb{R}^{n_u}$ *such that it transforms the nominal system* (5.1) *by means of some state-feedback control law into a target PH system with a stable equilibrium at the desired point* $(r,\rho) = (r^\star, 0)$ *with target (or desired) Lyapunov function (Hamiltonian), where* $\mathcal{M}_d(r) = \mathcal{M}_d^\top(r)$ *is full rank, but not necessarily positive definite, and* $r^\star = \arg\min \mathcal{V}_d(r)$ *is an isolated minimum.*

Consider the desired (or target) PH system in implicit representation

$$\begin{bmatrix}\dot r \\ \dot\rho\end{bmatrix} = \begin{bmatrix}0 & \mathcal{J}(r) \\ -\mathcal{J}^\top(r) & -\mathcal{W}(r,\rho)\end{bmatrix}\begin{bmatrix}\partial_r^\top \mathcal{H}_d \\ \partial_\rho^\top \mathcal{H}_d\end{bmatrix} + \begin{bmatrix}0 \\ b_d(r)\end{bmatrix}\lambda_d, \tag{5.3a}$$

$$0 = b_d^\top(r)\partial_\rho^\top \mathcal{H}_d, \tag{5.3b}$$

with target energy function

$$\mathcal{H}_d(r,\rho) = \frac{1}{2}\rho^\top \mathcal{M}_d^{-1}(r)\rho + \mathcal{V}_d(r),$$

where, similar to Proposition 5.1, we define $\Delta_d(r) \coloneqq b_d^\top \mathcal{M}_d^{-1}(r) b_d$ and the set

$$\mathcal{X}_d \coloneqq \{r \in \mathbb{R}^{n_r} \mid \operatorname{rank}(\Delta_d) = n_\lambda\},$$

such that the target system (5.3) is well-defined for all $r \in \mathcal{X}_d$, $b_d(r)\lambda_d$ represents the new constraint forces with $b_d : \mathcal{X}_d \to \mathbb{R}^{n_r \times n_\lambda}$ and $\lambda_d \in \mathbb{R}^{n_\lambda}$ are the new implicit variables, $\mathcal{M}_d : \mathcal{X}_d \to \mathbb{R}^{n_r \times n_r}$ is the non-singular target inertia matrix that satisfies $\mathcal{M}_d = \mathcal{M}_d^\top$, $\mathcal{J} : \mathcal{X}_d \to \mathbb{R}^{n_r \times n_r}$ is non-singular, $\mathcal{V}_d : \mathcal{X}_d \to \mathbb{R}$ is the target potential energy, $\mathcal{W} : \mathcal{X}_d \times \mathbb{R}^{n_r} \to \mathbb{R}^{n_r \times n_r}$ and $\mathcal{H}_d : \mathcal{X}_d \times \mathbb{R}^{n_r} \to \mathbb{R}$ is the new shaped Hamiltonian.

Proposition 5.2 (Implicit matching equations [10])**:** *Assume* $S \coloneqq \begin{bmatrix} \mathcal{G} & b \end{bmatrix}$ *is full rank. System* (5.1) *can be transformed into* (5.3) *for any* r *in* $\mathcal{X} \cap \mathcal{X}_d$ *whenever the following kinetic (quadratic in* ρ*), potential (independent of* ρ*) and constraint matching equations*

$$S_\perp \Big(\partial_r^\top (\mathcal{M}^{-1}\rho) - \mathcal{J}^\top \partial_r^\top (\mathcal{M}_d^{-1}\rho) - \mathcal{W}_1 \mathcal{M}_d^{-1} \Big) \rho = 0, \tag{5.4a}$$

$$S_\perp \Big(\partial_r^\top \mathcal{V} - \mathcal{J}^\top \partial_r^\top \mathcal{V}_d \Big) = 0, \tag{5.4b}$$

$$S_\perp \mathcal{J}^\top b = 0, \tag{5.4c}$$

are satisfied. As a consequence, the uniquely defined control law is given by

$$u_{_I} = S^\dagger \Big(\partial_r^\top \mathcal{H} - \mathcal{J}^\top \partial_r^\top \mathcal{H}_d - \mathcal{W} \partial_\rho^\top \mathcal{H}_d + \mathcal{J}^\top b \lambda_d \Big), \tag{5.5}$$

where $S^\dagger = \begin{bmatrix} I_{n_u} & 0 \end{bmatrix} (S^\top S)^{-1} S^\top$*,* $\mathcal{J} = \mathcal{M}^{-1}\mathcal{M}_d$*,* $b_d = \mathcal{J}^\top b$*,* $S_\perp$ *is the full rank left annihilator of* S*,* $\mathcal{W}(r,\rho) \coloneqq \frac{1}{2}\mathcal{W}_1(r,\rho) + S(r)K_u(r)S^\top(r)$*,* $\mathcal{W}_1(r,\rho) \in \mathbb{R}^{n_r \times n_r}$ *is linear in* ρ *and* $K_u(r) \in \mathbb{R}^{(n_u+n_\lambda)\times(n_u+n_\lambda)}$*.* ■

Proposition 5.3 (Implicit stability [10])**:** *Assume that the conditions of* Proposition 5.2 *are satisfied and define the new domain*[29]

$$\mathcal{X}_I \coloneqq \Big(\Big\{ r \in \mathcal{X}_d \mid b_\perp \mathcal{M}\mathcal{M}_d^{-1}\mathcal{M} b_\perp^\top \succ 0,\ \phi = 0 \Big\} \times \mathbb{R}^{n_r} \Big) \cap \mathcal{X}_c.$$

Then $x^\star = (r^\star, 0) \in \mathcal{X}_a = \{(r,\rho) \in \mathcal{X}_I \mid S_\perp \partial_r^\top \mathcal{V} = 0\}$ *is a stable equilibrium of the closed-loop system* (5.3) *for any* $K_u + K_u^\top \succeq 0$ *if* $r^\star = \arg\min \mathcal{V}_d|_{\mathcal{X}_I}$ *is an isolated minimum*[30] *and*

$$\rho^\top \mathcal{M}_d^{-1} \mathcal{W}_1 \mathcal{M}_d^{-1} \rho \Big|_{\mathcal{X}_I} = 0.$$

Furthermore, if $y_{_I} \coloneqq (K_u + K_u^\top)^{\frac{1}{2}} S^\top \mathcal{M}_d^{-1}\rho$ *is a detectable output of* (5.3)*, then the equilibrium point* $x^\star = (r^\star, 0)$ *is asymptotically stable.* ■

Remark: The implicit variables λ and λ_d may be computed from the hidden (or secondary) constraint

$$\frac{\mathrm{d}\, b^\top \partial_\rho^\top \mathcal{H}}{\mathrm{d}t} = \partial_r (b^\top \partial_\rho^\top \mathcal{H}) \partial_\rho^\top \mathcal{H} + b^\top \mathcal{M}^{-1} \dot{\rho} = 0. \tag{5.6}$$

[29] For non-integrable (non-holonomic) constraints $\mathcal{X}_I = \Big(\Big\{ r \in \mathcal{X}_d \mid b_\perp \mathcal{M}\mathcal{M}_d^{-1}\mathcal{M} b_\perp^\top \succ 0 \Big\} \times \mathbb{R}^{n_r} \Big) \cap \mathcal{X}_c$.
[30] Note that $\mathcal{H}_d|_{\mathcal{X}_I}$ is the restriction of $\mathcal{H}_d$ to $\mathcal{X}_I$.

5.1.1 A Class of Holonomic Systems

The set of PDEs from the matching conditions (5.4) may be solved algebraically for a class of UMSs in implicit PH representation with holonomic constraints. The following assumption defines the system class.

Assumption 5.1:

(a) *The inertia matrix $\mathcal{M}$ is constant.*

(b) *The potential energy function $\mathcal{V}$ is linear in r.*

(c) *The full rank input matrix-valued function $\mathcal{G}$ is polynomial.*

(d) *The constraints ϕ are polynomials.*

Proposition 5.4 ((Implicit) Algebraic IDA-PBC [10])**:** *Consider a holonomic (all constraints* (5.1b) *are integrable) implicit PH system* (5.1) *fulfilling* Assumption 5.1. *The implicit state-feedback control law* (5.5) *with $r^\star - r = \tilde{r}$, $K_u + K_u^\top \succeq 0$, target inertia matrix*

$$\mathcal{M}_d = \mathcal{M} B^\star \begin{bmatrix} A + CDC^\top & CD \\ DC^\top & D \end{bmatrix} B^{\star\top} \mathcal{M}, \qquad \textit{where} \qquad B^{\star\top} = \begin{bmatrix} b_\perp^\star \\ b^{\star\top} \end{bmatrix},$$

and target potential energy function

$$\mathcal{V}_d = \frac{1}{2}\psi^\top K_\psi \psi + \tilde{r}^\top b^\star \mu^\star, \quad \textit{where} \quad \psi(r) = \int_{r^\star}^{r} \bar{S}^\top(s) S^\top(s) \mathcal{M}_d^{-1} \mathcal{M} \, \mathrm{d}s,$$

stabilizes the closed-loop system (5.3) *at $x^\star = (r^\star, 0)$, if there exists a constant vector $\mu^\star \in \mathbb{R}^{n_\lambda}$ and matrices $A \in \mathbb{R}^{(n_r - n_\lambda)\times(n_r - n_\lambda)}$ that satisfies $A = A^\top \succ 0$, $C \in \mathbb{R}^{(n_r - n_\lambda)\times n_\lambda}$, non-singular symmetric $D \in \mathbb{R}^{n_\lambda \times n_\lambda}$, and $\bar{S}(r) \in \mathbb{R}^{(n_u + n_\lambda)\times n_\psi}$, with $n_\psi \leq n_u + n_\lambda$, such that*

$$S_\perp \Big(\partial_r^\top \mathcal{V} + \mathcal{M} Z_c D b^{\perp\top} b^\star \mu^\star \Big) = 0, \tag{5.7a}$$

$$S_\perp \mathcal{M} \Big(b_\perp^{\star\top} A b_\perp^\star + Z_c D Z_c^\top \Big) b = 0, \tag{5.7b}$$

$$\partial_r (S \bar{S}_i) \mathcal{M}^{-1} \mathcal{M}_d - \mathcal{M}_d \mathcal{M}^{-1} \partial_r^\top (S \bar{S}_i) = 0, \tag{5.7c}$$

$$Z_\perp Z_a Z_\perp^\top \succ 0, \tag{5.7d}$$

where $b^\star = b(r^\star)$, $Z_c = {b_\perp^\star}^\top C + b^\star$, $Z = \begin{bmatrix} I_{n_r - n_\lambda} & -C \end{bmatrix} B^{\star -1} \mathcal{M}^{-1} S(r^\star) \bar{S}(r^\star)$ *has full rank,* $Z_a = A b_\perp^\star \, \partial_r (b\mu^\star)|_{r=r^\star} \, {b_\perp^\star}^\top A$, $\bar{S}_i$ *is the* i*-th column of* $\bar{S}$,

$$\begin{bmatrix} S_\perp^\top & \mathcal{M}_d^{-1}\rho \end{bmatrix}^\top \mathcal{W}_1 = 0, \tag{5.8a}$$

$$K_\psi \succ -Z^+ \Big(Z_a - Z_a Z_\perp^\top (Z_\perp Z_a Z_\perp^\top)^{-1} Z_\perp Z_a \Big) {Z^+}^\top, \tag{5.8b}$$

where $K_\psi = K_\psi^\top \in \mathbb{R}^{n_\psi \times n_\psi}$ *and* $Z^+ = (Z^\top Z)^{-1} Z^\top$. *Furthermore, if* y_I *is a detectable output of* (5.3)*, then the equilibrium point* $x^\star = (r^\star, 0)$ *is asymptotically stable.* ■

The new algebraic matching conditions (5.7a) and (5.7b) are given by direct substitution of $\mathcal{H}_d$ in (5.4) with (5.8a). The integrability condition (5.7c) guarantees the existence of ψ, which implies the existence of $\mathcal{V}_d$. The necessary and sufficient conditions for $x^\star$ to be an isolated minimum of $\mathcal{H}_d \,|_{\mathcal{X}_c}$ are given by (5.7d) and (5.8b), respectively. In addition, (5.8a) is useful to compute $\mathcal{W}_1$ and (5.8b) set a lower bound in the choice of K_ψ. The procedure for the design of the implicit algebraic IDA-PBC approach is summarized in the following algorithm.

Require: Holonomic system (5.1) fulfilling Assumption 5.1

1: Select $r^\star$, $b_\perp^\star$ and $S_\perp$
2: Find a numerical solution for C (if possible) and constraints for A, D and $\mu^\star$ via (5.7a) and (5.7b)
3: Select $\bar{S}$ via (5.7c) with full rank condition on Z, and pick $Z_\perp$
4: Choose $\mathcal{W}_1$, $A \succ 0$, D (non-singular), $\mu^\star$, K_ψ, and K_u, from (5.7d), (5.8) and $K_u + K_u^\top \succeq 0$

Algorithm 5.1 – Algorithm for the implicit algebraic IDA-PBC

5.1.2 Reduction to Explicit Coordinates

The following proposition states a (local) coordinates reduction that removes the constraints (5.3b) and constraint forces $b_d(r)\lambda_d$.[31]

Proposition 5.5 (Implicit reduction [10])**:** *Assume all constraints* (5.3b) *are integrable (holonomic constraints) and the identity*

$$\Big\{r \mid \phi(r) = 0,\ \partial_r \phi = b_d^\top \mathcal{J}^{-1}\Big\} = \Big\{q \mid r = h(q)\Big\}$$

holds for all r and q in some subsets of $\mathcal{X}_d$ and $\mathbb{R}^{n_r - n_\lambda}$, respectively. Then, system (5.3) *with $r \in \mathcal{X}_d$, $p = T_1^\top \rho \in \mathbb{R}^{n_r - n_\lambda}$ and $\rho \in \mathbb{R}^{n_r}$ can be reduced to*

$$\begin{bmatrix}\dot{q}\\ \dot{p}\end{bmatrix} = \begin{bmatrix}0 & J_q(q)\\ -J_q^\top(q) & -T_1^\top \Gamma T_1\Big|_{r=h(q)}\end{bmatrix}\begin{bmatrix}\partial_q^\top H_d\\ \partial_p^\top H_d\end{bmatrix} \tag{5.9}$$

with

$$H_d(q,p) = \frac{1}{2} p^\top \Big(T_1^\top \mathcal{M}_d T_1\Big|_{r=h(q)}\Big)^{-1} p + \mathcal{V}_d(h(q)),$$
$$\Gamma = \partial_r(T^{-\top}p)\mathcal{J} - \mathcal{J}^\top \partial_r^\top (T^{-\top}p) + \mathcal{W},$$

if there exists a diffeomorphism $(r,\rho) \mapsto (r, T^\top \rho)$ and $q \mapsto h(q)$ s.t. $T = \begin{bmatrix}T_1 & T_2\end{bmatrix}$, $T_1 : \mathcal{X}_d \to \mathbb{R}^{n_r \times (n_r - n_\lambda)}$, $T_2 : \mathcal{X}_d \to \mathbb{R}^{n_r \times n_\lambda}$, $\mathcal{J} T_1|_{r=h(q)} = \partial_q h(q) J_q(q)$, $b_d^\top T_1 = 0$ and $b_d^\top T_2$ has full rank. ■

Proposition 5.5 is carried out for closed-loop systems of the form (5.3). However, the latter can be easily adapted for open-loop systems of the form (5.1), where $\mathcal{X}_d$, $\mathcal{J}(r)$ and $\mathcal{H}_d(r,\rho)$ are replaced by $\mathcal{X}$, I_{n_r} and $\mathcal{H}(r,\rho)$, respectively. Moreover, the implicit input matrix $\mathcal{G}$ is reduced to $G = T_1^\top \mathcal{G}$. Indeed, for holonomic systems with $J_q = I_{n_r - n_\lambda}$ the following is satisfied

$$T_1^\top \Gamma T_1 = \partial_q^\top (T_1^\top \rho) - (\partial_q T_1^\top \rho) = \sum_{i=1}^{n_r} \Big(\partial_q^\top (\partial_q^\top h_i) - \partial_q (\partial_q^\top h_i)\Big)\rho_i = 0,$$

where the first equality is obtained by using the chain rule and the last one results from the integrability condition of h (symmetric $\partial_q(\partial_q^\top h_i)$), with h_i as the i-th element of the column vector h.

[31] We perform the reduction from implicit to explicit coordinates.

5.2 Classical Energy-Based Control for Implicit UMS

This section provides an alternative approach to the typical energy-based control using a more general class of energy function for the control of UMSs in implicit PH representation. This approach is performed in two steps. First, we analyze the passivity properties of the system and identify its passive output. Second, we define a (generalized) admissible storage function for the stabilization at an energy level-set.

5.2.1 Passivity

Consider the constrained Hamiltonian equations (5.1) and its total mechanical energy (5.2). Then, taking the time-derivative of (5.2) along the trajectories of (5.1) yields

$$\dot{\mathcal{H}}(r,\rho) = \left(\partial_\rho \mathcal{H}\right) \mathcal{G}(r)\, u.$$

The operator $u \mapsto y := \mathcal{G}^\top \partial_\rho^\top \mathcal{H}$ is passive with storage function (5.2).[32]

5.2.2 Controller Design

Since the implicit UMS (5.1) is passive, with input u and output y, then the following assumption is introduced.

Assumption 5.2: *There exists a mapping $\eta : \mathbb{R}^{n_r} \to \mathbb{R}^{n_u}$ such that*

$$\left(\frac{\partial\, \eta(r)}{\partial r}\right)^\top = \mathcal{G}(r).$$

That is, there exists a function η such that $\dot{\eta} := y$.

Problem Formulation: *Find a mapping $u : \mathcal{X} \times \mathbb{R}^{n_r} \to \mathbb{R}^{n_u}$ such that the system* (5.1) *in closed-loop with the state-feedback control law u achieves*

$$\lim_{t\to\infty} \mathcal{H} = \mathcal{H}^\star, \qquad \lim_{t\to\infty} y = 0, \qquad \lim_{t\to\infty} f(\eta) = 0. \tag{5.10}$$

The goal is to stabilize the passive output y and reach the desired (or target) mechanical energy $\mathcal{H}^\star \in \mathbb{R}$ which imposes a restriction on the underactuated variables.

[32] From now on, we will consider a passive system (instead of cyclo-passive) since we assume $\mathcal{H}(r,\rho)$ is bounded from below.

We now recall the standard procedure of the classical energy-based control approach [6,9] for implicit UMSs of the form (5.1). Examine whether there exists a control law to achieve the control objectives in (5.10) via the following (generalized) function.[33]

$$\mathcal{U}(r,\rho) = \frac{1}{2}k_H\big(\mathcal{H}(r,\rho) - \mathcal{H}^\star\big)^2 + f(\eta) + \frac{1}{2}\| y \|^2_{K_\Omega}, \tag{5.11}$$

where $k_H \in \mathbb{R}$ is a positive constant, $K_\Omega \in \mathbb{R}^{n_u \times n_u}$ verifies $K_\Omega = K_\Omega^\top \succ 0$ and $f : \mathbb{R}^{n_u} \to \mathbb{R}$ such that $f(\eta) \geq 0$.

Taking the time-derivative of (5.11) along the trajectories of (5.1) yields

$$\dot{\mathcal{U}}(r,\rho) = y^\top \Big[k_H\big(\mathcal{H}(r,\rho) - \mathcal{H}^\star\big)u + \partial_\eta^\top f + K_\Omega\, \dot{y}\Big].$$

Selecting

$$k_H\big(\mathcal{H}(r,\rho) - \mathcal{H}^\star\big)u + \partial_\eta^\top f + K_\Omega\, \dot{y} = -K_\nabla\, y \tag{5.12}$$

for some $K_\nabla \in \mathbb{R}^{n_u \times n_u}$, $K_\nabla = K_\nabla^\top \succ 0$, results in

$$\dot{\mathcal{U}} = -\| y \|^2_{K_\nabla} \leq 0.$$

Now, it is discussed under what condition the controller u can be obtained from (5.12).

Taking the time-derivative of $y = \mathcal{G}^\top \partial_\rho^\top \mathcal{H}$ along the trajectories of (5.1) yields

$$\dot{y} = (\mathcal{G}^\top \mathcal{M}^{-1}\mathcal{G})u + (\mathcal{G}^\top \mathcal{M}^{-1} b)\lambda + \mathcal{N}_1(r,\rho), \tag{5.13}$$

where $\mathcal{N}_1(r,\rho) = \dot{\mathcal{G}}^\top \partial_\rho^\top \mathcal{H} + \mathcal{G}^\top \dot{\mathcal{M}}^{-1}\rho - \mathcal{G}^\top \mathcal{M}^{-1}\partial_r^\top \mathcal{H}$. Replacing (5.13) into (5.12) gives

$$\mathcal{N}_2(r,\rho)u + K_\Omega(\mathcal{G}^\top \mathcal{M}^{-1} b)\lambda = -K_\nabla\, y - \partial_\eta^\top f - K_\Omega\, \mathcal{N}_1(r,\rho), \tag{5.14}$$

where $\mathcal{N}_2(r,\rho) = k_H\big(\mathcal{H} - \mathcal{H}^\star\big) I_{n_u} + K_\Omega(\mathcal{G}^\top \mathcal{M}^{-1}\mathcal{G})$. From the hidden constraint (5.6), we get

$$(b^\top \mathcal{M}^{-1}\mathcal{G})u + \Delta(r)\lambda + \mathcal{N}_3(r,\rho) = 0, \tag{5.15}$$

where $\mathcal{N}_3(r,\rho) = \partial_r(b^\top \partial_\rho^\top \mathcal{H})\partial_\rho^\top \mathcal{H} - b^\top \mathcal{M}^{-1}\partial_r^\top \mathcal{H}$. Now, we can rewrite (5.14) and (5.15) in matrix notation as

$$\begin{bmatrix} \mathcal{N}_2(r,\rho) & K_\Omega(\mathcal{G}^\top \mathcal{M}^{-1} b) \\ b^\top \mathcal{M}^{-1}\mathcal{G} & \Delta(r) \end{bmatrix} \begin{bmatrix} u \\ \lambda \end{bmatrix} = - \begin{bmatrix} K_\nabla\, y + \partial_\eta^\top f + K_\Omega\, \mathcal{N}_1(r,\rho) \\ \mathcal{N}_3(r,\rho) \end{bmatrix},$$

[33] According to Definition 2.3, the function $\mathcal{U}$ does not necessarily qualify as a Lyapunov candidate function.

such that

$$u = -\begin{bmatrix} I_{n_u} & 0 \end{bmatrix} \begin{bmatrix} \mathcal{N}_2(r,\rho) & K_\Omega(\mathcal{G}^\top \mathcal{M}^{-1} b) \\ b^\top \mathcal{M}^{-1} \mathcal{G} & \Delta(r) \end{bmatrix}^{-1} \begin{bmatrix} K_\nabla\, y + \partial_\eta^\top f + K_\Omega \mathcal{N}_1(r,\rho) \\ \mathcal{N}_3(r,\rho) \end{bmatrix} \tag{5.16}$$

is free of singularities if

$$\det\left(\begin{bmatrix} \mathcal{N}_2(r,\rho) & K_\Omega(\mathcal{G}^\top \mathcal{M}^{-1} b) \\ b^\top \mathcal{M}^{-1} \mathcal{G} & \Delta(r) \end{bmatrix} \right) \neq 0, \qquad \forall\, (r,\rho). \tag{5.17}$$

Lemma 5.1 (Positive definite condition [9])**:** *If the total mechanical energy $\mathcal{H}$ of the system* (5.1) *is bounded from below, then there exists a positive parameter K_Ω such that*

$$\begin{bmatrix} \mathcal{N}_2(r,\rho) & K_\Omega(\mathcal{G}^\top \mathcal{M}^{-1} b) \\ b^\top \mathcal{M}^{-1} \mathcal{G} & \Delta(r) \end{bmatrix} \succ 0. \qquad \blacksquare$$

Subsequently, stability can be proved by invoking Theorem 2.2 to analyse the motion of the system (5.1) under the control law (5.16) with the aim of investigating whether the closed-loop solution satisfies the control objectives stated in the problem formulation.

Keep in mind that one application of this approach is to solve the swing-up control problem for the cart-pole system in implicit PH representation.

Chapter 6

Energy-Based Control for Implicit UMS: The Cart-Pole Analysis

This chapter provides the design, stability analysis and experimental validation of the control algorithms discussed in Chapter 5. The well-known benchmark cart-pole system is taken as a case study owing to its nonlinear, underactuated and non-minimum phase properties, which remain a topic of interest in the field of nonlinear control systems. The design of the nonlinear control scheme has been carried out on the basis of the implicit PH representation of the cart-pole system in SNF. This chapter is organized as follows. Section 6.1 provides the constrained PH representation for the cart-pole system and its formulation in SNF. Section 6.2 performs the design of a swing-up controller based on the classical energy-based control approach with mild modifications for the cart-pole system in SNF. The effectiveness of the nonlinear controller is verified by simulations and real-time experiments. Section 6.3 performs the design of a (local) stabilizing controller under a novel algebraic IDA-PBC technique, as well as the formulation of a novel approach to ensure an optimal (local) transient response. The effectiveness of the nonlinear controller is verified by simulations and real-time experiments. Section 6.4 describes the overall (implicit) control strategy for the cart-pole system in SNF. The chosen scheme is based on a two-stage control strategy, such that one controller will swing-up the pendulum and another will (locally) stabilize it. Section 6.5 presents comparative results, where the (implicit) control algorithms designed in this chapter are contrasted with the (explicit) control algorithms discussed in Chapter 4. All numerical simulations presented in the following were performed using MATLAB®/ Simulink (R2018a) platform.

6.1 Model Derivation

Consider the cart-pole system as shown in Figure 4.4 satisfying the following ideal assumptions.

- The pendulum is a point mass located at the top of the pole.
- There exists no Coulomb friction.

The parameters of the cart-pole system are shown in Table 4.2. Additionally, x_p and y_p denotes the pendulum displacements relative to the cart. The implicit model has a constraint $\phi = \frac{1}{2}\left(x_p^2 + y_p^2 - l^2\right)$ and (implicit) generalized coordinates $r = \mathrm{col}(x_p, y_p, x_c)$. To compute the Lagrangian function, we introduce the total kinetic and potential energy

$$\mathcal{K} = \frac{1}{2}(m_c + m_p)\dot{x}_c^2 + m_p\dot{x}_c\dot{x}_p + \frac{1}{2}m_p\dot{x}_p^2 + \frac{1}{2}m_p\dot{y}_p^2,$$
$$\mathcal{P} = m_p g_r(y_p - l),$$

respectively. We build the constrained EL equations of motion

$$\frac{\mathrm{d}}{\mathrm{d}t}\left(\frac{\partial \mathcal{L}}{\partial \dot{r}}\right)^\top - \left(\frac{\partial \mathcal{L}}{\partial r}\right)^\top = b(r)\lambda + \bar{\mathcal{G}}u - \bar{\mathcal{R}}\dot{r}, \tag{6.1}$$

where $\mathcal{L} = \mathcal{K} - \mathcal{P}$, $b(r) = \partial_r^\top \phi$, $\bar{\mathcal{G}} = \mathrm{col}(0, 0, 1)$ and $\bar{\mathcal{R}} = \bar{\mathcal{R}}^\top \succeq 0$ denotes natural damping. We rewrite (6.1) in matrix form as follows

$$\begin{bmatrix} M_{11} & M_{12} \\ M_{12}^\top & M_{22} \end{bmatrix}\begin{bmatrix} \ddot{r}_p \\ \ddot{r}_c \end{bmatrix} + \begin{bmatrix} \partial_{r_p}^\top \mathcal{P} \\ \partial_{r_c}^\top \mathcal{P} \end{bmatrix} = \begin{bmatrix} \partial_{r_p}^\top \phi \\ \partial_{r_c}^\top \phi \end{bmatrix}\lambda + \begin{bmatrix} 0 \\ 1 \end{bmatrix} u - \begin{bmatrix} \bar{r}_1 & 0 \\ 0 & \bar{r}_2 \end{bmatrix}\begin{bmatrix} \dot{r}_p \\ \dot{r}_c \end{bmatrix}, \tag{6.2}$$

where $r_p = \mathrm{col}(x_p, y_p)$, $r_c = x_c$, $M_{11} = \mathrm{diag}(m_p, m_p)$, $M_{12} = \mathrm{col}(m_p, 0)$, $M_{22} = m_c + m_p$ and $\bar{r}_1 = \mathrm{diag}(r_1, r_1)$. According to [37], we can transform (6.2) into

$$\begin{bmatrix} M_{11} & 0 \\ 0 & 1 \end{bmatrix}\begin{bmatrix} \ddot{r}_p \\ \ddot{r}_c \end{bmatrix} + \begin{bmatrix} \partial_{r_p}^\top \mathcal{P} \\ 0 \end{bmatrix} = \begin{bmatrix} \partial_{r_p}^\top \phi \\ 0 \end{bmatrix}\lambda + \begin{bmatrix} -M_{12} \\ 1 \end{bmatrix}\upsilon - \begin{bmatrix} \bar{r}_1 & 0 \\ 0 & 0 \end{bmatrix}\begin{bmatrix} \dot{r}_p \\ \dot{r}_c \end{bmatrix}. \tag{6.3}$$

System (6.3) takes the so-called SNF and can be transformed into the constrained PH representation, with no natural damping, as follows

$$\begin{bmatrix} \dot{r} \\ \dot{\rho} \end{bmatrix} = \begin{bmatrix} 0 & I_3 \\ -I_3 & 0 \end{bmatrix}\begin{bmatrix} \partial_r^\top \mathcal{H} \\ \partial_\rho^\top \mathcal{H} \end{bmatrix} + \begin{bmatrix} 0 \\ b(r) \end{bmatrix}\lambda + \begin{bmatrix} 0 \\ \mathcal{G} \end{bmatrix}\upsilon, \tag{6.4a}$$

$$b^\top(r)\partial_\rho^\top \mathcal{H} = 0, \tag{6.4b}$$

with total stored energy

$$\mathcal{H}(r,\rho) = \frac{1}{2}\rho^\top \mathcal{M}^{-1}\rho + \mathcal{V}(r), \tag{6.5}$$

where the inertia matrix, potential energy and input vector are now given by

$$\mathcal{M} = I_3, \qquad \mathcal{V}(r) = g_r(y_p - l), \qquad \mathcal{G} = \begin{bmatrix} -1 & 0 & 1 \end{bmatrix}^\top, \tag{6.6}$$

respectively. The potential energy has been initially chosen to be zero at the origin, i.e. $\mathcal{V}(0) = 0$, and is clearly bounded from below.

System (6.4) has a subset of two equilibrium points, where

- $r = \text{col}(0, -l, x_c^\star)$ and $\rho = 0$ is the stable equilibrium point; and
- $r = \text{col}(0, \ \ l, x_c^\star)$ and $\rho = 0$ is the unstable equilibrium point,

with $x_c^\star$ set as an arbitrary target value for the cart position.

6.2 Implicit Swing-Up Controller

Note: For the sake of convenience, here and throughout the rest of this section, we will use $\dot{r}$ instead of ρ. Since $\dot{r} = \mathcal{M}^{-1}\rho$ and $\mathcal{M} = I_3$ gives $\dot{r} = \rho$.

This section deals with the tracking of homoclinic orbits (limit cycles) that contains the desired (unstable) equilibrium of the system.[34] Consider an ideal cart-pole system (massless bar) in SNF given by (6.4) and assume there is no friction, i.e. $r_1 = 0$.

Problem Formulation: *Find a mapping $\upsilon : \mathcal{X} \times \mathbb{R}^3 \to \mathbb{R}$ such that the trajectories of the pendulum can be brought into a homoclinic orbit (limit cycle) reaching the desired energy level-set $\bar{\mathcal{E}} \to \bar{\mathcal{E}}^\star$ and holding the cart stable at the target position $x_c \to x_c^\star$ with $\dot{x}_c \to 0$.*

[34] For the formal explanation of the homoclinic orbit, see Definition 4.1.

Under the design procedure described in Section 5.2, we proceed to analyze the passivity properties of the system. The mechanical energy from (6.5) can be rewritten as

$$\mathcal{E}(r,\dot{r}) = \frac{1}{2}\dot{r}^\top \mathcal{M}(r)\dot{r} + \mathcal{V}(r). \tag{6.7}$$

Taking the time-derivative of (6.7) along the trajectories of the system (6.4) yields $\dot{\mathcal{E}} = \dot{r}^\top \mathcal{G} v$. The operator $v \mapsto y \coloneqq \mathcal{G}^\top \dot{r}$ is passive with storage function (6.7).

Following Section 5.2, we can synthesize a control law but the requirements of the *problem formulation* are not met because the system (6.4) is passive with a combined output of actuated and underactuated variables, i.e., $y = -\dot{x}_p + \dot{x}_c$. Therefore, we introduce a mild modification in order to stabilize the cart position x_c instead of y.

6.2.1 New Energy Function

This section focuses on finding a new energy function $\bar{\mathcal{E}} = \mathcal{E} + \mathcal{E}_\mu$, which allows to fulfill the requirements of the *problem formulation*.[35]

Let $\bar{\mathcal{E}} : \mathcal{X} \times \mathbb{R}^3 \to \mathbb{R}$ be the new (open-loop) energy function defined as

$$\bar{\mathcal{E}}(r,\dot{r}) = \frac{1}{2}\dot{r}^\top \bar{\mathcal{M}}(r)\dot{r} + \mathcal{V}(r), \tag{6.8}$$

where

$$\bar{\mathcal{M}}(r) = \begin{bmatrix} 1 & 0 & 1 \\ 0 & 1 & 0 \\ 1 & 0 & k_c \end{bmatrix}, \qquad \mathcal{V}(r) = g_r\,(y_p - l)$$

and $k_c \in \mathbb{R}$ is a strictly positive constant. Clearly, $\bar{\mathcal{M}}(r) = \bar{\mathcal{M}}^\top(r) \succ 0$ if and only if $k_c > 1$. The new energy function $\bar{\mathcal{E}}$, which is slightly different from the original mechanical energy $\mathcal{E}$, takes similarly a constant value for each equilibrium point, i.e.,

- $\bar{\mathcal{E}}(r,\dot{r}) = 0$ at the unstable equilibrium point and
- $\bar{\mathcal{E}}(r,\dot{r}) = -2g_r l$ at the stable equilibrium point.

[35] We define $\mathcal{E}_\mu : \mathcal{X} \times \mathbb{R}^3 \to \mathbb{R}$ as $\mathcal{E}_\mu(r,\dot{r}) \coloneqq \dot{x}_p\dot{x}_c + \frac{1}{2}(k_c - 1)\dot{x}_c^2$.

6.2.2 Stabilization around the Homoclinic Orbit

Let us verify that the new energy (6.8) is a suitable function for the controller design. In view of (6.8), if the system (6.4) reaches $\bar{\mathcal{E}} = 0$ and $\dot{x}_c = 0$, then

$$\frac{1}{2}\left(\dot{x}_p^2 + \dot{y}_p^2\right) = g_r\,(l - y_p) \tag{6.9}$$

represents a particular trajectory that corresponds to a homoclinic orbit.[36] In general, if the system can be brought to the homoclinic orbit (6.9), then the task of swinging-up the pendulum has been solved. This means that the pendulum will eventually get close to its unstable equilibrium point if it follows the homoclinic orbit.

Based on (6.8), a new controller is derived in order to approach the trajectories of the pendulum into the homoclinic orbit (6.9). Define the target storage function as[37]

$$\mathcal{U}(r, \dot{r}) = \frac{1}{2}k_{\mathcal{E}}(\bar{\mathcal{E}} - \bar{\mathcal{E}}^{\star})^2 + \frac{1}{2}k_{\phi}(x_c - x_c^{\star})^2 + \frac{1}{2}K_{\Omega}\,\dot{x}_c^2, \tag{6.10}$$

where $k_{\mathcal{E}}$, k_{ϕ}, $K_{\Omega} \in \mathbb{R}$ are strictly positive constants, $x_c^{\star} \in \mathbb{R}$ is the target cart position and $\bar{\mathcal{E}}^{\star} \in \mathbb{R}$ is the non-negative target energy fixed as $\bar{\mathcal{E}}^{\star} = 0$.

Taking the time-derivative of (6.10) along the trajectories of (6.4) yields

$$\dot{\mathcal{U}}(r, \dot{r}) = \dot{x}_c\Big[\big[k_{\mathcal{E}}(\bar{\mathcal{E}} - \bar{\mathcal{E}}^{\star})\beta + K_{\Omega}\big]\upsilon + k_{\mathcal{E}}(\bar{\mathcal{E}} - \bar{\mathcal{E}}^{\star})\alpha + k_{\phi}(x_c - x_c^{\star})\Big], \tag{6.11}$$

where $\alpha(r, \dot{r}) = x_p(g_r y_p - \dot{x}_p^2 - \dot{y}_p^2)/l^2$ and $\beta(r) = k_c - y_p^2/l^2$. Clearly, $\beta(r) > 0$ if and only if $k_c > 1$.

One can choose υ such that

$$\Big[k_{\mathcal{E}}(\bar{\mathcal{E}} - \bar{\mathcal{E}}^{\star})\beta + K_{\Omega}\Big]\upsilon + k_{\mathcal{E}}(\bar{\mathcal{E}} - \bar{\mathcal{E}}^{\star})\alpha + k_{\phi}(x_c - x_c^{\star}) = -K_{\nabla}\,\dot{x}_c \tag{6.12}$$

for some strictly positive constant $K_{\nabla} \in \mathbb{R}$, which leads to

$$\dot{\mathcal{U}}(r, \dot{r}) = -K_{\nabla}\,\dot{x}_c^2. \tag{6.13}$$

Moreover, the singularities in (6.12) are avoided provided that

$$\Big|k_{\mathcal{E}}(\bar{\mathcal{E}} - \bar{\mathcal{E}}^{\star})\beta + K_{\Omega}\Big| \neq 0, \qquad \forall\,(r, \dot{r}).$$

[36] Via reduction to explicit coordinates, (6.9) is equivalent to (4.6).
[37] Also known as (generalized) admissible energy function or (generalized) admissible storage function.

According to Lemma 3.1, the expression above holds if the following lower bound constraint for K_Ω is fulfilled

$$K_\Omega > (2g_r l + \bar{\mathcal{E}}^\star) k_\mathcal{E} \max_r(\beta) \quad \Rightarrow \quad K_\Omega > (2g_r l + \bar{\mathcal{E}}^\star) k_\mathcal{E} k_c. \tag{6.14}$$

Now, the control law υ can be rewritten from (6.12) as

$$\upsilon(r, \dot{r}) = -\frac{K_\nabla \, \dot{x}_c + k_\mathcal{E}(\bar{\mathcal{E}} - \bar{\mathcal{E}}^\star)\alpha + k_\phi(x_c - x_c^\star)}{k_\mathcal{E}(\bar{\mathcal{E}} - \bar{\mathcal{E}}^\star)\beta + K_\Omega}. \tag{6.15}$$

6.2.3 Stability Analysis

In view of (6.13) is negative semi-definite and the homoclinic orbit is not an isolated equilibrium point, the stability analysis will be performed based on LaSalle's invariance principle, see Theorem 2.2.[38] Since $\mathcal{U}$ in (6.10) is a non-increasing function, see (6.13), every solution of the system (6.4) in closed-loop with (6.15) starts in Ω_I and remains in Ω_I for all $t \geq 0$. The set Ω_I is defined as

$$\Omega_I = \Big\{(r, \dot{r}) \in \mathcal{X} \times \mathbb{R}^3 \mid b^\top \partial_\rho^\top \mathcal{H} = 0, \ \phi = 0, \ \mathcal{U}(r, \dot{r}) \leq c\Big\},$$

where c is an appropriate positive constant, such that Ω_I is closed and bounded.[39] Let Γ_I be the set of all points in Ω_I such that $\dot{\mathcal{U}} = 0$. The set Γ_I is defined as

$$\Gamma_I = \Big\{(r, \dot{r}) \in \Omega_I \mid \dot{\mathcal{U}} = 0\Big\}.$$

Let $\mathbb{M}_I$ be the largest invariant set in Γ_I. Via LaSalle's theorem every solution starting in Ω_I approaches $\mathbb{M}_I$ as $t \to \infty$.

Since $\dot{\mathcal{U}} = 0$ holds identically in Γ_I. From (6.13), if $\dot{\mathcal{U}} = 0$, then $\dot{x}_c = 0$, $\mathcal{U} = \text{const.}$, $x_c = \text{const.}$ and $\ddot{x}_c = \upsilon = 0$ in Γ_I. Using (6.10), it is clear that $\bar{\mathcal{E}} = \text{const.}$ in Γ_I. The resulting constants can be summarized as

$$\bar{\mathcal{E}} = \text{const.}, \qquad x_c = \text{const.}, \qquad \dot{x}_c = 0, \qquad \upsilon = 0. \tag{6.16}$$

From (6.15) and (6.16), it follows that the control law has been chosen such that

$$0 = k_\mathcal{E}(\bar{\mathcal{E}} - \bar{\mathcal{E}}^\star)\alpha + k_\phi(x_c - x_c^\star). \tag{6.17}$$

[38] LaSalle's invariance principle can be used when, instead of an isolated equilibrium point, the system has an equilibrium set [15].

[39] The states of (6.4a) are bounded given the constraint (6.4b), see Proposition 5.1.

Now, it is evident that $(\bar{\mathcal{E}} - \bar{\mathcal{E}}^\star)\alpha$ must be constant in Γ_I. Since $\bar{\mathcal{E}}$ is also constant and $\bar{\mathcal{E}}^\star$ is fixed to be 0, two cases are discussed below.

- $\underline{\bar{\mathcal{E}} = 0}$: This is the simplest case. Here, $x_c = x_c^\star$. Recall that $\bar{\mathcal{E}} = 0$ means that the trajectories of the pendulum are in the homoclinic orbit (6.9).

- $\underline{\bar{\mathcal{E}} \neq 0}$: In this case, the only solution for α is to be a constant in Γ_I. Besides, using (6.8) we can rewrite α as $\alpha(x_p, y_p) = x_p \left[3g_r y_p - \bar{d}\right]/l^2$, where $\bar{d} = 2(\mathcal{E} + g_r l)$. Analyzing (6.4), shows that if $\upsilon = 0$, then the cart-pole dynamics (6.4) is reduced to a simple pendulum. Therefore, if and only if the pendulum gets stuck at the equilibrium points, then α is constant and equal to 0. Hence, $x_c = x_c^\star$. Note that, at the unstable equilibrium point it is implied that $\bar{\mathcal{E}} = 0$, which is a contradiction. The other equilibrium point may be avoided by including the following assumption.

Assumption 6.1: *To avoid the pendulum get stuck at the downward (stable) position, it is imposed that the new energy $\bar{\mathcal{E}}(r, \dot{r}) > -2g_r l$, for all $(r, \dot{r})$.*

Assumption 6.1 implies that a nonzero initial value must be assigned to the new kinetic energy in (6.8), i.e., $x_p(0) = 0$ and $y_p(0) = -l$ (downward pendulum position) is admissible if and only if $\dot{x}_p(0) \neq 0$ and $\dot{y}_p(0) = 0$. From the above, it is concluded that (6.17) is fulfilled only when $\bar{\mathcal{E}} = 0$, $x_c = x_c^\star$ and $\dot{x}_c = 0$.

Finally, the largest invariant set $\mathbb{M}_I$ in Γ_I is given by

$$\mathbb{M}_I = \left\{(r, \dot{r}) \in \Omega_I \mid \dot{x}_p^2 + \dot{y}_p^2 = 2g_r(l - y_p),\ x_c = x_c^\star,\ \dot{x}_c = 0\right\}.$$

From LaSalle's invariance principle, it has been proved that the control law (6.15) bring the system (6.4) for any $(r, \dot{r}) \in \Omega_I$ to the invariant set $\mathbb{M}_I$, starting and remaining in Ω_I. Recall that, Theorem 2.2 refers to those sets Ω_I that are compact (closed and bounded), nothing can be said for those sets Ω_I that are not compact.

6.2.4 Damping Injection

In order to improve convergence (physically motivated), with no compromising stability, the well-known damping injection method can be used. The control input υ is set as

$$\upsilon \coloneqq \upsilon + \hat{\upsilon}. \tag{6.18}$$

To prove the passivity of the closed-loop it suffices to compute (6.11) with (6.18). Solving for $\hat{\upsilon}$ yields

$$\dot{\mathcal{U}}(r, \dot{r}) = \dot{x}_c \Big[k_{\mathcal{E}} (\bar{\mathcal{E}} - \bar{\mathcal{E}}^\star)\beta + K_\Omega \Big] \hat{\upsilon}.$$

Define the input $\hat{\upsilon}$ and the output $\hat{y} \coloneqq \dot{x}_c \Big[k_{\mathcal{E}} (\bar{\mathcal{E}} - \bar{\mathcal{E}}^\star)\beta + K_\Omega \Big]$. The operator $\hat{\upsilon} \mapsto \hat{y}$ is passive with storage function (6.10).

Notice that $\dot{x}_c \hat{y} \geq 0$, then the damping injection can be formulated as $\hat{\upsilon} = -k_y \dot{x}_c$, where $k_y \in \mathbb{R}$ is a strictly positive constant.

6.2.5 Simulation Results

Consider the parameters of the cart-pole system from Table 4.1, with no friction, i.e., $r_1 = 0$. The tuning gains are chosen as shown in Table 6.1. These gains satisfy the inequality in (6.14). The desired cart position is set to $x_c^\star = 0$ with target energy $\bar{\mathcal{E}}^\star = 0$. The objective is to swing-up the pendulum from the initial states $x_p(0) = 0$, $y_p(0) = -l$, $x_c(0) = 0$, $\dot{x}_p(0) = -l\pi/180$, $\dot{y}_p(0) = 0$ and $\dot{x}_c(0) = 0$. These initial conditions satisfy Assumption 6.1.

k_c	$k_{\mathcal{E}}$	k_ϕ	K_Ω	K_∇	k_y
2	1	100	20	0	4

Table 6.1 – Parameters of the implicit swing-up controller

Figure 6.1 depicts the phase portraits of $(x_p, \dot{x}_p)$ and $(y_p, \dot{y}_p)$ and the time responses of x_c, $\dot{x}_c$, $\mathcal{U}$ and $\bar{\mathcal{E}} - \bar{\mathcal{E}}^\star$ under the swing-up control problem. Simulations show that the controller (6.15) brings the trajectories of the pendulum into the homoclinic orbit (6.9) fulfilling the requirements stated in the *problem formulation*, i.e., $\bar{\mathcal{E}} \to \bar{\mathcal{E}}^\star$, $x_c \to x_c^\star$ and $\dot{x}_c \to 0$.

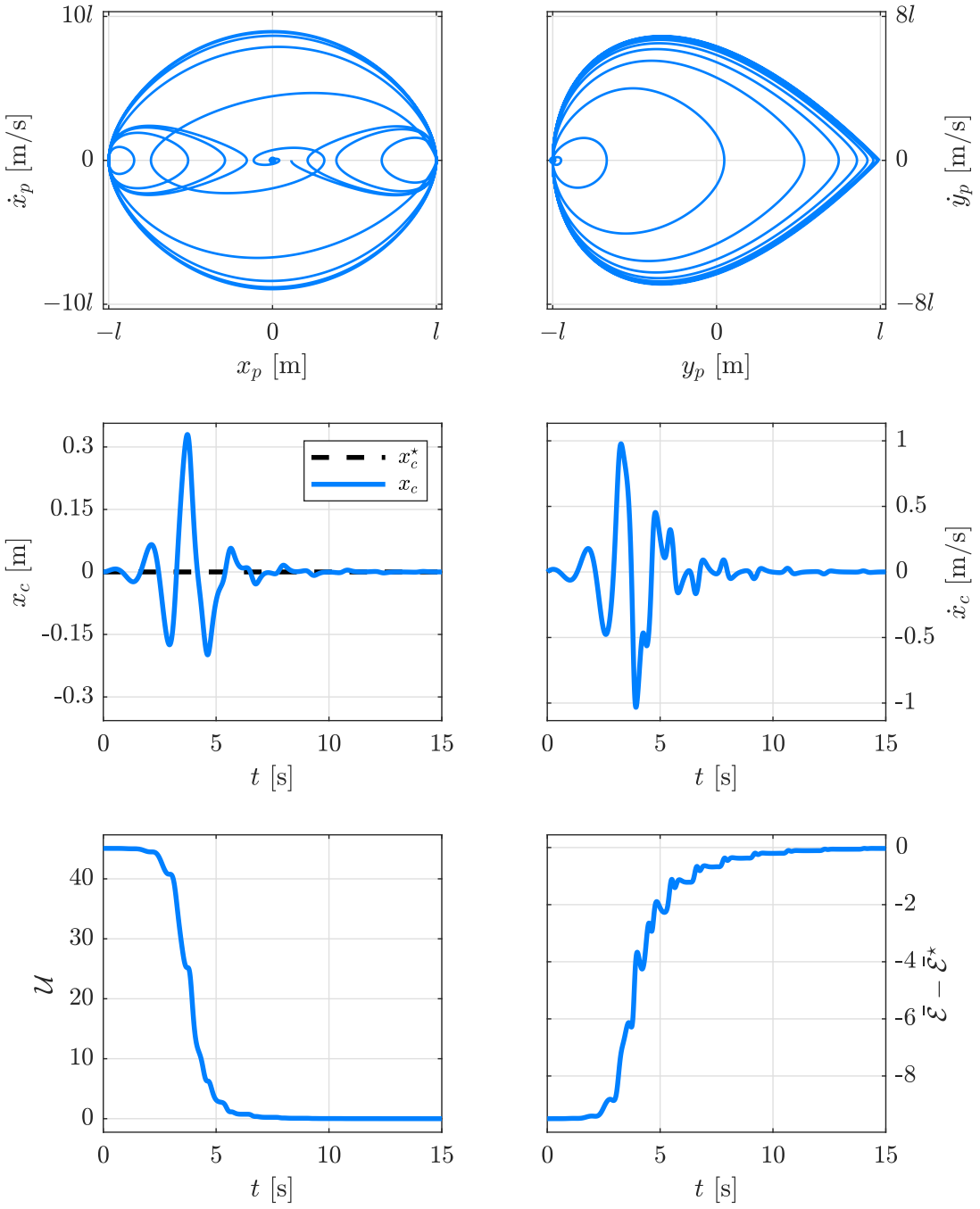

Figure 6.1 – Simulation results with no damping

6.2.6 Experimental Validation

Real-time experiments are contrasted with simulations including damping in the cart-pole dynamics. Consider the parameters of the cart-pole system from Table 4.1, including

friction, and the controller parameters from Table 6.1. The target values and initial conditions are the same as in the previous section.

Figure 6.2 depicts the phase portraits of $(x_p, \dot{x}_p)$ and $(y_p, \dot{y}_p)$ for a given $\bar{\mathcal{E}}^\star = 0$, where unmodeled dynamics, e.g. friction, impede the increase in amplitude of x_p, $\dot{x}_p$, y_p and $\dot{y}_p$. To reduce the effect of the friction and other unmodeled dynamics, we study the effectiveness of positive energy $\bar{\mathcal{E}}(r, \dot{r})$.

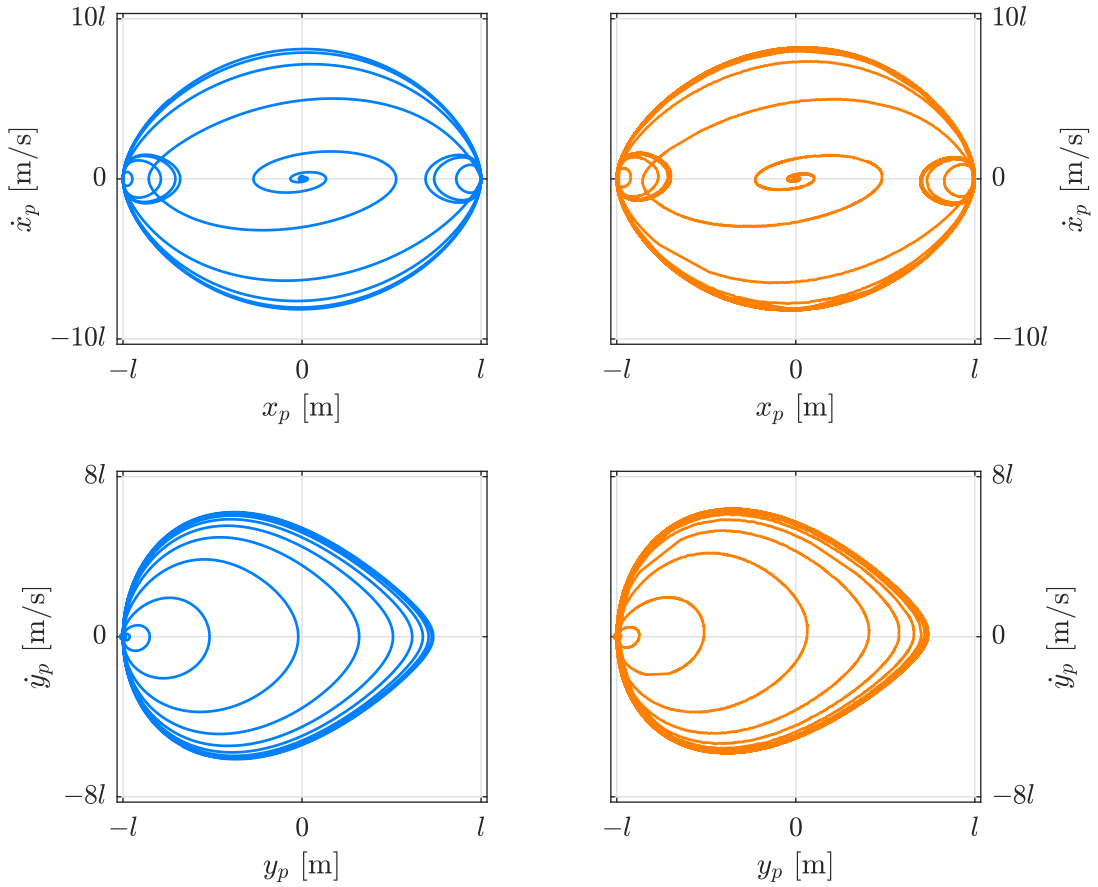

Figure 6.2 – Simulation (blue) and experimental (red) results with damping

According to [6, 41], a good practical approach is to choose a target energy $\bar{\mathcal{E}}^\star > 0$ such that the trajectories of the pendulum reach the homoclinic orbit (6.9).

Now, consider the same controller parameters and set the target energy as $\bar{\mathcal{E}}^\star = 1.44$. Figure 6.3 depicts that x_c, $\dot{x}_c$ and $\bar{\mathcal{E}}$ remain bounded near to their target values.

As shown in Figure 6.4, the controller (6.15) brings the trajectories of the pendulum into the homoclinic orbit (6.9).

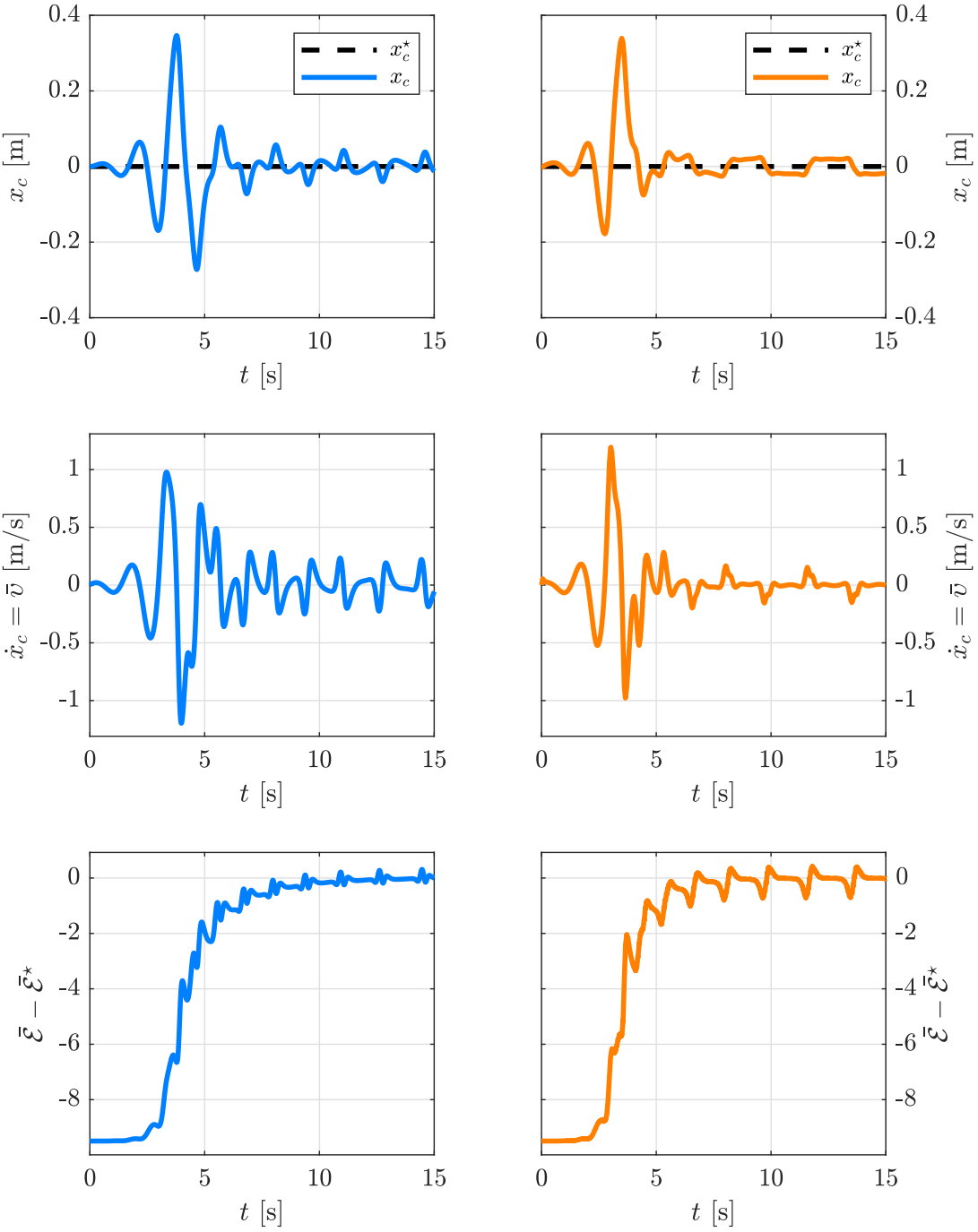

Figure 6.3 – Simulation (blue) and experimental (red) results with damping

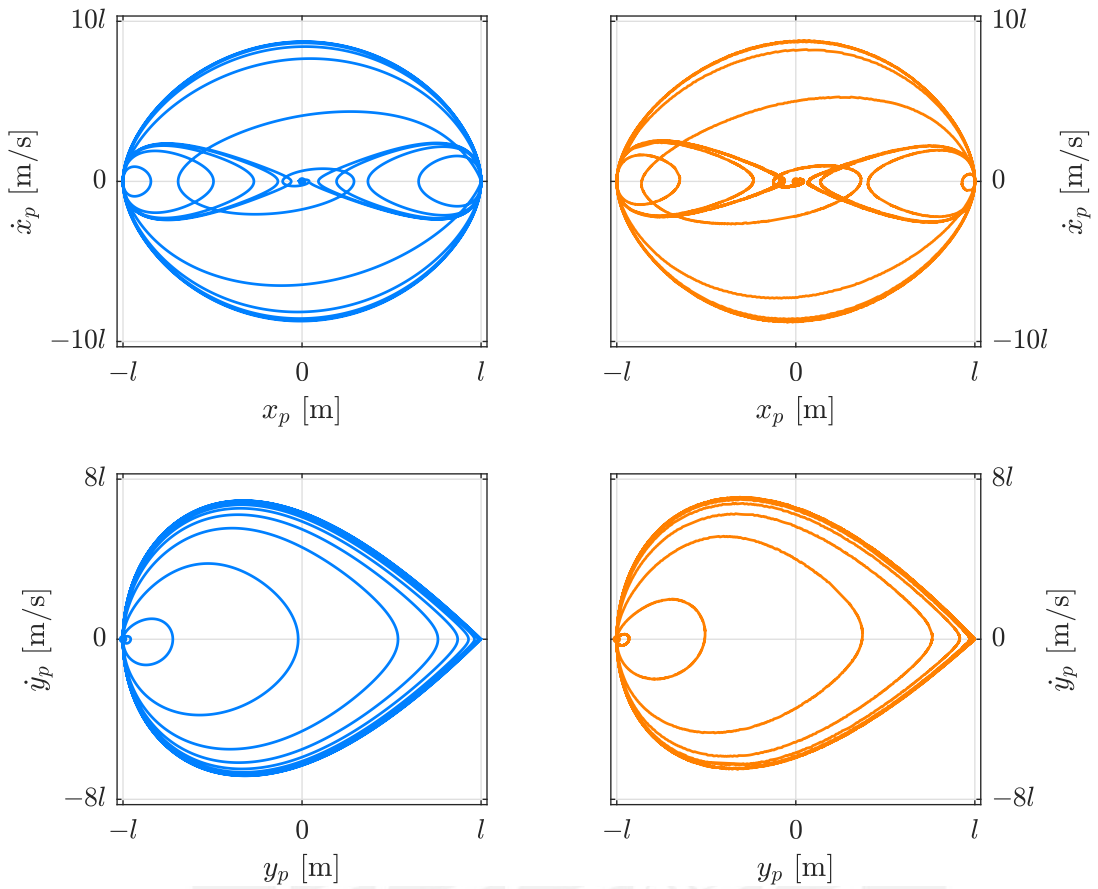

Figure 6.4 – Simulation (blue) and experimental (red) results with damping

6.3 Implicit IDA-PBC

This section deals with the (local) stabilization at the unstable equilibrium point of the cart-pole system in implicit PH representation. A novel algebraic IDA-PBC [10] technique is performed for the cart-pole system in SNF.

6.3.1 Controller Design

Consider an ideal cart-pole system (massless bar) in SNF given by (6.4) and assume there is no friction, i.e., $r_1 = 0$. We now select $r^\star = \begin{bmatrix} 0 & l & x_c^\star \end{bmatrix}^\top \in \mathcal{X}_a$ which denotes the upright (unstable) position.

Problem Formulation: *Find a mapping $\upsilon : \mathcal{X} \times \mathbb{R}^3 \to \mathbb{R}$ such that it stabilizes the upright vertical position of the pendulum and places the cart at any arbitrary position. Consider the desired equilibrium $r^\star \in \mathcal{X}_a$, where $x_c^\star \in \mathbb{R}$ is the only constant assignable equilibrium point.*

We shall test Proposition 5.4. First, we compute $b = \partial_r^\top \phi = \begin{bmatrix} x_p & y_p & 0 \end{bmatrix}^\top$ and $b^\star = b(r^\star) = \begin{bmatrix} 0 & l & 0 \end{bmatrix}^\top$, S is found via $S = \begin{bmatrix} \mathcal{G} & b \end{bmatrix}$ and the full rank left annihilator of S and $b^\star$ are given by

$$S_\perp = \begin{bmatrix} y_p & -x_p & y_p \end{bmatrix}, \qquad b_\perp^\star = \begin{bmatrix} 1 & 0 & 0 \\ 0 & 0 & 1 \end{bmatrix},$$

respectively. Second, collect and match the coefficients from (5.7a), we obtain

$$D\mu^\star l^3 + g_r = 0, \tag{6.19a}$$
$$D\mu^\star l^2 (c_1 + c_2) = 0, \tag{6.19b}$$

where c_i is an element located in the i-th row of vector $C \in \mathbb{R}^2$, for $i = \{1, 2\}$. Clearly, from (6.19b) we can choose $c_1 = 0$ and $c_2 = 0$, and from (6.19a) yields $D = \frac{D_x}{l^2}$ and $\mu^\star = -\frac{g_r}{D_x l}$, for some constant D_x. Next, from (5.7b) we get

$$c_1 D\, l = 0, \tag{6.20a}$$
$$c_1^2 D + c_1 c_2 D - D\, l^2 + a_{11} + a_{12} = 0, \tag{6.20b}$$
$$c_1 D\, l + c_2 D\, l = 0, \tag{6.20c}$$

where a_{ij} is an element located in the i-th row and j-th column of matrix $A \in \mathbb{R}^{2\times 2}$, for $i, j = \{1, 2\}$. Clearly, from (6.20b) yields $a_{12} = D_x - a_{11}$. We define $a_1 \coloneqq a_{11}$ and $a_2 \coloneqq a_{22}$. Thus, the resulting matrices are summarized as

$$A = \begin{bmatrix} a_1 & D_x - a_1 \\ D_x - a_1 & a_2 \end{bmatrix}, \qquad C = \begin{bmatrix} 0 \\ 0 \end{bmatrix}, \qquad D = \frac{D_x}{l^2}, \qquad \mu^\star = -\frac{g_r}{D_x l}$$

for some constants a_1, a_2 and D_x. Third, we compute $B^\star = \begin{bmatrix} b_\perp^{\star\top} & b^\star \end{bmatrix}$ and the target inertia matrix is given by

$$\mathcal{M}_d = \begin{bmatrix} a1 & 0 & D_x - a_1 \\ 0 & D_x & 0 \\ D_x - a_1 & 0 & a_2 \end{bmatrix}.$$

Then, we pick $S\bar{S} = \mathcal{G}$, which satisfies (5.7c) with full rank Z, and select $Z_\perp = \begin{bmatrix} 1 & 1 \end{bmatrix}$. Fourth, from (5.7d) and (5.8b) we realize that $D_x < 0$ and $K_\psi > 0$, respectively. Then, according to (5.8a) a suitable choice for $\mathcal{W}_1$ is $\mathcal{W}_1 = 0$. At this point, we compute $\psi = -\bar{S}^\top S^\top \mathcal{M}_d^{-1} \mathcal{M}\, \tilde{r}$ and the target potential energy function is given by

$$\mathcal{V}_d = \frac{1}{2} K_\psi \frac{\left[D_x(x_c^\star - x_c) + (D_x - a_1 + a_2)x_p\right]^2}{\left[(2D_x - a_1 + a_2)a_1 - D_x^2\right]^2} + \frac{1}{D_x} g_r (y_p - l).$$

Finally, all conditions of Proposition 5.4 are satisfied and we can directly compute the implicit state-feedback control law via (5.5), which is rewritten as follows

$$\upsilon = S^\dagger \Big(\partial_r^\top \mathcal{H} - \mathcal{J}^\top \partial_r^\top \mathcal{H}_d - \mathcal{W} \partial_\rho^\top \mathcal{H}_d + \mathcal{J}^\top b \lambda_d \Big), \tag{6.21}$$

where $S^\dagger = \begin{bmatrix} 1 & 0 \end{bmatrix} (S^\top S)^{-1} S^\top$, $\mathcal{W} = \frac{1}{2}\mathcal{W}_1 + S K_u S^\top$, $\mathcal{J} = \mathcal{M}^{-1}\mathcal{M}_d$ and the implicit variable λ_d is calculated via the hidden constraint (5.6). Stability in a neighborhood of $x^\star = (r^\star, 0)$ is guaranteed by selection of

$$A \succ 0, \qquad D_x < 0, \qquad K_\psi > 0 \qquad \text{and} \qquad K_u + K_u^\top \succeq 0. \tag{6.22}$$

6.3.2 Local Optimal Controller

Proposition 5.5 is easily adapted to systems of the form (6.4), where $\mathcal{X}_d$, $\mathcal{J}$ and $\mathcal{H}_d$ are replaced by $\mathcal{X}$, I_3 and $\mathcal{H}$, respectively. Consider $r = h(q) = \begin{bmatrix} l\sin\theta & l\cos\theta & x_c \end{bmatrix}^\top$, $q = \begin{bmatrix} \theta & x_c \end{bmatrix}^\top$, $J_q = I_2$, $T_1 = I_3^{-1}\, \partial_q h\, I_2$, $M = \left(T_1^\top \mathcal{M}\, T_1\right)\Big|_{r=h(q)}$, $V = \mathcal{V}(h(q))$ and $G = T_1^\top \mathcal{G}$, we obtain[40]

$$M(q) = \begin{bmatrix} l^2 & 0 \\ 0 & 1 \end{bmatrix}, \qquad V(q) = g_r l(\cos\theta - 1), \qquad G(q) = \begin{bmatrix} -l\cos\theta \\ 1 \end{bmatrix}. \tag{6.23}$$

From this result we can construct the nominal system in explicit PH representation

$$\begin{bmatrix} \dot{q} \\ \dot{p} \end{bmatrix} = \begin{bmatrix} 0 & I_2 \\ -I_2 & 0 \end{bmatrix} \begin{bmatrix} \partial_q^\top H \\ \partial_p^\top H \end{bmatrix} + \begin{bmatrix} 0 \\ G(q) \end{bmatrix} \upsilon, \tag{6.24}$$

with total stored energy $H(q,p) = \frac{1}{2} p^\top M^{-1}(q) p + V(q)$.

[40] Since Γ is not relevant for the open-loop reduction, we avoid T_2.

System (6.24) can be transformed into the explicit EL representation

$$M(q)\ddot{q} + C(q,\dot{q})\dot{q} + \partial_q^\top V = G(q)\upsilon. \tag{6.25}$$

Solving for $\ddot{q}$ and defining the state vector $\mathbf{x} \in \mathbb{R}^4$ as $\mathbf{x} = \text{col}(q, \dot{q}) = \text{col}(\theta, x_c, \dot{\theta}, \dot{x}_c)$ and the control input $\upsilon \in \mathbb{R}$. Makes clear that (6.25) can be represented by the following affine nonlinear state-space equation $\dot{\mathbf{x}} = f(\mathbf{x}) + g(\mathbf{x})\upsilon$, for some $f, g : \mathbb{R}^4 \to \mathbb{R}^4$.

Consider the linearization of the nominal system (6.25) in closed-loop with (6.21)

$$\begin{aligned}\dot{\tilde{\mathbf{x}}} &= \left.\frac{\partial \left[f(\mathbf{x}) + g(\mathbf{x})\upsilon_{IDA}(\mathbf{x})\right]}{\partial \mathbf{x}}\right|_{\mathbf{x}=\mathbf{x}^\star} \tilde{\mathbf{x}} \\ &= \left.\frac{\partial f(\mathbf{x})}{\partial \mathbf{x}}\right|_{\mathbf{x}=\mathbf{x}^\star} \tilde{\mathbf{x}} + g(\mathbf{x})\Big|_{\mathbf{x}=\mathbf{x}^\star} \left.\frac{\partial \upsilon_{IDA}(\mathbf{x})}{\partial \mathbf{x}}\right|_{\mathbf{x}=\mathbf{x}^\star} \tilde{\mathbf{x}},\end{aligned}$$

where $\tilde{\mathbf{x}} = \mathbf{x} - \mathbf{x}^\star$ and the desired equilibrium $\mathbf{x}^\star = \text{col}(q^\star, 0) = \text{col}(0, x_c^\star, 0, 0)$. The state matrix, input-to-state matrix and (linear) feedback gain vector are provided by

$$\mathbf{A} = \left.\frac{\partial f(\mathbf{x})}{\partial \mathbf{x}}\right|_{\mathbf{x}=\mathbf{x}^\star}, \qquad \mathbf{B} = g(\mathbf{x})\Big|_{\mathbf{x}=\mathbf{x}^\star}, \qquad \mathbf{K}_{LIN} = \left.\frac{\partial \upsilon_{IDA}(\mathbf{x})}{\partial \mathbf{x}}\right|_{\mathbf{x}=\mathbf{x}^\star},$$

respectively.[41] As discussed in Section 4.4.2, we can perform the optimal LQR method. The procedure for calculating the unknown parameters of (6.21) with optimal (local) transient response is summarised in the following algorithm.

Require: The linearization of the nominal system (6.25) in closed-loop with (6.21)
1: Determine $\mathbf{A}$, $\mathbf{B}$ and $\mathbf{K}_{LIN}$
2: Check whether the pair $(\mathbf{A}, \mathbf{B})$ is controllable
3: Find $\mathbf{K}_{LQR}$ for the linearized system $\dot{\tilde{\mathbf{x}}} = \mathbf{A}\tilde{\mathbf{x}} + \mathbf{B}\upsilon$ via the LQR method with suitable weighting matrices $\mathbf{Q} = \mathbf{Q}^\top \succeq 0$ and $\mathbf{R} = \mathbf{R}^\top \succ 0$
4: Calculate the unknown parameters of υ_{IDA} using $\mathbf{K}_{LIN} = -\mathbf{K}_{LQR}$

Algorithm 6.1 – Algorithm for optimal local gains

6.3.3 Stability Analysis

Since, at the equilibrium point, the system (6.25) in feedback with (6.21) is (locally) equivalent to $\dot{\tilde{\mathbf{x}}} = (\mathbf{A} - \mathbf{B}\mathbf{K}_{LQR})\tilde{\mathbf{x}}$, then asymptotic stability can be verified invoking Theorem 2.3.

[41] To find $\upsilon_{IDA}(\mathbf{x})$, we compute $\dot{r}^\top = \dot{h}^\top = \dot{q}^\top \partial_q^\top h$ and given $\dot{r} = \mathcal{M}^{-1}\rho$, then $\rho = \mathcal{M}\dot{h}$. In general, we have $r = h(q)$ and $\rho = h^\dagger(q, \dot{q})$, where $h^\dagger(q, \dot{q}) = \mathcal{M}\dot{h}(q, \dot{q})$.

In view of (6.23), it can be observed that (6.25) is equivalent to (4.2) with negligible damping, i.e., $r_1 = 0$. For the stability analysis, we considered the linearized dynamics of the (explicit) nominal system (4.31) using the parameters from Table 4.1. The gain vector $\mathbf{K}_{LQR}$ is computed following Algorithm 6.1. Here, two cases are addressed.

- Negligible damping ($r_1 = 0$): The optimal LQR feedback gain is

$$\mathbf{K}_{LQR} = \begin{bmatrix} -50.2405 & -7.7460 & -11.2019 & -8.7091 \end{bmatrix} \tag{6.26}$$

  and the (closed-loop) eigenvalues are

$$\Lambda = \begin{Bmatrix} -3.2107 & -5.8772 & -2.6738 \pm 1.0821\imath \end{Bmatrix}. \tag{6.27}$$

- With damping ($r_1 = 0.0276$): The optimal LQR feedback gain is

$$\mathbf{K}_{LQR} = \begin{bmatrix} -50.7416 & -7.7460 & -11.1672 & -8.7544 \end{bmatrix} \tag{6.28}$$

  and the (closed-loop) eigenvalues are

$$\Lambda = \begin{Bmatrix} -3.2099 & -5.8788 & -2.6737 \pm 1.0821\imath \end{Bmatrix}. \tag{6.29}$$

Via Lyapunov's indirect method, (local) asymptotic stability is guaranteed because in both cases the eigenvalues of the closed-loop system are in the open left-half plane.

6.3.4 Simulation Results

Consider the system parameters from Table 4.1, with no friction, i.e., $r_1 = 0$. From Algorithm 6.1, one solution gives us the following tuning gains $a_1 = 0.0967$, $a_2 = 0.2105$, $D_x = -0.0311$, $K_\psi = 1$ and $K_u = 1.1243\, I_2$. These gains satisfy the inequalities in (6.22). The desired cart position is set to $x_c^\star = 0\,\mathrm{m}$. The objective is to stabilize the cart-pole system from the initial states $x_p(0) = 0.1655$, $y_p(0) = 0.4548$, $x_c(0) = 0$ and $\rho(0) = 0$. These initial conditions satisfy the constraint (6.4b).

Figure 6.5 depicts the time responses of the (position) states x_p, y_p, x_c and the target Hamiltonian $\mathcal{H}_d$ under the stabilization control problem. Simulations show that the implicit controller (6.21) stabilizes the system (6.4) fulfilling the requirements stated in the *problem formulation*, i.e., $x_p \to 0$, $y_p \to l$, $x_c \to x_c^\star = 0$ and $\rho \to 0$.

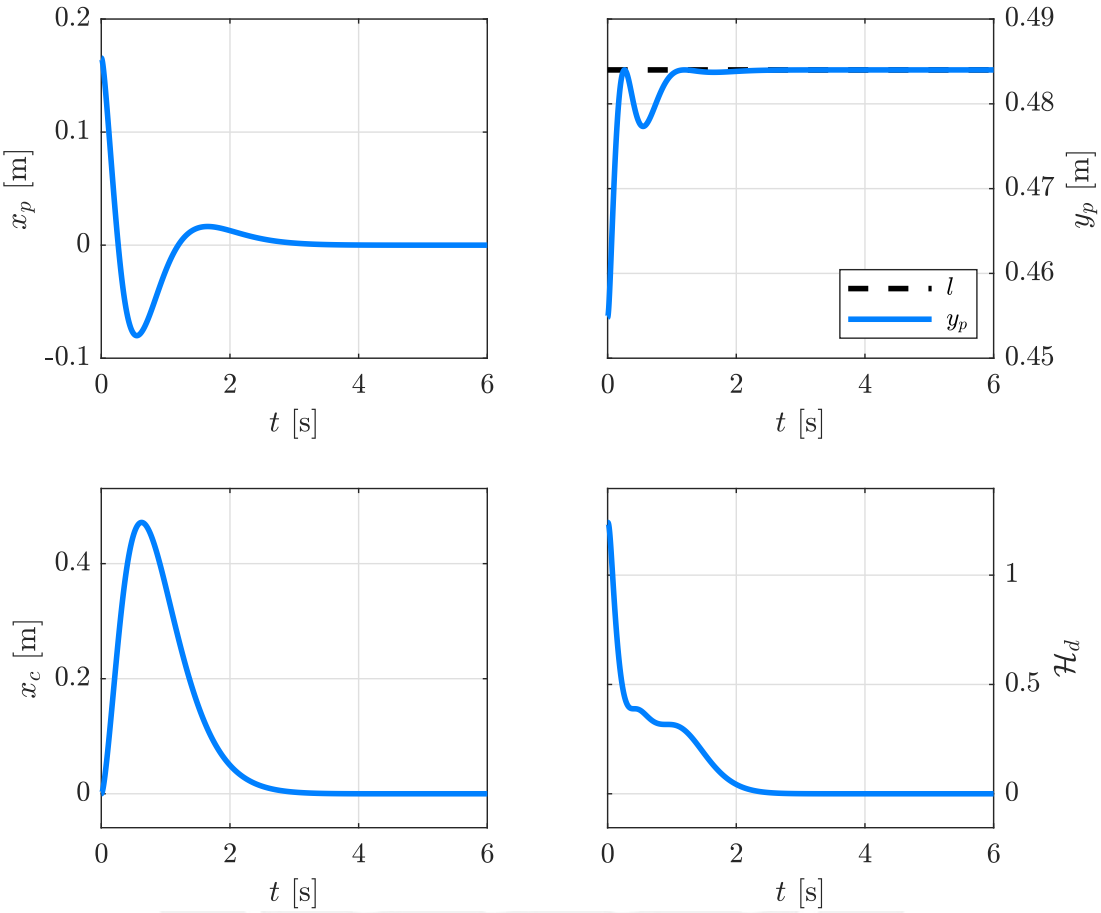

Figure 6.5 – Simulation results with no damping

6.3.5 Experimental Validation

Real-time experiments are contrasted with simulations including damping in the cart-pole dynamics. Consider the parameters of the cart-pole system from Table 4.1, including friction. From Algorithm 6.1, one solution gives us the following tuning gains as shown in Table 6.2 These gains satisfy the inequalities in (6.22). The desired equilibrium is set to $x_c^\star = 0.5\,\text{m}$ for $t \in [0, 5[$ s, $x_c^\star = -0.5\,\text{m}$ for $t \in [5, 10[$ s and $x_c^\star = 0\,\text{m}$ for $t \in [10, 15]$ s. The objective is to stabilize the cart-pole system from the initial states $x_p(0) = 0$, $y_p(0) = 0$, $x_c(0) = 0$ and $\rho(0) = 0$. These initial conditions satisfy the constraint (6.4b).

a_1	a_2	D_x	K_ψ	K_u
0.0978	0.2102	-0.0309	1	$1.1302\, I_2$

Table 6.2 – Implicit IDA-PBC parameters

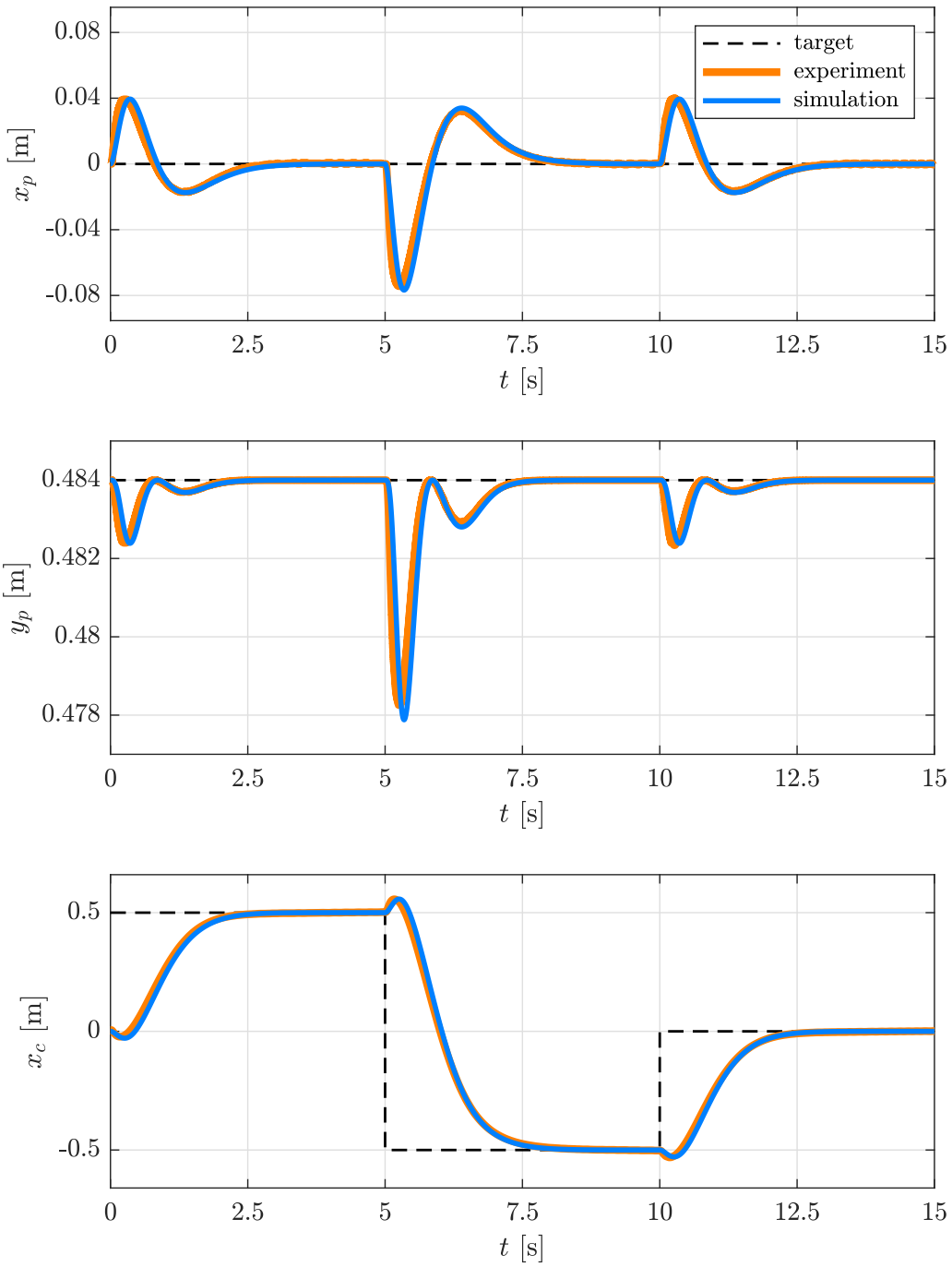

Figure 6.6 – Simulation and experimental results with damping

Figure 6.6 depicts the time responses of the (position) states x_p, y_p, x_c and Figure 6.7 depicts the (real) control input $\bar{v}$ under the regulation control problem. Simulations and real-time experiments show that the implicit controller (6.21) stabilizes the system (6.4) fulfilling the requirements stated in the *problem formulation*, i.e., $x_p \to 0$, $y_p \to l$

and $x_c \to x_c^\star$ with continuous, smooth and bounded (real) control input $\bar{v}$. It can be seen that simulations and real-time experiments show almost the same performance.

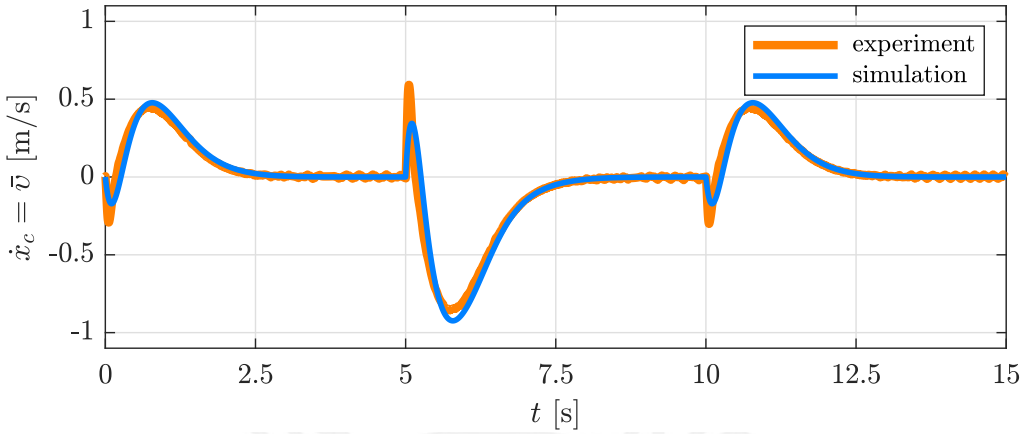

Figure 6.7 – Simulation and experimental results with damping

6.4 Implicit Control Scheme

Figure 6.8 depicts an overview of the implicit control strategy which integrates both controllers: (i) implicit swing-up and (ii) implicit IDA-PBC. The first controller will swing-up the pendulum and the second will stabilize it.[42]

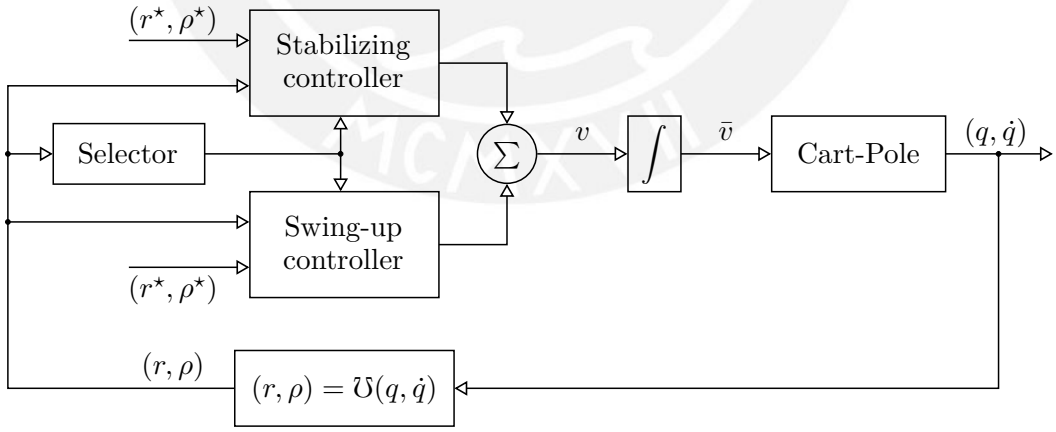

Figure 6.8 – Overview of the implicit control system

Since the control scheme is initialized with the swing-up controller, then an algorithm is required to decide when to switch to the stabilizing controller.

[42] In this section, *stabilizing controller* refers to the implicit IDA-PBC.

The block named *Selector* is an algorithm that decides which of the controllers must be active and operates on the basis of the conditions outlined in Section 4.5. Note that whenever one controller is activated, the other remains deactivated. This is computationally efficient since it avoids computing both control algorithms simultaneously.

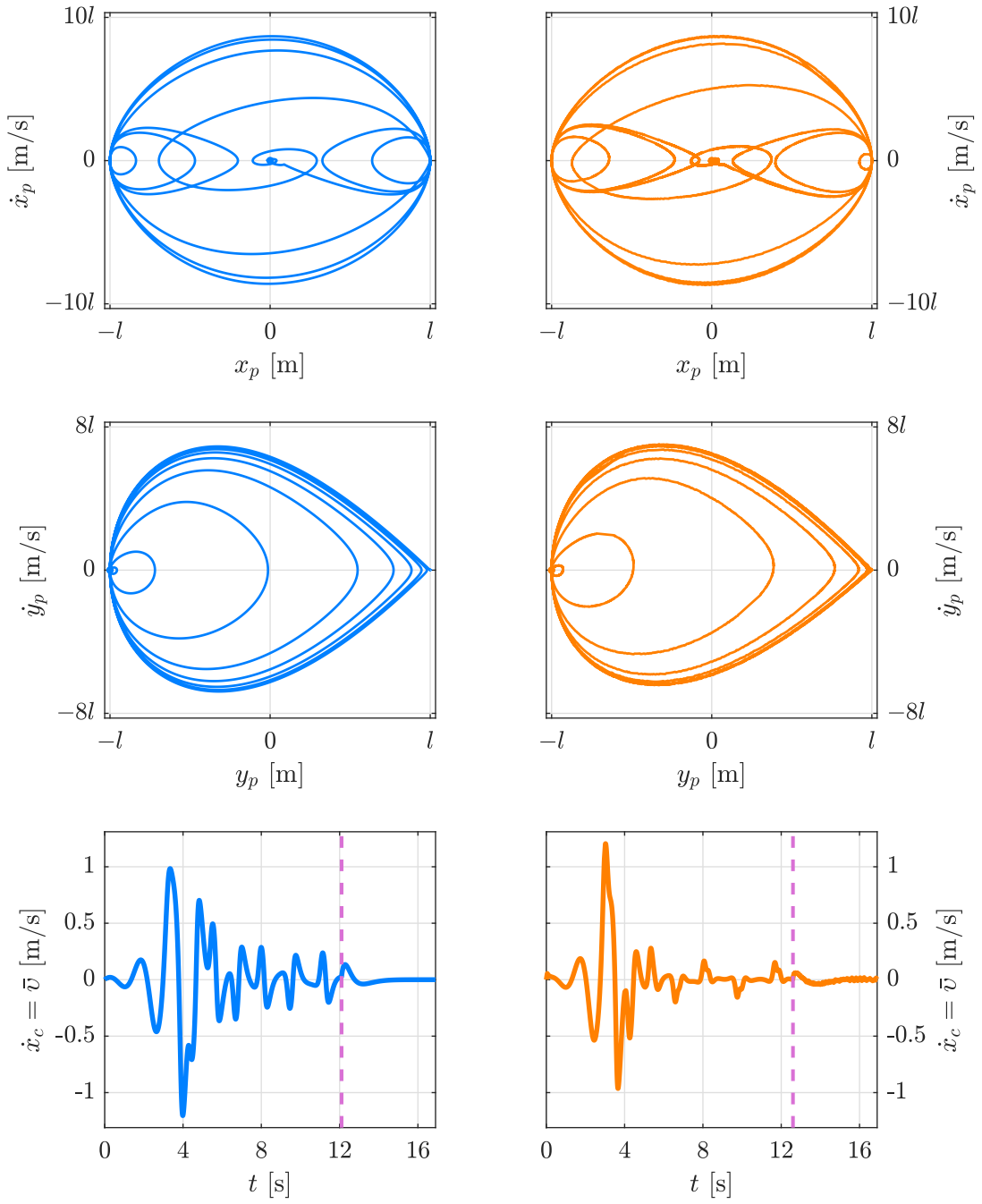

Figure 6.9 – Simulation (blue) and experimental (red) results with damping

Additionally, the block of coordinate transformation , namely $(r, \rho) = \mho(q, \dot{q})$, is defined as $\mho^\top := \begin{bmatrix} h^\top & h^{\dagger\top} \end{bmatrix}$, where $h^{\dagger\top} = \dot{q}^\top \partial_q^\top h \, \mathcal{M}$.

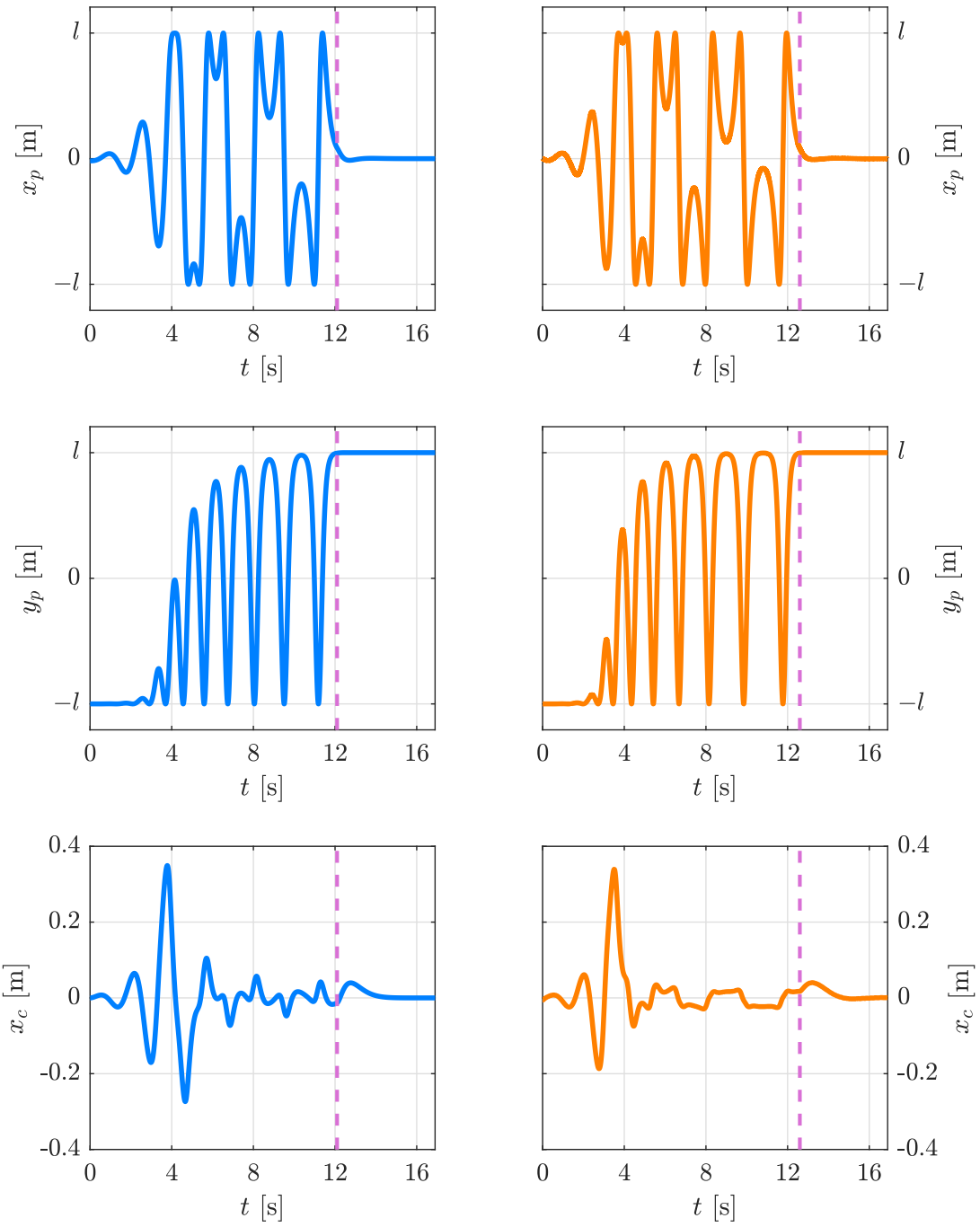

Figure 6.10 – Simulation (blue) and experimental (red) results with damping

Real-time experiments are contrasted with simulations including damping in the cart-pole dynamics. (i) For the swing-up controller, consider the system parameters from

Table 4.1, the controller parameters from Table 6.1, the (new) target energy set as $\bar{\mathcal{E}}^\star = 1.44$ and the initial states from Section 6.2.6. (ii) For the stabilizing controller, consider the system parameters from Table 4.1 and the controller parameters from Table 6.2. For both controllers, the target cart position is set to $x_c^\star = 0\,\mathrm{m}$.

The first and second row of Figure 6.9 depicts the phase portrait of $(x_p, \dot{x}_p)$ and $(y_p, \dot{y}_p$, respectively. The third row depicts the (real) control input $\bar{v}$ under the (implicit) control scheme provided by Figure 6.8. Figure 6.10 depicts the time responses of the (position) states x_p, y_p and x_c. The switch occurs at $t = 12.1\,\mathrm{s}$ in the simulations and at $t = 12.6\,\mathrm{s}$ in the real-time experiments. Note that the (real) control input $\bar{v}$ is bounded.

6.5 Comparative Results

6.5.1 Analytical Comparison

Stabilizing Controller Using Proposition 5.5 with (5.9), $q = \begin{bmatrix}\theta & x_c\end{bmatrix}^\top$, $r = h(q) = \begin{bmatrix} l\sin\theta & l\cos\theta & x_c\end{bmatrix}^\top$, $J_q = M^{-1}(q)M_d(q)$, $T_1 = \mathcal{J}^{-1}\partial_q h\, J_q$, $M_d = \left(T_1^\top \mathcal{M}_d\, T_1\right)\Big|_{r=h(q)}$ and $M(q)$ from (6.23), we obtain

$$M_d^{-1}(q) = M^{-1}(q)\,\partial_q^\top h\,\mathcal{M}(r)\,\mathcal{M}_d^{-1}(r)\,\mathcal{M}(r)\,\partial_q h\,M^{-1}(q).$$

After some direct calculations, the (reduced) target inertia matrix takes the form

$$M_d(q) = \begin{bmatrix} k_e k_u l^2 + k_u^2 K_D\,(l\cos\theta)^2 & -k_a k_u K_D l\cos\theta \\ -k_a k_u K_D l\cos\theta & k_e k_a + k_a^2 K_D \end{bmatrix}, \tag{6.30}$$

where

$$k_e = \frac{1}{k_a(D_x - a_1 + a_2)}, \quad k_u = \frac{1}{k_e D_x} \quad \text{and} \quad K_D = \frac{D_x - a_1}{k_u k_a\left[a_1 a_2 - (D_x - a_1)^2\right]}.$$

The (reduced) target potential energy function $V_d(q) = \mathcal{V}_d(h(q))$ takes the form

$$V_d(q) = k_e k_u g_r l(\cos\theta - 1) + \frac{1}{2}K_I\left[k_a(x_c - x_c^\star) - k_u l\sin\theta\right]^2, \tag{6.31}$$

where

$$K_I = \frac{K_\psi}{k_e^2\,k_u^2\,k_a^2\,\left[a_1 a_2 - (D_x - a_1)^2\right]^2}.$$

From this result we can see that the closed-loop system in explicit coordinates has the same target inertia matrix $M_d(q)$ and potential energy function $V_d(q)$ compared with (4.24) and (4.25), respectively. In synthesis, both approaches (implicit IDA-PBC and explicit PID-PBC) have the same target Hamiltonian $H_d(q, \dot{q})$ for the closed-loop.

Swing-Up Controller Using Proposition 5.5 with (6.4), $q = \begin{bmatrix} \theta & x_c \end{bmatrix}^\top$, $r = h(q) = \begin{bmatrix} l\sin\theta & l\cos\theta & x_c \end{bmatrix}^\top$, $\mathcal{J} = I_3$, $J_q = I_2$, $T_1 = I_3^{-1}\,\partial_q h\, I_2$, $M = (T_1^\top \mathcal{M}\, T_1)\big|_{r=h(q)}$ and $V = \mathcal{V}(h(q))$, we obtain

$$\bar{M}(q) = \begin{bmatrix} l^2 & l\cos\theta \\ l\cos\theta & k_c \end{bmatrix} \qquad \text{and} \qquad V(q) = g_r l\,(\cos\theta - 1)\,.$$

The (reduced) new energy function takes the form

$$\bar{E}(q, \dot{q}) = \frac{1}{2}\dot{q}^\top \bar{M}(q)\dot{q} + V(q). \tag{6.32}$$

From this result we can see that the closed-loop system in explicit coordinates has the same new energy function $\bar{E}(q, \dot{q})$ compared with (4.5). This fact also implies that the closed-loop system in explicit coordinates has the same (target) storage function $U(q, \dot{q})$ compared with (4.7).

6.5.2 Experimental Comparison

Implicit Control Scheme (i) For the swing-up controller, consider the system parameters from Table 4.1, the controller parameters from Table 6.1, the (new) target energy set as $\bar{\mathcal{E}}^\star = 2.54$ and the initial states from Section 6.2.6. (ii) For the stabilizing controller, consider the system parameters from Table 4.1 and the controller parameters from Table 6.2.

Explicit Control Scheme (i) For the swing-up controller, consider the system parameters from Table 4.1, the controller parameters from Table 4.3, the (new) target energy set as $\bar{E}^\star = 2.54$ and the initial states from Section 4.3.6. (ii) For the stabilizing controller, consider the system parameters from Table 4.1 and the controller parameters from Table 4.4.

For both control schemes, the target cart position is set to $x_c^\star = 0\,\text{m}$ for $t \in [0, 10[$ s, $x_c^\star = 0.5\,\text{m}$ for $t \in [10, 15[$ s, $x_c^\star = -0.5\,\text{m}$ for $t \in [15, 20[$ s and $x_c^\star = 0\,\text{m}$ for $t \in [20, 25]$ s.

For comparative purposes, we have measured the generalized coordinates in explicit representation, i.e., $(q, \dot{q})$ instead of (r, ρ). Real-time experiments show that the trajectories of the pendulum are brought into a homoclinic orbit. Evidently, we improve the time of reachability by injecting more energy into the system.

Figure 6.11 depicts the phase portrait of $(\theta, \dot{\theta})$. We can observe that the system promptly converges into the homoclinic orbit ensuring that their trajectories enter the basin of attraction of the (local) stabilizing controller.

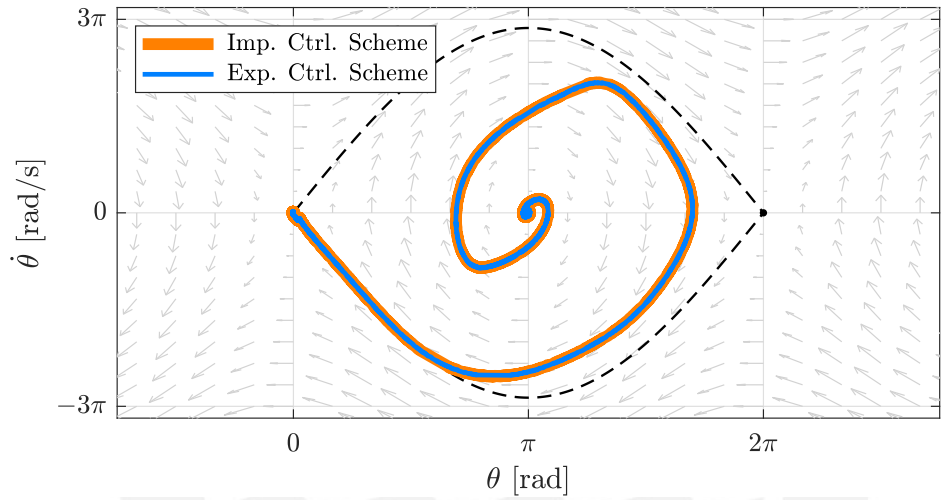

Figure 6.11 – Experimental results

Figure 6.12 depicts the time responses of the states θ, x_c and the (real) control input $\bar{v}$. In both representations (implicit and explicit), the switch occurs at $t = 4.6\,\mathrm{s}$, approximately. The main control task formulated at the beginning of the document has been fulfilled, i.e., formulate a control strategy to swing-up the pendulum from the stable equilibrium to the unstable equilibrium point and then to stabilize the pendulum at the upright vertical position with the cart at some desired position.

This chapter closes by concluding that both control schemes (implicit and explicit) exhibit almost the same performance. The difference is almost negligible, but it is visible in the transient responses, specifically, after an aggressive change of reference. This slight deviation can be appreciated in the graph corresponding to the transient response of the (real) control input $\bar{v}$ at $t = 15\,\mathrm{s}$. It is noteworthy here that we are dealing with a physical system which is vulnerable to uncertainties and disturbances, such as, unmodeled dynamics, friction, rail vibration, lack of accuracy in the sensors, among others.

A video of the experiments can be watched at youtu.be/SRR5zJ6SHH4.

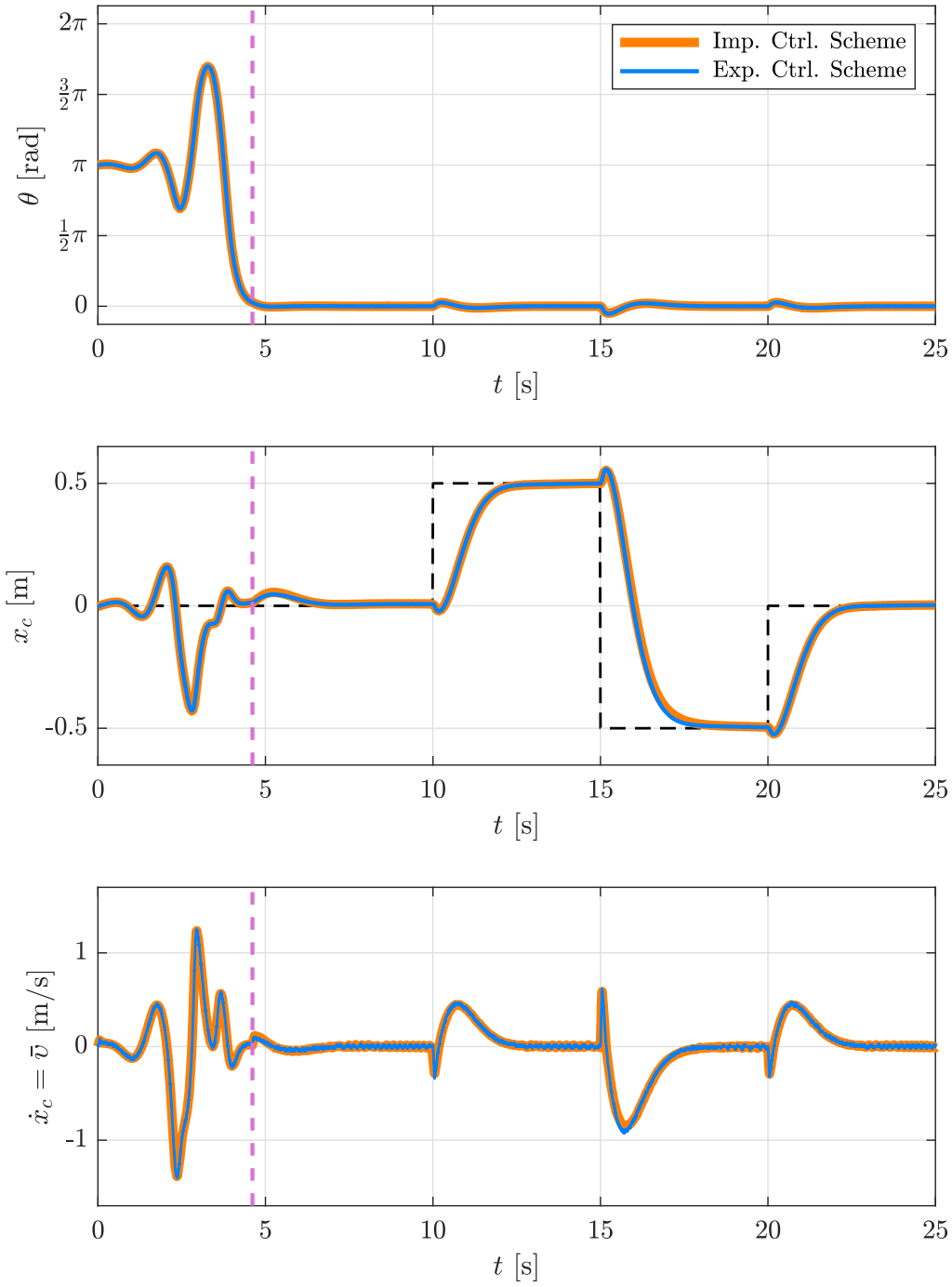

Figure 6.12 – Experimental results

ET LUX IN TENEBRIS LUCET
MCMXVII

Chapter 7

Conclusions and Future Work

The swing-up and (local) stabilization control problem is formulated and solved for the cart-pole system in implicit PH representation. Towards this end, an (implicit) control scheme based on a two-stage control strategy is proposed so that one controller will swing-up the pendulum and another will (locally) stabilize it. The effectiveness of the control strategies has been verified by simulations and real-time experiments. Moreover, the physical setup can be controlled via an inner velocity loop or via an inner current loop. We decided on the inner velocity loop because dealing with the current loop involves knowing the (exact) values of more system parameters, such as, masses, inertias, gear features, frictions, among others. The velocity loop with an integrator in the input can be approximated to the cart-pole system in SNF.

The swing-up controller is designed under an alternative approach that does not require the closed-loop system to have a Hamiltonian form. It consists in defining a more general class of target (or desired) energy function to drive the trajectories of the pendulum at a homoclinic orbit (or limit cycle). However, slight modifications have been performed for the cart-pole system in SNF since the typical approach does not permit stabilization of the cart trajectories at a given reference point. This modification consists of: (i) finding a new energy function for the open-loop dynamics and (ii) defining a (generalized) admissible storage function for the closed loop. Simulations with no physical damping revealed tracking of the homoclinic orbit. In real-time experiments, we observed that increasing the target energy is a practical and straightforward solution to the unmodeled dynamics (e.g. viscous friction) problem.

The (local) stabilizing controller is designed using a novel algebraic solution to the IDA-PBC problem (avoiding the computation of PDEs) [10]. Additionally, another novel approach is formulated to identify the controller parameters and ensure an optimal (local) transient response. It is noteworthy here that no modifications were needed because the design procedure in [10] works perfectly for the cart-pole system in SNF. Simulations and real-time experiments reveal asymptotic stability, even in the presence of unmodeled dynamics, i.e., unmodeled friction. Conclusively, the proposed (implicit) control scheme guarantees the swing-up and asymptotic stabilization of the pendulum at its upright vertical position holding the trajectories of the cart at the desired point.

For comparison purposes, an (explicit) control scheme is additionally implemented for the cart-pole system in explicit EL representation. Experiments show that the behavior is almost the same in both control schemes (implicit and explicit). This is proved analytically via the reduction from implicit to explicit coordinates, where it can be observed that: (i) both swing-up controllers (implicit and explicit) have the same target storage function and (ii) both (local) stabilizing controllers (implicit IDA-PBC and explicit PID-PBC) have the same target Hamiltonian. Concerning the (local) stabilizing controllers, the IDA-PBC approach in [10] permits to control a wider class of UMSs compared to the PID-PBC method. In addition, for a class of UMSs we can find an algebraic solution to the IDA-PBC problem (avoiding PDEs). Regarding the swing-up controllers, they have been designed under the same methodology. Therefore, they are equivalent but in different representations (implicit and explicit).

A future research topic consists of analyzing whether the algebraic IDA-PBC approach in [10] works for UMSs with higher degrees of underactuation, e.g. the double or triple inverted pendulum on a cart. The swing-up control problem has been solved in [6] for the double inverted pendulum on a cart in explicit EL representation using the typical energy-based control method. However, no results have been reported for the same system in implicit PH representation. Indeed, the most challenging task is the formulation of the control strategy for those system in SNF. To the best of author's knowledge, there are no reported energy-based control strategies for the triple inverted pendulum on a cart. Another research topic consists of studying the swing-up control problem for UMSs with unmodeled frictions and parametric uncertainties.

List of Acronyms

ARE	Algebraic Riccati Equation
DAE	Differential Algebraic Equation
DOF	Degrees of Freedom
EL	Euler-Lagrange
IDA	Interconnection and Damping Assignment
IDA-PBC	Interconnection and Damping Assignment Passivity-Based Control
LQR	Linear Quadratic Regulator
PBC	Passivity-Based Control
PCH	Port-Controlled Hamiltonian
PCHD	Port-Controlled Hamiltonian with Dissipation
PDE	Partial Differential Equation
PFL	Partial Feedback Linearization
PH	Port-Hamiltonian
PID	Proportional–Integral–Derivative
PID-PBC	PID Passivity-Based Control
ODE	Ordinary Differential Equation
SMC	Sliding Mode Control

SNF	Spong's Normal Form
UMS	Underactuated Mechanical System
ZSD	Zero-State Detectable
ZSO	Zero-State Observable

List of Figures

List of Tables

ET LUX IN TENEBRIS LUCET
MCMXVII

Bibliography

[1] A. S. Huaman Loayza and C. G. Pérez Zuñiga, "Design of a fuzzy sliding mode controller for the autonomous path-following of a quadrotor," *IEEE Latin America Transactions*, vol. 17, no. 06, pp. 962–971, 2019.

[2] A. S. Huaman-Loayza, "Path-following of a quadrotor using fuzzy sliding mode control," in *2018 IEEE XXV International Conference on Electronics, Electrical Engineering and Computing (INTERCON)*. IEEE, 2018, pp. 1–4.

[3] A. S. Huaman Loayza, *Desarrollo de una plataforma de simulación y control basado en el modelamiento de un robot articular de cinco grados de libertad para fines académicos*. Universidad Peruana de Ciencias Aplicadas (UPC), 2017.

[4] A. S. Huaman-Loayza, "Accurate trajectory tracking for a 3d-plotter using optimal preview control and unknown input observer," in *2018 IEEE XXV International Conference on Electronics, Electrical Engineering and Computing (INTERCON)*. IEEE, 2018, pp. 1–4.

[5] I. Fantoni and R. Lozano, *Non-linear control for underactuated mechanical systems*. Springer Science & Business Media, 2001.

[6] X. Xin and Y. Liu, *Control design and analysis for underactuated robotic systems*. Springer Science & Business Media, 2014.

[7] M. Takegaki and S. Arimoto, "A new feedback method for dynamic control of manipulators," *Journal of Dynamic Systems, Measurement, and Control*, vol. 103, no. 2, pp. 119–125, 1981.

[8] F. Castaños, D. Gromov, V. Hayward, and H. Michalska, "Implicit and explicit representations of continuous-time port-hamiltonian systems," *Systems & Control Letters*, vol. 62, no. 4, pp. 324–330, 2013.

[9] F. Castaños and D. Gromov, "Passivity-based control of implicit port-hamiltonian systems with holonomic constraints," *Systems & Control Letters*, vol. 94, pp. 11–18, 2016.

[10] O. B. Cieza and J. Reger, "Ida-pbc for underactuated mechanical systems in implicit port-hamiltonian representation," in *2019 18th European Control Conference (ECC)*. IEEE, 2019, pp. 614–619.

[11] J. E. Vidal Sandoval, *Implicit IDA-PBC Design and Implementation for a Portal Crane System*. Pontificia Universidad Católica del Perú.

[12] J. K. Roberge, "The mechanical seal," Ph.D. dissertation, Massachusetts Institute of Technology, 1960.

[13] J. F. Schaefer, "On the control of unstable mechanical systems," in *Proc. of the Third Congress of IFAC*, vol. 1, 1966, pp. 6c–1.

[14] H. Kwakernaak and R. Sivan, *Linear optimal control systems*. Wiley-interscience New York, 1972, vol. 1.

[15] H. Khalil, *Nonlinear Systems*, 3rd ed. Prentice Hall, 2002.

[16] S. Mori, H. Nishihara, and K. Furuta, "Control of unstable mechanical system control of pendulum," *International Journal of Control*, vol. 23, no. 5, pp. 673–692, 1976.

[17] K. Furuta, M. Yamakita, and S. Kobayashi, "Swing up control of inverted pendulum," in *Proceedings IECON'91: 1991 International Conference on Industrial Electronics, Control and Instrumentation*. IEEE, 1991, pp. 2193–2198.

[18] K. Barya, S. Tiwari, and R. Jha, "Comparison of lqr and robust controllers for stabilizing inverted pendulum system," in *2010 International Conference on Communication Control and Computing Technologies*. IEEE, 2010, pp. 300–304.

[19] K. J. Åström, "Hybrid control of inverted pendulums," in *Learning, control and hybrid systems*. Springer, 1999, pp. 150–163.

[20] J. Zhao and M. W. Spong, "Hybrid control for global stabilization of the cart–pendulum system," *Automatica*, vol. 37, no. 12, pp. 1941–1951, 2001.

[21] J. Aracil and F. Gordillo, "The inverted pendulum: A benchmark in nonlinear

control," in *Proceedings World Automation Congress, 2004.*, vol. 16. IEEE, 2004, pp. 468–482.

[22] S. Riachy, Y. Orlov, T. Floquet, R. Santiesteban, and J.-P. Richard, "Second-order sliding mode control of underactuated mechanical systems i: Local stabilization with application to an inverted pendulum," *International Journal of Robust and Nonlinear Control: IFAC-Affiliated Journal*, vol. 18, no. 4-5, pp. 529–543, 2008.

[23] R. Santiesteban, T. Floquet, Y. Orlov, S. Riachy, and J.-P. Richard, "Second-order sliding mode control of underactuated mechanical systems ii: Orbital stabilization of an inverted pendulum with application to swing up/balancing control," *International Journal of Robust and Nonlinear Control: IFAC-Affiliated Journal*, vol. 18, no. 4-5, pp. 544–556, 2008.

[24] M.-S. Park and D. Chwa, "Swing-up and stabilization control of inverted-pendulum systems via coupled sliding-mode control method," *IEEE Transactions on Industrial Electronics*, vol. 56, no. 9, pp. 3541–3555, 2009.

[25] R. Olfati-Saber, "Fixed point controllers and stabilization of the cart-pole system and the rotating pendulum," in *Proceedings of the 38th IEEE Conference on Decision and Control (Cat. No. 99CH36304)*, vol. 2. IEEE, 1999, pp. 1174–1181.

[26] R. Balan, V. Maties, and S. Stan, "A solution of the inverse pendulum on a cart problem using predictive control," in *Proceedings of the IEEE International Symposium on Industrial Electronics, 2005. ISIE 2005.*, vol. 1. IEEE, 2005, pp. 63–68.

[27] P. J. Gawthrop and L. Wang, "Intermittent predictive control of an inverted pendulum," *Control Engineering Practice*, vol. 14, no. 11, pp. 1347–1356, 2006.

[28] A. Mills, A. Wills, and B. Ninness, "Nonlinear model predictive control of an inverted pendulum," in *2009 American control conference*. IEEE, 2009, pp. 2335–2340.

[29] W.-D. Chang, R.-C. Hwang, and J.-G. Hsieh, "A self-tuning pid control for a class of nonlinear systems based on the lyapunov approach," *Journal of Process Control*, vol. 12, no. 2, pp. 233–242, 2002.

[30] F. Mazenc and S. Bowong, "Tracking trajectories of the cart-pendulum system," *Automatica*, vol. 39, no. 4, pp. 677–684, 2003.

[31] B. Srinivasan, P. Huguenin, and D. Bonvin, "Global stabilization of an inverted

pendulum–control strategy and experimental verification," *Automatica*, vol. 45, no. 1, pp. 265–269, 2009.

[32] J. Van der Burg, R. Ortega, J. Scherpen, J. Acosta, and H. Siguerdidjane, "An experimental application of total energy shaping control: Stabilization of the inverted pendulum on a cart in the presence of friction," in *2007 European Control Conference (ECC)*. IEEE, 2007, pp. 1990–1996.

[33] J. Á. Acosta, R. Ortega, A. Astolfi, and I. Sarras, "A constructive solution for stabilization via immersion and invariance: The cart and pendulum system," *Automatica*, vol. 44, no. 9, pp. 2352–2357, 2008.

[34] J. Yi, N. Yubazaki, and K. Hirota, "Upswing and stabilization control of inverted pendulum system based on the sirms dynamically connected fuzzy inference model," *Fuzzy Sets and Systems*, vol. 122, no. 1, pp. 139–152, 2001.

[35] H. O. Wang, K. Tanaka, and M. F. Griffin, "An approach to fuzzy control of nonlinear systems: Stability and design issues," *IEEE transactions on fuzzy systems*, vol. 4, no. 1, pp. 14–23, 1996.

[36] C. W. Anderson, "Learning to control an inverted pendulum using neural networks," *IEEE Control Systems Magazine*, vol. 9, no. 3, pp. 31–37, 1989.

[37] M. W. Spong, "Partial feedback linearization of underactuated mechanical systems," in *Proceedings of IEEE/RSJ International Conference on Intelligent Robots and Systems (IROS'94)*, vol. 1. IEEE, 1994, pp. 314–321.

[38] C. C. Chung and J. Hauser, "Nonlinear control of a swinging pendulum," *Automatica*, vol. 31, no. 6, pp. 851–862, 1995.

[39] D. Angeli, "Almost global stabilization of the inverted pendulum via continuous state feedback," *Automatica*, vol. 37, no. 7, pp. 1103–1108, 2001.

[40] J. Aracil, F. Gordillo *et al.*, "A family of smooth controllers for swinging up a pendulum," *Automatica*, vol. 44, no. 7, pp. 1841–1848, 2008.

[41] K. J. Åström and K. Furuta, "Swinging up a pendulum by energy control," *Automatica*, vol. 36, no. 2, pp. 287–295, 2000.

[42] R. Lozano, I. Fantoni, and D. J. Block, "Stabilization of the inverted pendulum around its homoclinic orbit," *Systems & control letters*, vol. 40, no. 3, pp. 197–204,

2000.

[43] O. Kolesnichenko and A. S. Shiriaev, "Partial stabilization of underactuated euler–lagrange systems via a class of feedback transformations," *Systems & Control Letters*, vol. 45, no. 2, pp. 121–132, 2002.

[44] M. W. Spong and L. Praly, "Control of underactuated mechanical systems using switching and saturation," in *Control using logic-based switching*. Springer, 1997, pp. 162–172.

[45] A. Shiriaev, A. Pogromsky, H. Ludvigsen, and O. Egeland, "On global properties of passivity-based control of an inverted pendulum," *International Journal of Robust and Nonlinear Control: IFAC-Affiliated Journal*, vol. 10, no. 4, pp. 283–300, 2000.

[46] D. Chatterjee, A. Patra, and H. K. Joglekar, "Swing-up and stabilization of a cart–pendulum system under restricted cart track length," *Systems & control letters*, vol. 47, no. 4, pp. 355–364, 2002.

[47] J.-H. Yang, S.-Y. Shim, J.-H. Seo, and Y.-S. Lee, "Swing-up control for an inverted pendulum with restricted cart rail length," *International Journal of Control, Automation and Systems*, vol. 7, no. 4, pp. 674–680, 2009.

[48] R. Ortega and M. W. Spong, "Stabilization of underactuated mechanical systems via interconnection and damping assignment," *IFAC Proceedings Volumes*, vol. 33, no. 2, pp. 69–74, 2000.

[49] A. M. Bloch, N. E. Leonard, and J. E. Marsden, "Controlled lagrangians and the stabilization of mechanical systems. i. the first matching theorem," *IEEE Transactions on automatic control*, vol. 45, no. 12, pp. 2253–2270, 2000.

[50] A. M. Bloch, D. E. Chang, N. E. Leonard, and J. E. Marsden, "Controlled lagrangians and the stabilization of mechanical systems. ii. potential shaping," *IEEE Transactions on Automatic Control*, vol. 46, no. 10, pp. 1556–1571, 2001.

[51] J. A. Acosta, R. Ortega, A. Astolfi, and A. D. Mahindrakar, "Interconnection and damping assignment passivity-based control of mechanical systems with underactuation degree one," *IEEE Transactions on Automatic Control*, vol. 50, no. 12, pp. 1936–1955, 2005.

[52] G. Viola, R. Ortega, R. Banavar, J. Á. Acosta, and A. Astolfi, "Total energy shaping control of mechanical systems: simplifying the matching equations via

coordinate changes," *IEEE Transactions on Automatic Control*, vol. 52, no. 6, pp. 1093–1099, 2007.

[53] A. Donaire, R. Mehra, R. Ortega, S. Satpute, J. G. Romero, F. Kazi, and N. M. Singh, "Shaping the energy of mechanical systems without solving partial differential equations," *IEEE Transactions on Automatic Control*, vol. 61, no. 4, pp. 1051–1056, 2016.

[54] A. Donaire, R. Ortega, and J. G. Romero, "Simultaneous interconnection and damping assignment passivity-based control of mechanical systems using generalized forces," *Systems & Control Letters*, vol. 94, pp. 118–126, 2016.

[55] J. J. E. Slotine, W. Li *et al.*, *Applied nonlinear control*. Prentice hall Englewood Cliffs, NJ, 1991, vol. 199, no. 1.

[56] M. Vidyasagar, *Nonlinear systems analysis*. Siam, 2002, vol. 42.

[57] R. Sepulchre, M. Jankovic, and P. V. Kokotovic, *Constructive nonlinear control*. Springer Science & Business Media, 2012.

[58] R. Ortega, J. A. L. Perez, P. J. Nicklasson, and H. J. Sira-Ramirez, *Passivity-based control of Euler-Lagrange systems: mechanical, electrical and electromechanical applications*. Springer Science & Business Media, 2013.

[59] A. J. van der Schaft and A. Van Der Schaft, *L2-gain and passivity techniques in nonlinear control*. Springer, 2000, vol. 2.

[60] C. I. Byrnes, A. Isidori, and J. C. Willems, "Passivity, feedback equivalence, and the global stabilization of minimum phase nonlinear systems," *IEEE Transactions on automatic control*, vol. 36, no. 11, pp. 1228–1240, 1991.

[61] A. J. van der Schaft, "Port-hamiltonian systems: an introductory survey," in *Proceedings of the international congress of mathematicians*, vol. 3. Citeseer, 2006, pp. 1339–1365.

[62] A. J. van der Schaft, D. Jeltsema *et al.*, "Port-hamiltonian systems theory: An introductory overview," *Foundations and Trends® in Systems and Control*, vol. 1, no. 2-3, pp. 173–378, 2014.

[63] R. Ortega, A. Van Der Schaft, F. Castanos, and A. Astolfi, "Control by interconnection and standard passivity-based control of port-hamiltonian systems," *IEEE*

Transactions on Automatic control, vol. 53, no. 11, pp. 2527–2542, 2008.

[64] R. Ortega and E. Garcia-Canseco, "Interconnection and damping assignment passivity-based control: A survey," *European Journal of control*, vol. 10, no. 5, pp. 432–450, 2004.

[65] R. Ortega, A. J. van der Schaft, B. Maschke, and G. Escobar, "Interconnection and damping assignment passivity-based control of port-controlled hamiltonian systems," *Automatica*, vol. 38, no. 4, pp. 585–596, 2002.

[66] J. G. Romero, R. Ortega, and A. Donaire, "Energy shaping of mechanical systems via pid control and extension to constant speed tracking," *IEEE Transactions on Automatic Control*, vol. 61, no. 11, pp. 3551–3556, 2016.

[67] J. G. Romero, A. Donaire, R. Ortega, and P. Borja, "Global stabilisation of underactuated mechanical systems via pid passivity-based control," *Automatica*, vol. 96, pp. 178–185, 2018.

[68] M. Spong, S. Hutchinson, and M. Vidyasagar, *Robot Modeling and Control*. Wiley, 2005.